香港地區地震危險性分析
SEISMIC HAZARD ANALYSIS OF THE HONG KONG REGION

土力工程處報告系列第65號
GEO REPORT No. 65

李焯芬　丁原章　黃日恆
余演波　郭貴安　陳龐龍　及　黃新輝
C.F. Lee, Y.Z. Ding, R.H. Huang,
Y.B. Yu, G.A. Guo, P.L. Chen & X.H. Huang

香港特別行政區政府
土木工程署
土力工程處
GEOTECHNICAL ENGINEERING OFFICE
CIVIL ENGINEERING DEPARTMENT
THE GOVERNMENT OF THE HONG KONG
SPECIAL ADMINISTRATIVE REGION

香港地區地震危險性分析
SEISMIC HAZARD ANALYSIS OF THE HONG KONG REGION

土力工程處報告系列第65號
GEO REPORT No. 65

李焯芬　丁原章　黃日恆
余演波　郭貴安　陳龐龍　及　黃新輝
C.F. Lee, Y.Z. Ding, R.H. Huang,
Y.B. Yu, G.A. Guo, P.L. Chen & X.H. Huang

本報告源於一九九六年九月與香港大學的顧問合約
This report was originally produced in September 1996
under Consultancy Agreement with the University of Hong Kong

First published, January 1998
Reprinted, August 2000
Reprinted, May 2002

Prepared by:

Geotechnical Engineering Office,
Civil Engineering Department,
Civil Engineering Building,
101 Princess Margaret Road,
Homantin, Kowloon,
Hong Kong.

PREFACE

In keeping with our policy of releasing information, we make available some of our internal reports in a series of publications termed the GEO Report series. The reports in this series, of which this is one, are selected from a wide range of reports produced by the staff of the Office and our consultants. A charge is made to cover the cost of printing.

The Geotechnical Engineering Office also publishes guidance documents and presents the results of research work of general interest in GEO Publications. These publications and the GEO Reports may be obtained from the Government's Information Services Department. Information on how to purchase these publications is given on the last page of this report.

Andrew Malone
Principal Government Geotechnical Engineer
January 1998

FOREWORD

In June 1995, the Geotechnical Engineering Office, (GEO) awarded a one-year research contract to the University of Hong Kong (HKU), with the Guangdong Seismological Bureau (GSB) as sub-consultants, to undertake a seismic hazard analysis of the Hong Kong region. The study, which is a project under the GEO Research and Development Theme "Engineering Seismology", commenced in July 1995, with Professor C.F. Lee of the HKU and Professor Ding Yuanzhang of the GSB serving as project co-leaders.

In December 1995, the project team submitted its Phase 1 Study Report to the GEO. The report reviews and documents the pertinent seismological and geological data from GSB and other sources. The project team then extended its study with specific focus on the situation in the Hong Kong region. Firstly, the project team conducted a series of seismotectonic investigations in the field. Then, the distribution, stratigraphy and rock properties of the Quaternary strata in the region were studied. As part of the study, the Institute of Geology under the State Seismological Bureau of China was subcontracted to conduct thermoluminescene age dating (20 tests), ^{14}C age dating (3 tests) and thin section studies (22 tests). In the course of the study, the earthquake records obtained by the Royal Observatory (renamed Hong Kong Observatory in July 1997) were re-evaluated. These records, together with pertinent data from the GSB seismic monitoring network, were used to establish an updated earthquake catalogue for the Hong Kong region (bounded by latitude 22°00′ - 23°00′ and longitudes 113°45′ - 114°45′), for seismic events since 1972 with $M_L \geq 1.8$. Analysis was also made of the potential seismic source zones which may affect Hong Kong and their seismological parameters. Seismic ground motion attenuation models applicable to the region were studied and compared. Finally, peak ground acceleration and seismic intensity values corresponding to various probabilities of exceedance and return periods were computed and analysed.

The Hong Kong Observatory provided strong support throughout the study. Messrs K.W. Lai and W.K. Pun of the GEO joined the research team in the field studies and helped to resolve specific logistic issues. They, as well as Dr C J N Fletcher of the Hong Kong Geological Survey, provided useful comments on a draft of this report.

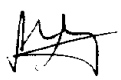

P L R Pang
Chief Geotechnical Engineer/Special Projects

ABSTRACT

Based on the results of previous investigations, the present study evaluates and re-assesses the potential source zones for the Hong Kong region and the related seismic ground motion parameters. The attenuation relations proposed by various investigations are compared and analyzed. The computation results thus obtained in the present study are compared to those of others for adjacent regions. Uncertainty analyses were then conducted.

The main conclusion of the present study is that the peak acceleration on bedrock is in the range of 75 - 115 gal for the Hong Kong region, corresponding to a probability of exceedance of 10% over a return period of 50 years. For Kowloon sites, this value is in the order of 92.7 gal. The seismic intensity of the region is rated as VII.

CONTENTS

1. REGIONAL SEISMOTECTONIC SETTING

1.1 Regional Structural Geology

The study area, for which the regional geology is analyzed herein, is bounded by latitudes 21°20′ - 23°20′ and longitudes 112°20′ - 115°40′. Rock outcrops in the study area include strata of various periods ranging from Sinian to Quaternary. Over geologic time, these strata were subject to the Caledonian Cycle, the Hercynian Cycle and the Indochina - Yenshanian Cycle of tectonic development, resulting in the three basic structural layers of a folded basement, overlying sediments and an upper stromatolithic basin. Of particular importance is the Yenshan movement, with its intense activity and scale of deformation. There were large areas of intrusion and extrusion of intermediate acidic magma, resulting in the formation of spectacular faulted metamorphic zones and a series of intermontane basins. These formed the basic features of the structural geology and geomorphology of the study area. Neotectonism in the study area is based mainly on a continuation of fault activity and differential movement of blocks, and is also characterized by the extrusion of basic magma. The crustal depth in the study area is within 20 km. Based on seismic wave velocity and density, the crust in the study area can be subdivided into three layers. The top layer consists of a surgical layer with a thickness of about 1.4 km, consisting mainly of Mesozoic to Cenozoic land sediments. The middle layer is a silica-alumina layer with a thickness of approximately 20 km, consisting of Palaeozoic strata, ancient basement and granitic rocks. The lower layer is a silica - magnesium layer, with a thickness of about 11.1 km, consisting of basaltic rocks. The interface between the middle and lower layers is the Conrad surface. The interface between the lower layer and upper mantle is the Mohorovicic surface.

1.2 Main Regional Fault Systems

Faults in the study area are well developed. There are three major fault systems on land, trending respectively EW, NE and NW (Figure 1). Offshore in the South China Sea, there are two major fault systems respectively trending ENE and NW.

The EW faults are typified by the Gaoyao-Huilai Fault. This fault is divided into a northern branch and a southern branch. The northern branch is known as the Dinghushan - Luofushan Fault, and is made up of a western segment (the Guangli - Sanshui Fault) and an eastern segment (Shougouling - Luofushan Fault). The southern branch is known as the Yunfu - Huilai Fault, and is consisted of the following four segments running from west to east respectively :

- a Yunfu to Gaoming segment known as the Dashi - Yangmei Fault, which controls the westerly distribution of Yenshanian biotite - granite and Cambrian formations;

- a Gaoming to Dongguan Shatin segment across the Pearl River Delta, overlain by Quaternary deposits, which controls the east-westerly alignment of the lower

reach of Beijiang River (Shunde - Shawan water course);

- a Dongguan Shatin to Haifeng Changpu segment known as the Zhangmutou - Changpu Fault, which features an east-westerly alignment of the Gaojiping group of volcanic rocks along the fault; and

- a Changpu to Huilai segment known as the Haifeng - Huilai Fault, which controls the east-westerly distribution of the Haifeng - Lufeng - Huilai Quarternary Basins.

The date of last motion on the Gaoyao - Huilai Fault Zone is 90,000 - 440,000 years B.P., based on thermoluminescence dating. This means that the fault zone was active between the middle period of Mid-Pleistocene and the early period of Late-Pleistocene.

Northeasterly (NE) trending faults, counting from east to west, consist mainly of the Wuhua - Shenzhen Fault, the Zijin - Boluo Fault, the Heyuan - Dongguan Fault and the Conghua - Guangzhou Fault, etc. These faults were intensely active during the Yenshanian Period, forming a series of Mesozoic - Cenozoic semi - fault-trough basins along the fault zone, such as the Guzhu Basin along the Zijin - Baluo Fault, the Heyuan - Yangcun Basin along the Heyuan - Dongguan Fault, and the Taiping Basin and Longgui Basin along the Conghua - Guangzhou Fault. Fault activity diminished somewhat during the Quaternary Period.

Northwesterly (NW) trending faults, counting from east to west, consist of the Dongguan - Shenzhen Fault, the Pearl River Estuary Fault, the Baini - Shawan Fault, the Xijiang Fault, etc. These faults were formed relatively late in time, with relatively recent activity. They control the development of surface water systems, estuaries and the Quaternary Series. For example, the Pearl River Estuary Fault and the Xijiang Fault control the east and west boundaries of the Pearl River fault depression basin. A number of Quaternary depression centres exist along the Xijiang Fault, with the Quaternary isopachs trending in a northwesterly direction. From the results of thermoluminescence dating, the last date of motion on these northwesterly trending faults is generally in the order of 100,000 years B.P. There was evident activity during the early phase of Late Pleistocene. Local segments were active even during the middle and late periods of Late Pleistocene. Hence, the NW trending faults are considered to be active faults.

The east-northeasterly (ENE) trending faults are typified by the Coastal Fault, which controlled the occurrence and evolution of the Pearl River Estuary exterior basin, facilitating the deposition of some 7000 m of Tertiary and about 250 m of Quaternary sediments. The strata isopachs depict an ENE trending. The results of marine geophysical investigation indicate that this fault cuts across the Quaternary deposits (Figure 2), reflecting activity during the Quaternary Period (Guangzhou Marine Geology Bureau 1992).

1.3 Structural Basins of Hong Kong and Vicinity

Block differential movement resulted in a number of basins and valleys. These basins are controlled mainly by faults and are hence termed fault depression basins. Figure 3 illustrates the main basins of Hong Kong and vicinity :

Duozhu Basin and Danshui Basin - Controlled by the northeasterly trending Wuhua - Shenzhen Fault; a fault basin of the semi-graben type; composed mainly of the Cretaceous system.

Longgui Basin - controlled by the northeasterly trending Conghua - Guangzhou Fault; a fault basin of the semi-graben type; composed mainly of the Lower Tertiary system.

Pearl River Delta Basin - a Quaternary Basin developed on the basis of the three Cretaceous - Tertiary red basins of Sanshui, Dongguan and Xinhui; the following six Quaternary segs evolved:

- Dongguan Seg, which evolved from the Tertiary Dongguan Basin, with a Quaternary system thickness of 35 - 45 m at its centre of deposition;

- Sanshui Seg, which evolved from the Cretaceous/Tertiary Sanshui Basin, with a Quaternary system thickness of 30 - 40 m at its centre of deposition;

- Shunde Seg, which evolved from an early Cretaceous red basin, with a Quaternary system thickness of 30 - 34 m at its centre of deposition;

- Zhongshan Seg, a new Seg formed during the Himalayan Movement, with a Quaternary system thickness of 40 - 60 m at its centre of deposition;

- Xinhui Seg, which evolved from the Cretaceous/Tertiary Xinhui Basin, with a Quaternary system thickness of 30 - 35 m at its centre of deposition;

- Doumen Seg, a newly formed Quaternary Seg with maximum depression and a Quaternary system thickness of 64 m.

Dapengwan (Mirs Bay) Basin - A Mesozoic/Cenozoic fault depression basin; controlled by the Kwai Chung - Sai Chung Fault on the east and the Kat O Chau - Chek Chau Fault on the west; composed of Upper Cretaceous conglomerate and coarse sandstone (interbedded with siltstone) of the Chek Chau Group and Tertiary

dark gray, thinly bedded siltstone and dolomitic siltstone (interbedded with mudstone) of the Ping Chau Group.

Dangan Basin - located north of the Dangan Island; controlled by the ENE trending Dangan Island Fault; composed of Lower Tertiary molasse.

Outer Pearl River Estuary Basin - located in the coastal waters outside of the Pearl River estuary; controlled by ENE trending Coastal Fault; a Cenozoic basin that evolved from Tertiary fault depression basin, with a thickness of 8000 - 10000 m of fragmentals interbedded with oil-bearing strata. This basin continued to subside during the Quaternary Period. The Wanshan Island uplift zone to the North clearly reflects the differential movement in the region.

In addition, well-developed Quaternary alluvial deposits have been founded in Fanling and Yuen Long. The results of ^{14}C and thermoluminescence dating confirm that they were formed during 16298 ± 831 to 32500 ± 490 years B.P.

1.4 Fault Activity in the Hong Kong Region

Faults in the Hong Kong region are well developed. They can be subdivided into the NE, NW and ENE trending groups (Figure 4).

1.4.1 NE Trending Faults

This group consists mainly of four fault zones, forming an integral part of the Lianhuashan Fault zone. Counting from southeast to northwest, they are respectively :

(1) The Po Toi Fault Zone

This fault passes through the strait between Dangan Island and Po Toi Island, extending northeasterly to south of the Huidong Pinghai Peninsula, Haifeng and then Dabu, forming the southeastern branch of the Lianhuashan Fault Zone. This fault zone trends NE 50°, dips SE at an angle of dip of 60° - 70°. The southwestern segment of this fault zone is intersected by the ENE trending Dangan Island Fault.

(2) The Lai Chi Kok - Tolo Channel Fault zone

This fault zone originates in Lai Chi Kok, Kowloon to the southwest, trending NE and extending into the Shatin Sea via Shatin, being offsetted by NW trending faults. It extends southwesterly into the East Lamma Channel, being intersected

by the Lau Fau Shan - Lamma Channel Fault. This fault zone trends NE 40° - 50°, dipping SE at a dip angle of 75° - 80°.

(3) The Sha Tau Kok - Pui O Wan Fault Zone

This fault zone trends NE 30° - 50°, dipping NW at a dip angle of 60° - 70°. It controls the geologic evolution of the strait and valleys, and is composed of the following four group of faults :

a. Sha Tau Kok - Sham Tseng Fault, which runs southwesterly from Sha Tau Kok via Lam Tsuen Valley to Sham Tseng.

b. Ma Tseuk Leng - Shiu Lam Fault, which runs southwesterly from Ma Tseuk Leng in the North to Wo Hop Sek, Tai Lam Chung Reservoir and Siu Lam.

c. Yam O Wan - Pui O Wan Fault, which runs southwesterly from Yam O Wan on the north slope of Lantau via Mui Wo to Pui O Wan on the south slope of Lantau.

d. Tung Chung - Shek Pik Fault, which runs southwesterly from Tung Chung on the north slope of Lantau via Muk Yue Shan to Shek Pik in southern Lantau.

(4) The Lo Wu - Tuen Mun Fault Zone

Located in northwest New Territories and on the southeast coast of Shenzhen Bay, this fault zone extends northeasterly to Meixian via Wuhua, and southwesterly to south of Macau to Gaolan Island. It forms the northwestern branch of the Lianhuashan Fault Zone, and is composed of the following five groups of fault :

a. San Tin Fault, which trends NE 40° and dips NW with a dip angle of 35° - 50°.

b. Lo Wu Fault, which runs from Tuen Mun via Yuen Long to Lo Wu, consisting of a subset of parallel faults such as the Wang Chau - Shan Ha Tsuen Fault and the Chu Wong Leng - Lam Kau Fault, controlling the geologic evolution of the Deep Bay, the Yuen Long Plain and the Tuen Mun Valley.

c. Tuen Mun Fault, which extends from Tuen Mun to the month of the Shenzhen River, with a trending of NE 15° in its southwest segment to NE 40° in its northeast segment.

d. Tsing Shan Fault, which originates in Pak Kok in west Tuen Mun, extending via east Tsing Shan to the mouth of the Shenzhen River. The southwest segment of the fault trends NE 10° - 20°, dipping NW with a dip

angle of 40° - 50°. Its northeast segment trends NE 50° - 55°, dipping at 50° - 67°. Thermoluminescene dating of a sample of fault material collected on the west beach of Wu Tip Wan (Co-ordinates 1316, 2552) gave an age of 265500 ± 21000 years B.P. (Table 1).

e. Lau Fau Shan Fault, which trends NE 60° and dips NW with a dip angle of 51° - 67°. A quartz vein of 20 m width and 4 km length was found along the fault between Lau Fau Shan and Tsim Bei Tsui.

It should be noted that geoscientists have different views on the use of the thermoluminescene dating method for determining the age of motion on faults.

1.4.2 ENE Trending Faults

This group consists of the following two fault zones, counting from north to south :

(1) Tsing Shan Wan - Tai Po Hoi Fault Zone

This fault zone is, in turn, made up of the following two faults :

a. Tsing Shan Wan - Ho Pui Reservoir Fault, which trends NE 65° - 70° from south Tuen Mun via Tai Lam Chung Reservoir to Ho Pui Reservoir. The western segment of this fault offsets the NE trending Tsing Shan fault and Tuen Mun Fault. A sample of fault material collected 900 m south of Nam Hang Pai in Yuen Long (Co-ordinates 2170, 3016) gave an age of 94700 ± 8100 years B.P. from thermoluminescene dating. Likewise, a sample collected on the west beach of Wu Tip Wan (Co-ordinates 1316, 2552) gave an age of 110,800 years B.P. (Table 1).

b. Tung Chung - Tai Po Hoi Fault, which originates in Tung Chung on western Lantau Island, extending easterly along northern Lantau via Tsuen Wan to Tai Po Hoi. A sample of fault material collected in one of the small parallel faults in Yim O Tuk on northern Lantau (Co-ordinates 1960, 2072) gave an age of last motion of 82000 ± 6800 years B.P., based on thermoluninescene dating.

(2) Dangan Island Fault Zone

Located north of Dangan Island, this fault forms part of the Coastal Fault, extending in an NE 70° direction and controlling the depositional basin in Dangan Strait.

1.4.3 NW Trending Faults

The northwesterly trending faults are highly developed in the study region. They are widely distributed within the region. There are three main fault zones which are located respectively on the east side and west side of the Kowloon Peninsula.

(1) Kat O Chau - Chek Chau Fault zone

Located on western Tai Pan Wan (Mirs Bay), consisting mainly of two faults:

a. Kai Kung Tau - Yeung Kok Tau Fault, which trends NW 310° from Kai Kung Tau on Kat O Chau to Yeung Kok Tau on Chek Chau. Subsidence of the northeast wall of the fault led to the formation of the Cenozoic depositional basin in Tai Pan Wan.

b. Kat O - Kung Chau Fault, which originates in Sham Chung on Kat O Chau in the north, extending southeasterly through Wang Mun Hoi, Jig Mun Tau, Wong Chuk Kok Hoi, Chek Chau Hau to Sha Pai. Thermoluminescene dating of a sample of fault material collected in Wong Nai Chau (at co-ordinates 5016, 4466) gave an age of last motion of 19600 ± 16900 years B.P.

(2) Lau Fau Shan - East Lamma Channel Fault Zone

The fault zone is located in Lau Fau Shan, Sham Tseng and Lamma Island. It consists of a series of parallel faults.

The following results were obtained from thermolumisescene dating: 105100 ± 8700 years B.P. for a Tai Tong, Yuen Long sample of fault material (Co-ordinates 2100, 2942); likewise, 91100 ± 7500 years B.P. for Tsing Lung Tau, Sham Tseng (Co-ordinates 2356, 2594); 93900 ± 7900 years B.P. for Cheung Tsui, Ma Wan (Co-ordinates 2465, 2370); 222200 ± 17800 years B.P. for Mo Tat Wan, Lamma Island (Co-ordinates 3314, 0786); and 33300 ± 2700 years B.P. for Yim O Tuk, Lantau Island (Co-ordinates 1970, 2072).

(3) Pearl River Month - Lantau Fault Zone

Within the study region, this fault zone outcrops west of Tung Chung on the Lantau Island, consisting of three parallel faults :

a. Tung Chung - Cheung Sha Beach Fault, which runs from Tung Chung in the North via Pak Kung Au to Cheung Sha Beach to the South. Thermoluminescene dating of a sample of fault material collected in a ditch at milestone 4 on Tung Chung Road (Co-ordinates 1243, 1174) gave an age of 101000 ± 8600 years B.P.

b. Sham Wat Wan - Sz Tsz Tau Shan Fault, which is located between Sham Wat Wan and Lo Kei Wan on Lantau Island.

c. Tai O - Tai Long Wan Fault, which is located between Tai O and Tai Long Wan on Lantau Island. Thermoluminescene dating of sample of fault material collected at Ngau Kwo Tin (Co-ordinates 0524, 1106) gave an age of 278700 ± 23000 years B.P.

1.4.4 Main Characteristics of Fault Activity

Faults with activity within the last 100,000 year are considered in this report to be active faults. Among the three groups of faults described above, the NW and ENE trending faults are considered to be the main active faults in the Hong Kong region. Their main tectonic features are as follows :

(1) The ENE trending faults are mainly distributed on Lantau Island and in the Tolo Channel and Dangan Island vicinities. The NW trending faults are located mainly on east and west Kowloon Peninsula, forming a rather dense zone of NW trending faults of considerable scale. The NW trending faults are, however, less prominent than the ENE trending faults in scale. Each NW trending fault ranges in length from a few km to a few tens of km.

(2) The faults often form negative relief geomorphologically, e.g. straits and valleys, thus controlling the evolution of water systems.

(3) Under the action of the prevailing tectonic stress field, the NW and ENE trending faults form a conjugate fault system. Thus, the NW trending faults show signs of left - rotational compression - shear, while ENE trending faults exhibit right rotational tension-shear features. This was observed in the field, e.g. the left rotational slickensides on the NW trending fault at Tai Tong, and simultaneously the left rotational displacement of an NE trending quartz vien due to an NW trending fracture.

(4) Both the ENE and the NW trending faults show signs of multi-stage activity, particularly the later, which generally feature two stages of calcite vein or quartz vein intrusion.

(5) Thermoluminescene dating indicated an age of last motion in the order of 80,000 - 100,000 years B.P., implying that fault activity continued to the early stage of Late Pleistocene.

2. SEISMIC ACTIVITY OF THE HONG KONG REGION

2.1 Seismicity of the Southeastern Coastal Seismic Belt

2.1.1 Spatial Distribution of Historical Earthquakes with $M_s \geq 4¾$

The study region forms part of the middle segment of the Southeastern Coastal Seismic Belt of China. There were 119 earthquakes recorded in the region with $M_s \geq 4¾$ since 1067

A.D. (Figure 5). These included 84 events with M_s between 4¾ and 5¼ (intensity VI); 21 events between 5½ and 5¾ (intensity VII); 7 events between 6 and 6½ (intensity VIII); 4 events between 6¾ and 7 (intensity IX) and 3 events between 7.3 and 7.5 (intensity X). These events largely trend in a northeasterly (NE) to east-northeasterly (ENE) direction. They are distributed along the inland zone of Huichang - Heyuan - Guangzhou and the coastal zone of Shantou - Yangjiang, which form the inner and outer zones of the Southeastern Coastal Seismic Belt respectively (Figure 6). The outer zone is relatively more active than the inner zone. In the past several centuries, events of $M_s \geq 7$ occurred only in the outer zone, along with several M_s 6 events. The largest event in the inner zone did not exceed M_s 6¾. There were also few M_s6 events in the inner zone. In the Shantou - Huichang, the Pearl River Delta and the Zhanjiang - Lingshan areas, seismicity also depicts a northwesterly (NW) trend, reflecting a close relation between seismicity and NE, ENE and NW trending active faults.

2.1.2 Temporal Sequence of Seismicity

Seismicity in the Southeastern Coastal Seismic Belt is characterized by periodic cycles of intense activity and low activity alternately. From records of historical seismicity, there were two cycles of seismic activity since 1400 A.D. The first cycle occurred between 1400 and 1710 A.D., while the second cycle began in 1711 and has yet to be completed. Each cycle lasts approximately 320 years (Figure 7). From a further analysis of the complete process of strain buildup and relief for seismicity, each cycle can be subdivided into four stages of development. The first stage is the strain buildup stage, lasting 73 - 112 years, with events of $M < 6$ only. The second stage is the precursory relief stage, lasting 112 - 155 years, with the possible occurrence of events of $6 \leq M < 7$. The third stage is the main relief stage, lasting 4 - 6 years, with events of $M \geq 7$. The fourth stage is the residual relief stage, lasting 88 - 94 years, with the possible occurrence of M 6 - 6¾ events. Presently this seismic belt is at the residual relief stage of the second cycle. It is expected that the second cycle will last until the year 2015.

2.2 Seismicity of the Hong Kong Region

2.2.1 Influence Fields of Several Relatively Large Earthquakes in Surrounding Region (Figure 8)

(a) M 5¾ Event, Dangan Islands, June 23, 1874

Based on historical records of the felt area, the epicenter is believed to be located in the coastal waters to the east of the Dangan Islands. The resulting intensity in Hong Kong was VI.

(b) M 5½ Event, Modaomen, August 12, 1905

In the earthquake catalogue of China, this event was originally rated as an M 5 event epicentred in Macau. During the seismic hazard study for the Daya Bay Nuclear Power Project, the seismic intensity of this event was re-assessed based on historical records. The epicentre was determined to be located offshore of

Modaomen, and the event was rated as M 5½ It resulted in an intensity of VI in Macau, with corresponding damage. The event was clearly felt in Hong Kong.

(c) M 6 Event, Honghau Bay, May 15, 1911

From historical records, the epicentre of this event is located offshore at approximately latitude 22.5° and longitude 115.0°. The event led to intensity VII damage in Gongping, Haifeng County. The intensity in Hong Kong was estimated to be V. To this date, M 2 - 3 events are still frequently recorded in the area.

(d) M 7.3 event, Nan Ao, February 13, 1918

The event is the largest event in Guangdong in the past century, with an epicentral intensity of X. Seismic motion was clearly felt in Guangzhou at more than 400 km away from the epicentre. The intensity recorded in Hong Kong was VI.

Besides the above, the M 6.1 event of Heyuan in 1962 and the M 6.4 event of Yangjiang in 1969 were both clearly felt in Hong Kong, with an intensity in the IV - V range.

2.2.2 Seismicity of the Hong Kong Region

Since the commissioning of the Guangdong Provincial Seismograph Network in 1970, a total of 212 events with Ms ≥ 2.0 were recorded up to 1995 in Hong Kong and its surrounding region, bounded by N 21° - 24° and E 112° - 116° (Figure 9). On land, reservoir - induced earthquakes occurred in the Heyuan district at a relatively high frequency. Otherwise, the seismic events are distributed mainly in the coastal region, i.e. Haifeng - Shenzhen - Toishan - Enping and the area to the south. This coastal seismic zone displays an ENE trending of seismicity. Hong Kong is situated within this zone. Hence, the level of microseismicity is higher in the Hong Kong region than in many cities and counties within the Pearl River Delta.

As part of the present study, the study team carried out a re-assessment of the pertinent earthquake data recorded by the Guangdong Provincial Seismograph Network and the local seismograph network of the Royal Observatory of Hong Kong, to accurately determine the epicentral locations of near-field micro-seismic events. An earthquake catalogue was thus newly established for the Hong Kong region bounded by latitudes 22°00′ - 23°00′ and longitudes 113°45′ - 114°45′ , beginning in 1972, with all blasts removed from the catalogue. A total of 53 events with $M_L \geq 1.8$ occurred within this region during the period 1972 - 1995, including two relatively minor events (Table 2). These include 19 events between 1972 and 1978 (average of 2.7 events per year); 11 events between 1979 and 1989 (average of one event per year); and 23 events between 1990 and 1995 (average of 3.8 events per year). The frequency of microseismicity has increased somewhat since 1990, but there has been little change in magnitude. This is consistent with the overall picture in the larger region since 1989,

which also features an enhancement in the frequency of microseismicity. However, seismicity in the Hong Kong region appears to be relatively diffused in distribution, with no sign of concentration at a specific point or in a specific zone. The microseismic events were mainly distributed in Shenzhen, the coastal waters of Lantau Island and round Tai Pang Wan (Mirs Bay) (Figure 10). These areas are also characterized by a relatively advanced stage of development of NW and ENE trending faults, thus reflecting a relationship between the two fault systems and local microseismicity, consistent with the age of faulting discussed in the previous chapter.

2.3 Trend Assessment for the Southeastern Coastal Seismic Belt

The Southeastern Coastal Seismic Belt is currently at the residual relief stage of the second cycle of seismic activity. This stage is expected to last until approximately 2015. While there will be some fluctuations in the level of seismic activity in the future, the overall level should be similar to that since 1920's. The maximum credible event for the next few decades is expected to be in the order of M 6 - 6¾. There will also be some periodic variations in seismic activity during this residual relief stage. Three periods of activity initiation can be identified for this stage. The third period of activity initiation occurred in 1989. The previous two periods of activity initiation were characterized by two M6 events, which occurred respectively in Heyuan (1962) and Yangjiang (1969). A pair of M 6 events (M 6.1 and M 6.2) occurred in the Beibuwan area of the outer zone respectively at the end of 1994 and early 1995. It is possible that another M 6 event may occur in another part of this seismic belt. However, the possibility of an M 7 or larger event occurring in the seismic belt during the residual relief stage is low. It is possible that several M5 events may occur in both the outer and inner zones of the Southeastern Coastal Seismic Belt.

3. POTENTIAL SOURCE ZONES FOR HONG KONG AND VICINITY

3.1 Introduction

A potential source zone (PSZ) represents an area in which damaging earthquakes can occur in the near future. It can be determined by synthesizing the analyses of relevant information including the geological structures, geophysics, crustal deformation and seismic activity of a region. The two fundamental principles of potential source zoning can be described as follows :

1) For an area where earthquakes had occurred in the past, it is highly pobable for earthquakes of similar magnitudes to occur again;

2) For areas of similar geological conditions, their seismic activities would also be similar.

In the process of identifying potential source zones with different magnitude values, it is also necessary to take into account the specific geological and structural conditions of a region. In general, the maximum magnitude of historical earthquakes can be used as the upper

bound magnitude of a potential source zone. If the maximum magnitude cannot represent the seismic activity trend, the upper bound magnitude can be estimated by adding 0.5 to 1.0 to the maximum magnitude value.

Based on the above principles, more than one hundred potential source zones were identified in the Southeastern Coastal Seismic Belt of China during the process of compiling the Seismic Intensity Zoning Map of China (1990). The present investigation adopted the zoning plans but adjusted and modified the potential source zones for the Hong Kong region. The potential source zones of substantial influences to Hong Kong are briefly described in the following (Figure 11).

3.2 Potential Source Zones for Hong Kong and Vicinity

3.2.1 Guangzhou Potential Source Zone (30)

This PSZ is located along the EW trending Gaoyao--Huilai Fault Zone. The alignments of the near EW trending Guangli--Sanshui Fault and Shougouling Fault pass through the entire zone. Besides, This PSZ also contains the NE trending Conghua- Guangzhou Fault and the NW trending Baini--Shawan Fault. These faults were still active during the Quaternary period. In particular, the rejuvenation of NW trending faults led to their activity until the late period of the Late Pleistocene epoch. The Sanshu Basin in this zone has a Middle Cenozoic Group of approximately 3000m thickness and is the deposition center during the Quaternary period with a 40m thick Quaternary System. Vertical deformation measurements indicate the zone has been subsiding. In 1372, 1683, 1824 and 1915, earthquakes of M4¾ to 5 occurred in the Guangzhou, Nanhai and Panyu areas, respectively. In recent years, microseismic events frequently occur in the zone. As a result, the zone could have an M6 event as its upper bound.

3.2.2 Dongguan Potential Source Zone (17)

This PSZ is located in the Dongguan Basin. The Dongguan Basin is dominated by the NE trending Shaowu--Heyuan Fault, the ENE trending Shougouling--Luofushan Fault and Pearl River Estuary Fault. The basin has a Quaternary System of about 35m thickness. The basin is actually an end-in-tension basin dominated by the three faults. The zone has no records of historical damaging earthquakes. In recent years, there are few small seismic events in the zone. As a result, the zone has been assigned an M5.5 event as its upper bound.

3.2.3 Huizhou Potential Source Zone (19)

This PSZ is located in the Boluo, Huizhou and Huidong districts of Guangdong Province and is oriented along the NW direction. The NW trending Huizhou--Yanzhou Deep Fault passes through the entire zone longitudinally. The NE trending Zijing--Boluo Fault passes through the zone transversely. On the south boundary, there is the NE trending Wuhua--Shenzhen fault. Huizhou is a basin formed during Middle Cenozoic Era. There is no record of damaging earthquakes in the zone. Recently, there have been a few small seismic events. As a result, the zone could have been an M 5.5 event as its upper bound.

3.2.4 Haifeng Potential Source Zone (31)

This PSZ is traversed by the NE trending Lianhuashan Fault Zone, the EW trending Zhangmutou--Changpu fault and the ENE trending Daya Bay--Huilai Deep Fault. The Haifeng and Lufeng area are a Quarternary trough with an EW orientation. The Quarternary system can be up to 50 m thick. Two M 4¾ events occurred in Haifeng in 1963 and 1974 respectively. More recently, a series of small seismic events or seismic swarms have occurred in the Meilong and Houmen areas. Hence an upper bound of M 6 has been assigned to this PSZ.

3.2.5 Huiyang Potential Source Zone (33)

This PSZ is located in the Huiyang and Huidong cities of Guangdong Province and is oriented in the NW direction. On its north side, there is the NE trending Wuhua--Shenzhen Fault. On its south, the ENE trending Coastal Fault. On its east boundary, the NW trending Huizhou--Yanzhou Fault, which is adjacent to the Haifeng potential source zone. On its west boundary, the NW trending Kwai Chung-Sai Chung Fault. In the PSZ, there are the NNW trending Daya Fault and the ENE trending Daya Bay--Huilai Fault. Along the Wuhua--Shenzhen Fault, there are the Duozhu and Danshui Basins formed during the Mesozoic Era to Cenozoic Era.

There is no record of historical damaging earthquakes. Since the establishment of a seismograph station, a series of microseismic events have been recorded in the areas of Baihua, Xiachong and Daya Bay. The upper bound magnitude is taken as M6.0 for this zone.

3.2.6 Dapengwan Potential Source Zone (32)

This PSZ has the NW trending Dapengwan Fault as its eastern boundary, being adjacent to the Huiyang potential source zone. Its western boundary is the Luohu--Sai Kung Fault. The NW trending Kan Tau Tsuen--High Island Reservoir Fault Zone passes through its central area. This fault zone together with the Kwai Chung -- Sai Chung Fault dominated the development of the Dapengwan Basin in the Middle Cenozoic Era. As a result of fault activity, the basin developed up to several km thick formations of the early Cretaceous system and the Chek Chau Formation of Eogene system. More recently, the zone experienced microseismic activity. The upper bound magnitude is taken as 6.0 for this zone.

3.2.7 Shenzhen Potential Source Zone (23)

This PSZ is located in the region from Shenzhen to Hong Kong and is oriented in the NW direction. Its eastern boundary is the NW trending Sha Tau Kok sea--High Island Reservoir Fault, which is adjacent to the Dapengwan potential source zone. Its western boundary reaches the east branch of the Pearl River Estuary Fault Zone, i.e., Luogang--Taiping Fault and Laufushan--East Lamma Fault. Its north is the Wuhua--Shenzhen Fault. Its south, the Dapu--Haifeng fault. There is no record of historical damaging earthquake. In recent

years, small earthquakes frequently occur to the west of Shenzhen and Kowloon. The upper bound magnitude is then defined as 5.5.

In the Seismic Intensity Zoning Map of China (1990), the Dapengwan and Shenzhen potential source zones are combined together as one potential source zone with an upper bound magnitude of 5.5. In the present investigation, it was found that the active NW trending faults and the current small seismic events are mainly located in Dapengwan area and that these activities were almost not observed in the central area of Kowloon Peninsula. As a result, the combined potential source zone was separated into the Dapengwan (32) and Shenzhen (23) potential source zones with upper bound magnitudes of 6.0 and 5.5, respectively.

3.2.8 Lantau Island Potential Source Zone (38)

This PSZ is located in the areas of Pearl River Estuary, Lantau Island and the adjacent coastal waters. It is oriented in the NW direction. Its eastern boundary is the NW trending Luogong--Taiping Fault and Laufushan--East Lamma Channel Fault, which is adjacent to the Shenzhen potential source zone. Its western boundary is the NW trending Qiao Island--Guishan Island Fault. Its north side is an extension of the NE trending Wuhua--Shenzhen Fault. On the north side of Lantau Island, there is the ENE trending Tsing Shan Bay--Tolo Channel Fault. Furthermore, Lantau Island has a series of NW trending faults such as Penny's Bay Fault, Tung Chung--Cheung Chung Fault, Shem Wat Bay Fault, and Tai O Fault. Based on thermoluminescence age dating, the most recent activities of these faults occurred about 90 to 270 thousand years ago, i.e., from the late period of the Middle Pleistocene epoch to the early period of the Late Pleistocene epoch. Recently, the zone experienced some microseismic activity. The upper bound magnitude of the potential source zone is then taken as 6.0.

3.2.9 Pearl River Estuary Potential Source Zone (48)

The PSZ is located in the areas of Zhuhai and Wanshan Islands and is oriented in the NW direction. Its eastern boundary is the Qiao Island--Guishan Island Fault, which is adjacent to the Lantau Island potential source zone. Its western boundary is the NW trending Xijiang Fault. Its north boundary reaches the NE trending Cuiheng--Tiantou Fault (or the Wuguishan South Fault). Its central part has the ENE trending Hengqin Island--Shangchuan Island Fault. In the zone, the NW and ENE faults are more active. They were active during the middle and late periods of the Late Pleistocene epoch. In 1905, there was an M 5.5 event which occurred in Modaomen. In recent years, microseismic events have occurred frequently. The upper bound magnitude is thus taken as 6.5.

In the Seismic Intensity Zoning Map of China (1990), Lantau Island (38) and Pearl River Estuary (48) potential source zones were also combined as one potential source zone with an upper bound magnitude of 6.5. In the present investigation, it was found that the Lantau Island and Dapengwan potential source zones have relatively similar tectonic features and microseismicity patterns. Consequently, it is prudent to define the upper bound magnitude of the Lantau Island (38) potential source zone as 6.0 and separate the combined potential source zone into two independent zones.

3.2.10 Zhongshan Potential Source Zone (35)

This PSZ is located in the Zhongshan and Shunde areas of Guangdong Province. The Luogang--Taiping Fault forms the zone's eastern boundary. The Xijiang Fault is its western boundary. The eastern extension of the EW trending Dashi--Yangmei Fault is its northern boundary, which is adjacent to the Guangzhou potential source zone. The Cuiheng--Tiantou Fault is its southern boundary. A Quarternary depression named the Zhongshan Depression was developed in the zone. The central position of the Quarternary system has a thickness of 35 m. Historically, there were many perceptible earthquakes in the zone. Recently, there were few microseismic events. The upper bound magnitude is then taken as 6.0.

3.2.11 Jiangmen Potential Source Zone (22)

This PSZ is located in the areas of Jiangmen, Xinhui, Kaiping and Taishan of Guangdong Province. It has a triangular shape in plane with an orientation in the NE direction. Its eastern boundary is the Xijiang Fault. Its western boundary is the Changcheng--Hailing Fault. In 1656, an M 4¾ event occurred in He Cheng. The upper bound magnitude is thus defined as 5.5.

3.2.12 Guanghai Potential Source Zone (39)

This PSZ is located in the areas of Guanghai, Yamen and Modaomen and is oriented in the ENE direction. On the north side, there is the Cuiheng--Tiantou Fault which was active about 70 thousand years ago (i.e., during the early period of Late Pleistocene Epoch). On the south side, the Hengqin Island--Shangchuan Island Fault was active about 170 thousand years ago (i.e., during the late period of Middle Pleistocene Epoch). In recent years, there were microseismic events in the region of Yamenkou and Guanghai Bay. The upper bound magnitude is taken as 6.0 for this PSZ.

3.2.13 Gaolan Island Potential Source Zone (40)

This PSZ is located in the areas of Shangchuan Island, Gaolan Island and the surrounding coastal region, and is oriented in the ENE direction. Its northern boundary is the Hengqin Island--Shangchuan Island Fault, being adjacent to the Guanghai potential source zone. Its eastern boundary is the Xijiang Fault. Its southern boundary reaches the Coastal Fault Zone. These faults were active in the Quaternary Period. In recent years, there was some microseismic activity. The upper bound magnitude is taken as 6.0.

3.2.14 Outer Gaolan Island Potential Source Zone (83)

This PSZ is located in the southern coastal region of Gaolan Island and has a major orientation in the ENE direction. It is located on the Coastal Fault Zone where faulting activities were evident during the Quarternary Period. This fault zone dominates the boundary between the sea and the land. Its east side ends in the Xijiang Fault. There was some

microseismic activity recently in the Coastal Fault Zone. The upper bound magnitude is taken as 6.5.

3.2.15 Dangan Island Potential Source Zone (99)

The ENE trending Coastal Fault passes through the entire zone longitudinally. The Coastal Fault is not only an active fault since the Quarternary period. It is also the boundary of neotectonic zoning. Its north side is the Wanshan Islands uplift zone where sea eroded cliffs have risen up to 180 m. Its south side is the depression area of the Pearl River Estuary outside basin with a late Tertiary system of up to 7000m thickness and a Quarternary system of up to 250 m thickness. These observations indicate that the zone is a site of strong differential crustal movement associated with neotectonic activities.

The zone is the juncture of the ENE trending Coastal Fault Zone and the NW trending faults. This tectonic setting is very similar to that of the Nanao--Shantou region where an M 7.3 event occurred. Furthermore, both regions are located in the outer zone of the Southeastern Coastal Seismic Belt of China. In the Seismic Intensity Zoning Map of China (1990), the two regions have an intensity rating of VIII. These two regions thus have the highest intensity rating in Guangdong Province (Figure 13). In 1874, an M 5¾ earthquake occurred at the eastern end of the Dangan Island. This event caused damages in Hong Kong corresponding to an intensity of VI. In recent years, a series of seismic events have occurred along the Coastal Fault Zone. Previous investigations considered the upper bound magnitude of the Dangan Island potential source zone to be 7.5. The present investigation found that the zone has the tectonic setting for an M 7 event to occur, but considered an upper bound magnitude of 7.5 to be on the high side. Adjacent potential source zones in the outer zone such as the Honghai Bay (82) and the Outer Gaolan Island (83) have 6.5 as their upper bound magnitude values. It is reasonable that the Dangan Island potential source zone should have an upper bound magnitude which is 0.5 higher than those of the adjacent potential source zones. As a result, the upper bound magnitude is defined as 7.0 for the Dangan Island PSZ.

3.2.16 Honghai Bay Potential Source Zone (82)

This PSZ is located in the south sea region of Daya Bay and Honghai Bay and is oriented in the ENE direction. It is also located in the Coastal Fault Zone. Its western boundary is the Dapengwan fault and is adjacent to the Dangan Island potential source zone. In 1911, an earthquake of magnitude 6 occurred in Honghai Bay. In recent years, there have been some microseismic events. The upper bound magnitude is taken as 6.5.

3.3 Seismological Parameters for the Potential Source Zones

3.3.1 General

In seismic hazard analysis, it is necessary to identify seismic zones and potential source zones and to determine the seismological parameters. Hong Kong forms a part of the Southeastern Coastal Seismic Belt of China. This seismic belt can be further divided into an

outer zone and an inner zone according to the characteristics of seismic activity and regional geological structures. The Hong Kong region is located within the inner zone, being also adjacent to the outer zone.

The outer zone is characterized by relatively strong seismic activity. Historically several earthquakes of M 7 and above and many earthquakes of M 6 and above had occurred in this zone. The outer zone is located in the coastal region. It is possible that small events might have been omitted in both the historical earthquake records and modern seismic recording.

The inner zone is characterized by relatively low seismic activity. Its frequency and intensity of seismic activity are much lower than those of the outer zone. There is no record of any events of M 7 and above in the inner zone. There are only records of events of M 6 or there above. Moreover, the inner zone is equipped with relatively abundant seismic records and a modern seismic monitoring system with relatively high detection capability and accuracy. It is therefore almost impossible to miss out any seismic events that had occurred in the inner zone recently.

Based on the foregoing, the seismological parameters of the relevant seismic zones and potential source zones are defined as follows, in order to carry out seismic hazard analysis and calculations for Hong Kong region.

3.3.2 Lower Bound Magnitude

Lower bound magnitude is the minimum magnitude with evident earthquake effects. All events that had occurred in the Hong Kong region in the past are of shallow focal depth. Hong Kong has had several historical earthquakes of magnitude 4 which caused slight damage to buildings. As a result, the study team selected 4 as the low bound magnitude in carrying out the calculations for the seismic hazard analysis. Besides, magnitude 4 is also used as the lower bound magnitude in performing statistical analysis of the b-value and the average annual occurrence rate.

3.3.3 Background Magnitude

Background magnitude is the maximum magnitude of seismic events that can occur outside any potential source zone. Background magnitudes are defined as 5 and 5.5 for the inner and outer zones region respectively. In other words, any area in the inner and outer zones could experience an event of magnitude up to 5 and 5.5, respectively.

3.3.4 b-value in the Relationship between Magnitude and Frequency

The b-value reflects the proportional relationship between large and small earthquake frequencies in a seismic zone. It has a direct relation with the probability of future earthquakes. The relationship between magnitude (M) and frequency (N) can be written as follow :

$$\log N = a - bM \quad \text{.....(3.1)}$$

Usually the values of a and b in the above equation are determined using the historical earthquakes that occurred during a certain period of time. Small to medium magnitude earthquakes were often omitted in the historical records, with large magnitude earthquakes accounting for a major portion of the records. This bias will result in a lower b-value from a statistical analysis using equation (3.1). On the other hand, modern seismic monitoring technology can record a much more complete spectrum of seismic events. However, these instrumental records were obtained over a relatively short time frame. Medium to large earthquakes occupy only a very limited portion of the recorded data. This bias in contemporary seismic data will result in a higher b-value from the statistical analysis using equation (3.1). Thus, these two approaches cannot find a b-value which accurately represents the characteristics of seismic activity of a region. In order to overcome this bias in the data, the project team adopted a statistical method which calculates b-values for recorded events over different time periods and with different magnitudes. This method can be described as follows.

Step 1: All seismic events recorded since 1600 are grouped into the following three groups according to their magnitudes and time periods of occurrence. Table 3 illustrates the data base of recorded events used in the analysis.

Group a: From 1800 to 1995, historical earthquakes with $M \geq 6.0$

Group b: From 1900 to 1995, historical earthquakes with $M \geq 5.0$

Group c: From 1970 to 1995, seismic events with surface-wave magnitudes $(Ms) \geq 4.0$.

Step 2: Using equation (3.1), b-values can be statistically calculated for each of the three groups for both the inner and outer zones (Figure 14).

Step 3: Carrying out a regression analysis of "b" for both inner and outer zones.

The above calculation results in a b-value of 0.80 and 0.56 respectively for the inner and outer zones.

In an earlier seismic hazard analysis of the Hong Kong region, Pun and Ambraseys (1992) suggested a b-value of 0.75 for a large study region (about 430,000 km^2) including the inland areas of Guangdong Province and the coastal area of South China Sea. This region covers the inner and outer zones defined in this report.

3.3.5 Average Annual Occurrence Rate

The average annual occurrence rate refers to the number of earthquakes with $Ms \geq 4.0$ which occur every year in the inner zone or outer zone. This value has a substantial influence on the results of seismic hazard analysis. The statistical method adopted in the calculation of b-value is used again to determine the average annual occurrence rate for the inner and outer

zones. This calculation results in average annual occurrence rates of 1.151 and 0.873 for the outer zone and inner zone, respectively.

Current trends of regional seismicity indicate that the region is within a relatively active period of seismic occurrence. This situation will likely continue for many more years. It is possible that the seismic activity in the outer and inner zones will be more intense than those obtained from multi-year average results. Consequently, the above two values of the average annual occurrence rates are increased by 20%. This increase results in 1.38 and 1.05 as the average annual occurrence rates for the outer and inner zones, respectively. Table 4 illustrates the average annual occurrence rates and recurrence ratios for events of different magnitudes in the Southeastern Coastal Seismic Belt of China.

3.3.6 Spatial Weight of Magnitude Distribution in Potential Source Zones

The distribution of seismic activity in the potential source zone is non-uniform. It is therefore necessary to estimate the spatial weight of magnitude distribution in every potential source zone. (Further details of this process can be found in Section 5.1 of this report). The five factors in estimating the spatial weight of different are as follows :

1) Reliability of potential source zone.

2) Results of medium to long term earthquake forecasting.

3) Regional features of seismic activity.

4) Area size of the potential source zone.

5) Orientation and weight of active faults which cause earthquakes.

Based on the above factors, a spatial weight matrix was obtained for each of the potential source zones identified in the Southeastern Coastal Seismic Belt of China. Those of substantial effect to the seismic hazard analysis of Hong Kong region are listed in Table 5.

4. SEISMIC GROUND MOTION ATTENUATION MODELS

4.1 Attenuation of Ground Motion

Once an earthquake occurs, seismic wave will propagate from the source to the external region. The further the distance away from the source (where seismic energy is released), the smaller would be the amount of seismic energy and amplitude of ground motion. This process is known as attenuation. It is one of the most important tasks in seismic hazard analysis to determine the attenuation model of seismic ground motion. Attenuation of ground motion is usually represented and modelled using the attenuation equations of seismic intensity and peak ground acceleration (PGA).

Since China including Southern China has accumulated abundant records of historical earthquakes, the attenuation equations of seismic intensity can be determined using such records of historical earthquakes and reports from felt areas of recent strong earthquakes. There are, as yet, few strong motion instruments installed in Southern China. Hence, there are very limited ground motion records of strong earthquake events. It is very difficult to obtain the attenuation equations of PGA directly from the seismic records of strong earthquakes. Consequently, the attenuation equations of bedrock PGA in the subject region are determined using the deductive method suggested by Hu (1984). Firstly, the attenuation equations of bedrock PGA obtained for Western USA are adopted and used in this method. There is an abundance of ground acceleration data for the Western USA, thus giving a high degree of reliability to the resultant attenuation equations. In order to apply the attenuation equations of Western USA to Southern China, modifications are made using the records of historical earthquakes and the macroscopic data of recent strong earthquakes in Southern China and by comparing the geological conditions and seismic activities of the two regions. This process results in attenuation equations of PGA applicable to Southern China.

4.2 Attenuation Equations of Seismic Intensity

Different regions may have very different source features, propagation media and geological conditions. Therefore different regions may have different attenuation laws of seismic intensity and acceleration.

During the past decades, a number of researchers have investigated the historical earthquakes of Southern China and obtained a number of isoseismal maps of seismic intensity. Based on given isoseismal maps, attenuation equations of seismic intensity can be obtained for the Southern China region using either circular or elliptical attenuation models.

Based on the historical earthquake data compiled by Huang Riheng (1996) and the circular attenuation model, the present study team obtained the following attenuation equation of seismic intensity for Southern China.

$$I = 4.1839 + 1.4372M - 1.6099\ln (R + 14) \qquad \sigma_I = 0.515 \qquad (4.1)$$

Similarly, using the elliptical attenuation model, the present study team obtained the following equations :

$$\text{Long axis } I_l = 4.85474 + 1.31271M - 1.49944\ln (R + 15) \qquad \sigma_I = 0.515 \qquad (4.2a)$$

$$\text{Short axis } I_s = 3.20975 + 1.31271M - 1.24136\ln (R + 7) \qquad \sigma_{Is} = 0.556 \qquad (4.2b)$$

Joyner and Boore (1984) gave the attenuation equation of seismic intensity for the Western USA as follows :

$$I = 5.876 + 1.500M - 2.100\ln (R + 25) \qquad \sigma_I = 0.274 \qquad (4.3)$$

Based on a statistical analysis of 16 isoseismal maps from Southern China, and using the circular attenuation model, Zhou (1985) obtained the following attenuation equation :

$$I = 5.8520 + 1.4899M - 1.9986\ln (R + 25) \qquad \sigma_1 = 0.210 \qquad (4.4)$$

4.3 Attenuation Equations of Peak Ground Acceleration

In a seismic hazard analysis of Hong Kong by Pun(1990), the following attenuation equation of PGA given by Ambraseys(1990) was used :

$$\log a = -0.789 + 0.2128M \log R - 0.00255R + 0.25P \qquad (4.5a)$$

Another attenuation equation of PGA proposed by Ambrasseys and Bommer(1990) is given as :

$$\log a = -1.00 + 0.251M - \log R - 0.00268\ R \qquad \sigma_{\log a} = 0.26 \qquad (4.5b)$$

$$R^2 = D^2 + H^2 \quad (H < 25 \text{ km})$$

Joyner and Boore (1981) obtained the following attenuation equation of PGA for bedrock and stiff soils in Western USA :

$$\ln a = -2.349 + 0.573M - \ln R - 0.00587R \qquad \sigma_{\ln a} = 0.26 \qquad (4.6)$$

$$R^2 = D^2 + 7.3^2$$

It is a common practice to adopt the attenuation equation of PGA for Western USA as reference in the seismic hazard analysis of the Guangdong region. The attenuation equation of bedrock PGA is given as :

$$\ln a = 8.250 + 0.790M - 2.167\ln (R + 25) \qquad \sigma_{\ln a} = 0.649 \qquad (4.7)$$

Based on the magnitude--distance reflection method, Zhou (1986) modified equation (4.7) and obtained the following attenuation equation of bedrock PGA for Southern China :

$$\ln a = 8.237 + 0.781M - 2.080\ln (R + 25) \qquad \sigma_{\ln a} = 0.65 \qquad (4.8)$$

Wang (1988) gave the following attenuation equation of bedrock PGA for the Southern China region :

$$\ln a = 1.153 + 0.677M - 1.465\ln (R + 25) \qquad \sigma_{\ln a} = 0.684 \qquad (4.9)$$

Luo (1991) obtained the following attenuation equation of bedrock PGA for Taiwan :

$$\ln a = 4.920 + 1.024M - 1.065\ln (R + R_0) \qquad \sigma_{\ln a} = 0.572 \qquad (4.10)$$

$$R_0 = 0.0395e^{0.92M}$$

Huo (1989) obtained following attenuation equation of bedrock PGA for Northern China :

$$\log a = -0.935 + 1.241M - 0.046M^2 (D + R_0) \qquad \sigma_{\log a} = 0.1802 \quad (4.11)$$

$$R_0 = 0.3268e^{0.6135M}$$

By taking into account the saturation characteristics of near field ground motion in high intensity region and using the elliptical attenuation model, Huo et al (1992) obtained the following attenuation's equation of bedrock PGA for Southern China :

$$\text{Long axis } \log a_l = -1.2629 + 1.4956M - 0.0513M^2 - 2.2252\log (D + R_{0l}) \qquad (4.12a)$$

$$R_{0l} = 0.3618e^{0.6989M} \qquad \sigma_{\log al} = 0.247$$

$$\text{Short axis } \log a_s = -2.0301 + 1.4573M - 0.0501M^2 - 1.9731 \log (D + R_{0s}) \qquad (4.12b)$$

$$R_{0s} = 0.1201e^{0.7654M} \qquad \sigma_{\log as} = 0.247$$

Lee and Yu (1996) made the assumption that the ratio of the two intensities (with the same magnitude and epicentral distance) between Southern China and Western USA is equal to the corresponding ratio of the two peak ground accelerations. Using this assumption, they transferred the attenuation equation of bedrock PGA for Western USA into one that is applicable to Southern China. Using the circular attenuation model of the isoseismal intensity, they obtained the following equation :

$$\ln a = 6.6954 + 0.8599M - 1.87145\ln (D + R_0) - 0.0028D \qquad \sigma_{\ln a} = 0.525 \quad (4.13)$$

$$R_0 = 22.246e^{0.0292M}$$

Scott et al (1996) adopted the following attenuation equation of bedrock PGA given by Dahle (1990) to investigate the seismic-resistant design of buildings in the Hong Kong region.

$$\ln a = \begin{cases} -1.471 + 0.849M - \ln R - 0.00418R & R \le R_0 \\ -1.471 + 0.849M - 0.167\ln R_0 - 0.833\ln R - 0.00418R & R > R_0 \end{cases} \qquad (4.14)$$

$$R_0 = 100\text{km} \qquad \sigma_{\ln a} = 0.83$$

It is noted that Dahle (1990) obtained the above equation from the study of attenuation of intraplate seismic motion.

4.4 Results and Comparison of Attenuation Equations

For M_s = 5, 6 and 7, Figure 16 compares the attenuation curves obtained from some of the above equations. If M_s = 5, the different attenuation equations produce relatively scattered attenuation curves. If M_s = 6, the attenuation curves are close to each other except that the curve obtained from equation (4.14) decays more slowly. If M_s = 7, the two curves from equations (4.12a) and (4.14) are almost the same while the curve from equation (4.12b) is close to the other curves.

In the process of calculating the bedrock PGA, the study team performed seismic hazard analysis for the Hong Kong region and other 25 neighboring zones using equations (4.5) to (4.8), (4.12) and (4.13). The results are presented in Table 6. The results obtained from the attenuation equations outside the Southern China region are presented for the purpose of reference and comparison. The four equations (4.8), (4.9), (4.12) and (4.13) can be used for assessment of the attenuation relations of the Southern China region. The PGA values at 25 sites obtained from the three equations (4.8, 4.9 and 4.13) are more uniformly distributed over the subject region. This uniform distribution of PGA values does not represent the different states of seismic activity in the Pearl River Delta and its vicinity. Nor does it reflect the actual situation of seismic hazard at each site. For example, the results from equation (4.8) show that the Guangzhou and Dangan Island zones have PGA values greater than 150 gal. The results from equations (4.9) and (4.13) indicate that the Guangzhou and Dangan Island zones have PGA values of less than 125 gal. However, the results from equations (4.12a) and (4.12b) show that the region has sites with high values of PGA (such as outer Dangan Island) and sites with low values of PGA (such as Lingao site). This non-uniform distribution of PGA values reflects the site-related differences of seismic activity within the region. Furthermore, equations (4.12a) and (4.12b) were established using the elliptical attenuation model by taking into account the saturation characteristics of near field seismic motion in a high intensity region. These features of equations (4.12a) and (4.12b) are unique. As a result, equations (4.12a) and (4.12b) were adopted in the seismic hazard calculations for the Hong Kong region.

Furthermore, the study team also calculated the seismic intensity values of 25 sites using the attenuation equations of seismic intensity (4.1), (4.2a), (4.2b), and (4.4). The results are presented in Table 7. The results from equations (4.1), (4.2a), (4.2b) and (4.4) are similar. Equations (4.2a) and (4.2b) are established using the elliptical attenuation model. The results from equations (4.2a) and (4.2b) are compatible with those obtained from equations (4.12a) and (4.12b). Consequently, equations (4.2a) and (4.2b) are adopted as the basis for the calculation of seismic intensity in the seismic hazard analysis of the Hong Kong region.

5. PROBABILISTIC ANALYSIS OF SEISMIC HAZARD

5.1 Basic Principles

The seismic hazard of a subject region is usually given as the probability of ground motion exceeding a given value over a certain time period. If there are N seismic zones which contribute seismic hazard to the subject area, and if the n-th seismic zone has Pn ($Z \geq z$) as its

annual probability contribution to the ground motion exceeding the given value (z) in the subject area, then the subject area has the following annual probability of exceedance :

$$P(Z \geq z) = 1 - \prod_{n}^{N} (1 - P_n(Z \geq z)) \quad \text{.....(5.1)}$$

where Z = Ground motion parameter (i.e., acceleration or intensity)
z = A given value of the ground motion parameter.

In the above analysis, the key step is the determination of Pn ($Z \geq z$) which will be further discussed in the following. For simplicity of notation, the subscript of seismic zone number will be omitted in all of the following equations. All parameters describe the same seismic zone.

In the probability analysis of seismic hazard, two extreme differentiation methods are usually adopted for the statistical and assigned elements of seismological parameters. A seismic zone is a statistical element of such seismological parameters. It should possess statistical integrity and uniformity of seismic activity trends. The earthquake time history satisfies the segmental Poisson's process. If the average annual occurrence rate is ν in t years, then

$$P_{kt} = \frac{(vt)^k}{k!} e^{-vt} \quad \text{.....(5.2)}$$

where P_{kt} is the probability for k seismic events to occur in the next *t* years in the subject area. From equation (5.2), one can obtain the probability of at least one seismic event occurring in the subject area in the next *t* years as follows :

$$P(t) = 1 - e^{-vt} \quad \text{..... (5.3)}$$

The ratio of small to large seismic events in a seismic zone follows a modified magnitude-frequency relation. The corresponding magnitude--frequency density distribution function is :

$$f_M(M) = \frac{\beta \exp[(M - M_0)]}{1 - \exp[(-\beta(M_{uz} - M_0)]} \quad \text{.....(5.4)}$$

where $\beta = b \times \ln 10$, M_{uz} is the upper bound magnitude of a given seismic zone.

For each seismic zone, it is necessary to identify a number of potential source zones. A potential source zone is an assigned element of seismological parameters. A magnitude classification method is adopted to classify seismic events in a seismic zone into several classes according to their magnitudes. The average annual occurrence rate of each of the magnitude classes in a seismic zone can then be reasonably assigned to its corresponding potential source zones. This approach can accurately take into account the temporal and spatial non-uniformity of seismic activities in the seismic hazard analysis. Besides, this approach does not underestimate the influence of large seismic events to the seismic hazard of a subject area. For

the i-th potential source zone in a seismic zone, the average annual occurrence rate of each magnitude class can be represented using the following equation :

$$V_{iMj} = \frac{2v\exp\left[-\beta(M_j - M_0)\right]sh(-\beta\Delta M)}{1-\exp\left[-\beta(M_{uz} - M_0)\right]} f_{im_j} \quad \text{.....(5.5)}$$

where v = Average annual occurrence rate of a seismic zone
ΔM = Segment length of magnitude classification
M_j = The medium magnitude of the j-th magnitude class among the total classes starting from the minimum magnitude M_o to the upper bound M_u.
v_{iMj} = Average annual occurrence rate of the i-th potential source zone and the j-th magnitude class.
f_{iMj} = Seismic spatial distribution function or the spatial weight (W_{iMj}) of magnitude distribution in a potential source zone.

The f_{iMj} represents the probability for a seismic event of magnitude M_j ± (½) ΔM to occur in the i-th potential source zone. As a conditional probability of magnitude, it can indicate the non-uniformity of magnitude spatial distribution in a seismic zone. It can be determined by statistical method and comprehensive judgment. For a f_{iMj} associated with an assigned magnitude, its summation over the entire seismic zone is unity, i.e.,

$$\sum_{i=1}^{N_s} f_{iMj} = 1 \quad \text{.....(5.6)}$$

where Ns = the total number of potential source zones in a seismic zone.

Based on the segmental Poisson's distribution model and the theorem of total probability, the following equation is obtained to calculate the annual probabilities of exceedance for both seismic intensity and peak ground acceleration at the subject site.

$$P(Z \geq z) = 1 - \exp\left[-\sum_{i=1}^{N_s} \int_{Ai} \int_0 \sum_{j=1}^{N_M} V_{iMj} P(Z \geq z|E) f_i(\theta) d\theta dA \Big| A_i \right] \quad \text{.....(5.7)}$$

$$= 1 - \exp\left[-\frac{2v}{\beta} \sum_{i=1}^{N_s} \int_{Ai} \int_0 \sum_{j=1}^{N_m} P(Z \geq z \Big| E) f_M(M) sh(-\frac{1}{2}\Delta M) f_i(\theta) f_{iM_j} d\theta dA \Big| A_i \right]$$

where N_M = Number of magnitude classes in a seismic zone.
$f_i(\theta)$ = Orientational function of the i-th potential source zone
θ = Possible major fracture orientation.
Aj = Area of the i-th potential source zone
$P(Z \geq z|E)$ = Probability of site seismic intensity or PGA exceeding a given value when a definite event (with a magnitude equal to M_j ± (½) ΔM, and a specific orientation of the major axis of ellipse) occurs in the i th potential source zone.

5.2 Uncertainty Analysis of Attenuation Relations

Since the attenuation relations of seismic intensity and PGA are always associated with a degree of scattering, the attenuation equations given in the foregoing chapter can only provide anticipated values of intensity and acceleration. It is necessary to take into account the uncertainty characteristics of the attenuation relations in order to obtain more reliable results for the hazard analysis. The following equation can be used to make corrections due to uncertainties in the attenuation relations in a probability analysis.

$$P(Z \geq z) = \int_{-3\sigma}^{3\sigma} P(Z \geq z|\varepsilon) f(\varepsilon) d\varepsilon \quad \text{.....(5.8)}$$

where ε = Random variable of uncertainty in regression analysis.

$f(\varepsilon)$ = Probability density function of the uncertainty random variable in the attenuation relations. It is usually assumed to be the normal probability density function with a mean value of 0 and a standard deviation of σ.

The probability correction for the attenuation relations has been included in the computer program for seismic hazard analysis. The outputs are thus corrected seismic hazard calculations.

Based on the annual probability of exceedance for the site intensity and acceleration, the Bernoulli independent trial process leads to the following equation for the probability of seismic intensity and acceleration exceeding a given value z over t years :

$$P_T(Z \geq z) = 1 - [1 - P(Z \geq z)]^T \quad \text{.....(5.9)}$$

5.3 Comparison of Seismic Hazards in Surrounding Regions

Based on the seismic zones, the potential source zones and their seismological parameters as determined on this project, the probability hazard analysis approach as discussed in Sections 5.1 and 5.2 was applied to a trial calculation for part of the Pearl River Delta region. The purpose of this trial calculation is to verify the suggested approach by comparing the results of seismic hazard analyses conducted by GSB researchers over the years with the Seismic Intensity Zoning Map of China (1990). The results of the trial calculations can verify if the values of seismic ground motion parameters and the attenuation equations of ground motion are reasonable and appropriate.

Table 8 presents the results of the bedrock horizontal PGA and the seismic intensity at several sites in Pearl River Delta. The present results compare well with those given by a majority of other investigations. It is therefore concluded that the values of seismic ground motion parameters and the attenuation equations of seismic intensity and PGA determined on this project are acceptable and that the results obtained from these parameters and relations are reliable.

5.4 Seismic Hazard Analysis of the Hong Kong Region

The above approach and equations and data were applied to the calculations of 840 control points in the Hong Kong region. In particular, equations (4.2) and (4.12) are utilized in the calculations. The results are presented below.

5.4.1 Bedrock Peak Ground Acceleration

Figures 17-1 to 17-3 illustrate the isoseismal maps of bedrock peak PGA corresponding to probabilities of exceedance of 63%, 10% and 2% respectively for the Hong Kong region over a return period of 50 years. The isoseismal curves of the three groups are mainly oriented in the EW direction. The northern region has relatively low values of bedrock PGA while the southern region has relatively high values. The isoseismal curves for Hong Kong region with a 10% probability exceedance over 50 years are used as an example in the following discussions.

The northern sites such as Sha Tau Kok, Yuen Long and Tuen Mun have PGA values between 75 and 85 gal while Kowloon, Hong Kong Island and Lantau Island have values between 90 and 105 gal. The peak values in the region are found in Po Toi Islands and can be up to 115 gal. The difference between the maximum and minimum values of PGA is about 40 gal, which indicates that different sites in the region do not have substantial differences in their PGA values.

Examples are given in the following to specifically reveal the contributions of each major potential source zone to the bedrock PGA at each site in the subject region. Table 6 and Figure 18 present the contributions of five major potential source zones to the bedrock PGA at the Kowloon site(N22.31, E1141.17).

Bedrock PGA values for the Kowloon site are mainly contributed by five potential seismic source zones. Among these five zones, the Dangan Island potential source zone (99) makes the largest contribution. However, for a PGA value of 20 gal, the three potential source zones (23), (32) and (38) adjacent to Hong Kong collectively make a contribution in excess of 50% to the PGA value.

For the three probabilities of exceedance of 63%, 10% and 2% over the next 50 years, the corresponding values of bedrock PGA for the Kowloon site are 18.82, 92.70 and 190.70 gal respectively. Figure 19 illustrates the variation of probability of exceedance with Kowloon bedrock PGA over different return periods. From this figure, PGA values can be obtained for return periods of 1, 20, 50 or 100 years and for different probabilities of exceedance. The PGA values for different return periods and probabilities of exceedance at other sites in the Hong Kong region are basically similar to those of the Kowloon site. Figure 20 illustrates the variation of return period with bedrock PGA values at the Kowloon site.

5.4.2 Seismic Intensity

Figures 21-1 to 21-3 illustrate the isoseismal maps of seismic intensity for the Hong Kong region over return period of 50 years, for probabilities of exceedance of 63%, 10% and 2%, respectively. For a probability of exceedance of 63% over 50 years, the seismic intensity in the whole region is less than 6. For a probability of exceedance of 10% over 50 years, the seismic intensity in the whole region is between 6.95 and 7.30 and the majority of sites have seismic intensity values of around 7. The results of the present investigation thus indicate that the seismic intensity should be VII for the Hong Kong region, for a probability of exceedance of 10% over 50 years. This conclusion is similar to that given in the Seismic Intensity Zoning Map of China (1990).

As an example, the computation results for the Kowloon site(N22.31, E114.17) are given in the following to specifically show the contributions of the major potential source zones to seismic intensity. Table 10 and Figure 22 present such results for the Kowloon site. For a seismic intensity of VII, there are four potential source zones making substantial contributions to the seismic intensity at this site. For a seismic intensity of VI, there are many zones making different contributions to intensity at the site. The four potential source zones (23), (38), (32) and (48) adjacent to Hong Kong collectively make a contribution of more than 50% to the seismic intensity at this site.

For probabilities of exceedance of 63%, 10% and 2% over the next 50 years, the Kowloon site would have seismic intensity values of 5.91, 7.10 and 7.75, respectively. Figure 23 illustrates the variation of seismic intensity with probability of exceedance for different periods at the Kowloon site. Figure 24 illustrates the variation of seismic intensity with return period at the Kowloon site.

5.5 Uncertainty Analysis of Seismic Hazard Results

5.5.1 General

The results of seismic hazard analysis are dependent on the values of the various input parameters used for computation. These values are, to a certain extent, determined artificially and are hence not completely reliable. Consequently, it is necessary to conduct sensitivity analysis on the seismic hazard analysis results. Sensitivity analysis is one aspect of uncertainty analysis.

The present investigation has taken into account the corrections for uncertainties in attenuation relations in the computer programs. The attenuation equation of bedrock PGA has been corrected using the logarithmically normal distribution with standard derivation σ_{Ln} as the scatter function. The attenuation equation of seismic intensity has been corrected using the normal distribution with standard derivation σ as the scatter function.

At present, there are no rigorous mathematical formulations to calculate the effects of uncertainty in seismic ground motion parameters on seismic hazard analysis results. The present investigation adopted the sensitivity analysis technique to determine the effects of uncertainty. In such a sensitivity analysis, the numerical values of the seismic parameters are

varied over a given range. The results of the seismic hazard analysis are then calculated based on the different values of the seismic parameters. By comparing such results of the parametric analysis, the effects of uncertainty in seismic parameters can be determined.

5.5.2 Scheme and Weight of Potential Source Zones

From Tables 9 and 10, it can be observed that there are four potential source zones which contribute substantially to the bedrock PGA and seismic intensity of sites in the study region. They are Dangan Island (99), Lantau Island (38), Shenzhen (23) and Dapengwan (32) potential source zones. These zones together account for more than 98% of the peak PGA value of 75 gal. It is therefore prudent to concentrate the sensitivity analysis on these four zones.

In the sensitivity analysis, two values, i.e., 7.0 and 7.5, are assigned as the upper bound magnitude for the Dangan Island potential source zone. The other three zones also have two sets of values as their upper bound magnitude. With the first set, the Lantau Island (38), Shenzhen (23) and Dapengwan (32) potential source zones respectively would have 6.0, 6.0 and 5.5 as their upper bound magnitude values. With the second set, these three zones are combined into one zone with an upper bound magnitude of 6.0.

Moreover, two weight matrices of the potential source zones are adopted in the sensitivity analysis. One (W1) is given in Chapter 3. Another (W2) is given by invited peers. Eight cases were analyzed as shown in Table 11. The combination scheme 1 in Table 11 is exactly the same as that presented in Section 5.4.

As an example to illustrate the sensitivity analysis, Table 11 presents the detailed results of the sensitivity analysis for the Kowloon site. The results in Table 11 reveal that the different combination schemes have very limited influences on the seismic intensity whose values are always between 7.07 and 7.37 and have a maximum difference of 0.3. However, the different combination schemes have substantial influence on the bedrock PGA whose values are between 86 and 116 gal and have a maximum difference of 30 gal.

Despite this difference, the two weight matrices have little influence on the results of seismic intensity and PGA. This finding indicates that different experts have the similar opinion on the values of the weight matrices of the potential source zones. The increase of the upper bound magnitude of the potential source zone (99) from 7.0 to 7.5 results in an increase from 24 to 26 gal in the PGA, and 0.2 in the seismic intensity. The combination of zones 38, 23 and 32 results in a decrease of less than 10 gal in PGA and 0.04 in seismic intensity, respectively.

5.5.3 b-value

The values of 0.80 and 0.56 were used as b-values for the inner and outer seismic zones, respectively. In order to determine its effect, the two b-values were increased or reduced by 0.05. The results of the sensitivity analysis are presented in Table 12. It can be observed from the table that the variations of b-value have a limited effect on the seismic

intensity but a considerable effect on the peak PGA. The changes in the seismic intensity are about ± 0.08 and in the PGA are less than ± 10 gal.

5.5.4 Average Annual Occurrence Rate

The average annual occurrence rates were 1.05 and 1.38 for the inner and outer seismic zones, respectively. In the sensitivity analysis, 20% were added to or reduced from the two original values. The results are presented in Table 13, indicating that the 20% variation in the average annual occurrence rate has a limited influence on the results of seismic hazard analysis.

5.5.5 Orientation of the Major Axis of Ellipse

The above calculations are based on the elliptical attenuation model. If the orientation of the major axis of the ellipse varies by plus 15° or minus 15°, these variations would have a very limited influence on the results of seismic hazard analysis (Table 14).

5.6 Conclusions and Recommendations

From the above calculations and uncertainty analyses, the following conclusions and recommendations can be obtained for the seismic hazard of the Hong Kong region.

(1) The bedrock horizontal peak ground acceleration of the Hong Kong region over the next 50 years and for a probability of exceedance of 10% is between 76 and 115 gal. Kowloon (N22.31, E114.17), as the central site of the region, would have a bedrock horizontal peak ground acceleration of 92.70 gal. In view of the uncertainties involved in the analyses, refinement is not warranted and the central site value may be used as the value of bedrock horizontal peak ground acceleration for the Hong Kong region.

(2) The seismic intensity of the Hong Kong region over the next 50 years and for a probability of exceedance of 10% is between 6.90 and 7.30. As the zoning of seismic intensity should not be unduly fine, it is therefore suggested that seismic intensity VII be used for all sites within the Hong Kong region.

6. REFERENCES 參考文獻

1. 黃鎮國等，珠江三角洲形成發育演變，廣州：科普出版社廣州分社， 1982 ， 168 - 187

2. 胡聿賢、張敏政，缺乏強震觀測資料地區地震動參數的估算方法《地震工程與工程振動》， 1984(1)， 1 - 9

3. 周克森，重要工程場地的地震小區劃問題，第一屆兩岸地震學術討論文集，北京：地震出版社， 1986 ， 300 - 215

4. 李作明，香港地質簡介《廣東地質》， 1987 ，第 2 卷第 1 期

5. 林紀曾等，東南沿海地區地震活動特征的研究，海南島北部地震研究文集，北京：地震出版社， 1988 ， 173 - 184

6. 姚梅尹等，東南沿海地區幾次歷史地震的考證，海南島北部地震研究文集，北京：地震出版社， 1988 ， 211 - 216

7. 汪素雲等，華南地區地震動參數的衰減關係，海南島北部地震研究文集，北京：地震出版社， 1988 ， 284 - 293

8. 丁原章等，廣東省地震地質問題《廣東地質》， 1989 ，第四卷第一期， 63 - 73

9. 張虎男等，華南沿海新構造運動與地質環境，北京：地震出版社， 1990 ， 173 - 234

10. 國家地震局，中國地震烈度區劃圖說明書，地震出版社， 1991 年

11. 丁原章、梁勞，巴士系構造的地震危險性，華南地震， 1992(2)， 1 - 13

12. 霍俊榮、胡聿賢，地震動峰值參數衰減規律的研究，地震工程與工程振動， 1992 ，第 12 卷第 2 期， 1 - 11

13 霍俊榮、胡聿賢、馮啓民，關于通過烈度資料估計地震動的研究，地震工程與工程振動， 1992 ，第 12 卷第 3 期， 1 - 14

14. 丁原章，南海開發工作中的地震問題，華南地震， 1994 ，第 14 卷第 1 期， 1 - 6

15. 國家地震局，工程場地地震安全性評價工作規範 (DB001 - 94)，北京：地震出版社，1994

16. 丁原章等，香港地區地震危險性問題的回顧

17. Cornell, C.A. (1968). Engineering seismic risk analysis. *Bulletin of the Seismological Society of America*, vol. 58, 1583 - 1606.

18. Lau, R (1972). Seismicity of Hong Kong. *Royal Observatory, Hong Kong, Technical Note* no. 33, 30p. (Reprinted with revisions, 1977).

19. GCO (1991). *Review of Earthquake Data for the Hong Kong Region (GCO Publication No. 1/91).* Geotechnical Control Office, 115p.

20. British Geological Survey (1992). A review of the crustal structure and seismotectonics pertinent to Hong Kong. *British Geological Survey Technical Report* WC/92/17, 135p.

21. K.W. Lai etc. (1992). Spatial and Temporal Characteristics of Major Faults of Hong Kong.

22. Pun, W. K. & Ambraseys, N.N. (1992). Earthquake data review and seismic hazard anslysis for the Hong Kong region. *Earthquake Engineering and Structural Dynamics*, vol. 21, pp 433 - 443.

23. Pun, W.K. (1994). Earthquake resistance of buildigns in Hong Kong. *Asia Engineer*, Vol. 22, No. 3, pp 25 - 28.

24. Scott, D.M., Pappin, J.W. & Kwork, M.K.Y. (1994). Seismic design of buildings in Hong Kong. *Hong Kong Institution of Engineers Transaction*, vol. 1, no. 2, pp 37 - 50.

25. JP Busby etc. (1995). Interpretation of the Regional Gravity Survey of Hong Kong. *Hong Kong Geolgoical*, 1 (Autumn) 52 - 66

26. Pun, W.K., Ding, Y.Z. & Lee, C.F. (1996). Determination of seismic load for buildings in Hong Kong. *Proceedings of the Seminar on Earthquake Resisting Structures.* Hong Kong Institution of Engineers, Structural Division.

27. Lau, C.K. & Wong, K.Y. (1996). Seismic design of Tsing Ma Bridge. *Proceedings of the Seminar on Earthquake Resisting Structures.* Hong Kong Institution of Engineers, Structural Division.

28. 活斷層研究會編，日本之活斷層圖【付解說】，東京大學出版社， 1992.

LIST OF TABLES

Table 1 - Thermoluminescene Dating Results

No	Field No	Location	Coordinates		Depth m	Elevation mPD	Landform	Soil Type	Laboratory Code	TL age Year Bp	Fault Type
			Easting	Northing							
1	TM01	West of Wu Tip Wan	13160	25520	0.1	3	Sea shore	Quartz vien, Fault material	LG225	110,800	NEE
2	TM02	West of Wu Tip Wan	13160	25520	0.1	3	Sea shore	Fault material	LG226	265,500 ± 21,000	NNE
3	MT06	Mo Tat Wan, Lamma Island	33140	07860	0.1	4	Sea shore	Fault material	LG227	177,700 ± 15,100	NW
4	TT09	1.5Km south of Tai Tong	21000	29420	0.1	30	Stream	Fault breccia	LG228	105,100 ± 8,700	NW
5	NH10	9000m south of Nam Hang pai	21700	30160	0.1	100	Stream	Fault material	LG229	94,700 ± 8,100	NEE
6	TL012	Tsing Lun Tau	23560	25940	0.1	110	Stream	Fault breccia	LG230	91,100 ± 7,500	NW
7	MW16	Cheung Tsui, Ma Wan	24650	23700	0.1	5	Sea shore	Fault material	LG231	93,900 ± 7,900	NW
8	TC17	Milestone 4, Tung Chung Road	12430	11740	0.1	220	Gully	Fault material	LG232	101,000 ± 8,600	NW
9	TY20	Tsing Yi	26360	23760		20	Bridge Pier	Calcite vein	LG233	222,260 ± 17,800	NW
10	FX22	Fei Shue Ngam	50400	45450	0.1	5	Wave eroded hole	Fault breccia	LG234	> 1,000,000	NW
11	WN24	Wong Nai Chau	50160	44660	0.1	4	Wave eroded hole	Fault breccia	LG235	196,100 ± 16,900	NW
12	YL26	Shan Ha Tsuen	19180	32100			Terrace Alluvium	Upper layer silty fine sand	LG236	23,800 ± 2,000	
13	YL28	Shan Ha Tsuen	19180	32100			Terrace Alluvium	Lowe layer silty fine sand	LG237	29,300 ± 2,300	
14	YL29	400m west of Shan Ha Tsuen	18940	32000			Terrace Alluvium	Upper layer silty fine sand	LG238	20,500 ± 1,700	
15	YO31	Yim O Tuk	19700	20720	0.1	40	Slope	Fault material of quartz vein	LG239	33,300 ± 2,700	NW
16	YO32	Yim O Tuk	19600	20720	0.1	40	Slope	Fault gouge	LG240	82,000 ± 6,800	NEE
17	TO34	Ngong Shuen Au	21380	21240	0.1	50	Gully	Fault material	LG241	147,500 ± 11,800	NW
18	TO36	Po Chue Tam, Tai O	04140	13440	1	3	Terrace Alluvium	Upper layer silty sand cobbles	LG242	24,400 ± 2,000	
19	TO37	Po Chue Tam, Tai O	04140	13440	4	0.2	Terrace Alluvium	Lower layer silty with gravel	LG243	126,100 ± 10,100	
20	TO38	Ngau Kwo Tin	05240	11060	0.1	130	Gully	Fault material	LG244	278.700 ± 23,100	NW
21	FX39	Fei Shue Ngam	50400	45450	0.1	5	Wave eroded cave	Fault breccia	LG466	190,600 ± 15,800	NW
22	FX40	Fei Shue Ngam	50400	45450	0.1	5	Wave eroded cave	Fault breccia	LG467	201,800 ±16,100	NW
23	FX41	Fei Shue Ngam	50400	45450	0.1	5	Wave eroded cave	Fault breccia	LG468	177,500 ± 13,300	NW
24	WM42	Wang Mun Hoi	49500	43900	0.1	6	Wave eroded cave	Fault breccia	LG469	254,500 ± 20,400	NW
25	PT44	Pak Tam Chung	51780	28660	0.1	30	Stream	Fault breccia	LG470	118,700 ±9,700	NW
26	SW45	Shum Wat Wan	07285	12585	0.1	230	Stream	Fault breccia	LG471	196,800 ±16,300	NW
27	PS46	Pak Sha Chau	52150	44560	0.1	6	Wave eroded cave	Fault breccia	LG472	188,500 ±15,400	NW
28	MW50	Ma Wan	24580	23860	0.1	5	Seashore	Fault breccia	LG473	126,200 ± 10,300	NW

Notes: Samples collected by Guangdong Seismological Bureau
Test by thermoluminescene laboratory, Institute of Geology, State Seismological Bureau, Beijing, China
TL Thermoluminescene Dating

Table 2 - Earthquake Catalogue for the Hong Kong Region (Sheet 1 of 2)

Number	Date	Epicentre		Magnitude		Remarks
	Y/M/D	Latitude	Longitude	M_L	M_s	
1	1972 02 20	22°48′	114°30′	2.7	2.0	
2	1972 02 20	22°48′	114°30′	2.6	1.9	
3	1972 04 05	22°54′	114°36′	2.9	2.2	
4	1972 04 05	22°54′	114°36′	2.9	2.2	
5	1972 04 05	22°46′	114°39′	2.4	1.6	
6	1972 12 31	22°05′	113°54′	3.3	2.6	
7	1973 06 02	22°18′	114°54′	3.2	2.5	
8	1973 07 05	23°00′	113°54′	3.3	2.6	
9	1973 12 16	22°48′	114°00′	2.8	2.1	
10	1975 05 15	22°24′	114°18′	2.6	1.9	
11	1976 06 14	22°24′	114°24′	2.7	2.0	
12	1976 06 17	22°57′	114°27′	2.5	1.7	
13	1976 06 21	22°42′	114°18′	2.4	1.6	
14	1976 08 20	23°06′	114°18′	1.8	1.0	
15	1976 10 08	23°06′	114°18′	2.5	1.7	
16	1977 05 06	22°48′	114°24′	2.0	1.2	
17	1977 06 17	22°36′	114°00′	2.3	1.5	
18	1977 10 22	22°36′	114°30′	3.1	2.4	
19	1978 05 27	22°30′	114°30′	2.1	1.3	
20	1982 01 22	22°46′	114°36′	2.3	1.5	
21	1982 08 30	22°18′	114°01′	1.5	0.6	**
22	1982 10 07	22°18′	114°01′	1.5	0.6	**
23	1983 07 22	22°32′	114°06′	2.8	2.1	*
24	1983 07 28	22°33′	114°02′	1.8	1.0	
25	1983 10 01	22°33′	114°09′	1.5	0.6	
26	1983 12 06	22°30′	114°02′	2.8	2.1	*
27	1984 03 15	22°50′	113°59′	2.2	1.4	
28	1985 06 04	22°15′	113°34′	2.4	1.6	
29	1986 11 09	22°42′	114°54′	3.0	2.3	
30	1987 06 09	22°37′	114°04′	1.6	0.7	

Table 2 - Earthquake Catalogue for the Hong Kong Region (Sheet 2 of 2)

Number	Date	Epicentre		Magnitude		Remarks
	Y/M/D	Latitude	Longitude	M_L	M_s	
31	1987 07 18	22°38′	114°04′	1.2	0.3	
32	1988 01 24	22°34′	114°11′	2.3	1.5	
33	1990 06 13	22°24′	114°56′	3.0	2.3	
34	1990 06 11	22°41′	114°56′	3.3	2.6	
35	1990 06 11	22°45′	114°55′	3.0	2.3	
36	1990 06 29	22°35′	114°35′	1.8	1.0	
37	1993 03 01	22°36′	114°24′	2.8	2.1	
38	1995 05 11	22°17′	114°04′	3.1	2.4	
39	1995 05 11	22°19′	114°02′	2.4	1.6	**
40	1995 05 12	22°17′	114°04′	2.1	1.3	**
41	1995 05 12	22°17′	114°03′	2.2	1.4	**
42	1995 05 13	22°19′	114°02′	2.2	1.4	**
43	1995 05 13	22°19′	114°03′	2.4	1.6	**
44	1995 05 16	22°18′	114°03′	2.2	1.4	**
45	1995 05 18	22°17′	114°03′	2.0	1.2	**
46	1995 05 23	22°17′	114°02′	2.3	1.5	**
47	1995 05 26	22°18′	114°03′	2.3	1.5	**
48	1995 05 28	22°18′	114°03′	2.3	1.5	**
49	1995 05 29	22°18′	114°03′	2.4	1.6	**
50	1995 05 29	22°18′	114°04′	2.2	1.4	**
51	1995 05 29	22°18′	114°02′	2.2	1.4	**
52	1995 05 29	22°17′	114°03′	2.4	1.6	**
53	1995 06 23	22°17′	114°04′	2.2	1.4	**
54	1995 08 15	22°18′	114°02′	2.3	1.5	**
55	1995 11 20	22°18′	114°04′	2.1	1.3	**

Legend : * Epicentre determined by seismograph network data from the Royal Observatory of Hong Kong

** Ditto, with magnitude determined from Cheung Chau seismograph station data

Table 3 - Numbers of Occurrence for Earthquakes of Different Magnitudes at Different Times along the Southeastern Coastal Seismic Belt

1970 - 1995 M ≥ 4																												
Magnitude	4.0	4.1	4.2	4.3	4.5	4.6	4.7	4.75	4.8	4.9	5	5.1	5.2	5.25	5.3	5.5	5.6	5.75	6	6.1	6.2	6.25	6.4	6.5	6.75	7	7.3	7.5	Total
Inner Zone	3	1	2	4	4	1	1		1	1	1					1													20
Outer Zone	3	1	1	2	1	1	2		1		3	2	1		2					1	1								22
Total	6	2	3	6	5	2	3		2	1	4	2	1		2	1				1	1								42

1990 - 1995 M ≥ 5																												
Magnitude										5	5.1	5.2	5.25	5.3	5.5	5.6	5.75	6	6.1	6.2	6.25	6.4	6.5	6.75	7	7.3	7.5	Total
Inner Zone										2	1	1	3	1	1		2							1				13
Outer Zone										6	2	1	1	2	2	1		1	1	1	2	1		1		1		23
Total										8	3	2	4	3	3	1	2	1	1	1	2	1		2		1		36

1800 - 1995 M ≥ 5																												
Magnitude																		6	6.1	6.2	6.25	6.4	6.5	6.75	7	7.3	7.5	Total
Inner Zone																		1	1					1				3
Outer Zone																		3	1	1	2	1		1		1		10
Total																		4	2	1	2	1		2		1		13

Table 4 - Annual Occurrence Rate and Recurrence Cycle for Earthquakes of Different Magnitude in the Southeastern Coastal Seismic Belt

Magnitude M_s	Inner Zone		Outer Zone	
	Average Annual Rate of Occurrence (events/yr.)	Return Period (yr.)	Average Annual Rate of Occurrence (events/yr.)	Return Period (yr.)
4.0	1.05	0.95	1.38	0.72
4.5	0.44	2.29	0.65	1.55
5.0	0.18	5.59	0.30	3.33
5.5	0.073	13.6	0.14	5.15
6.0	0.030	33.2	0.065	15.3
6.5	0.012	80.9	0.031	33.0
7.0	--	--	0.014	70.8

Table 5 - Weight Matrix (W_1) for Distribution of Magnitude for Major Potential Source Zones in Study Region

Seismic Zone	#	Potential Source Zone Number	4.0-5.5	5.6-6.0	6.1-6.5	6.6-7.0	θ_1	$W_{\theta 1}$	θ_2	$W_{\theta 1}$
Inner Zone	17	Dongguan	0.0165				0	1.0	0	0
	19	Huizhou	0.0127				20	1.0	0	0
	22	Jiangmen	0.0277				120	0.7	40	0.3
	23	Shenzhen	0.0155				120	0.7	40	0.3
	29	Zhaoquing	0.0287	0.0573			120	0.5	10	0.5
	30	Guangzhou	0.0304	0.0593			120	0.5	10	0.5
	31	Haifeng	0.0280	0.0454			120	0.5	30	0.5
	32	Dapengwan	0.0166	0.0271			120	1	0	0
	33	Huiyang	0.0235	0.0332			120	0.5	30	0.5
	35	Zhongshan	0.0282	0.0531			120	0.7	40	0.3
	38	Lantau	0.0182	0.0289			120	0.8	20	0.2
	39	Guanghai	0.0261	0.0468			120	1	0	0
	40	Gaolan Island	0.0253	0.0458			120	0.5	20	0.5
	48	Pearl River.Mouth	0.0212	0.0335	0.0939		120	0.7	40	0.3
Outer Zone	82	Honghai Bay	0.0298	0.0341	0.0405		120	0.5	20	0.5
	83	Outer Gaolan Island	0.0232	0.0256	0.0398		20	0.6	120	0.4
	84	Outer Xiachuan Island	0.0273	0.0338	0.0379		20	0.6	120	0.4
	99	Dangan Islands	0.0266	0.0366	0.0558	0.0947	120	0.5	20	0.5

Table 6 - PGA Values for 25 Sites from Different Attenuation Models (10% Exceedance in 50 Years)

Site	Ambrasseys -Bommer (Europe)	Joyner-Boore (Western U.S.A. bedrock and firm ground)	Zhou (Western U.S.A. bedrock)	Zhou (Southern China bedrock)	Wang (Southern China bedrock)	Luo (Taiwan bedrock)	Huo (Southern China bedrock)	Lee & Yu (Southern China bedrock)	Huo (Western U.S.A. bedrock)	Anders Dahle, etc. (Interaplate)
Guangzhou	97.83	114.31	121.01	159.69	84.64	93.76	76.50	88.39	60.14	92.45
Huangpu	95.41	112.12	117.46	155.15	82.76	91.41	71.15	85.41	57.09	91.17
Kowloon	104.90	115.95	125.78	168.29	92.82	105.15	92.70	93.33	66.30	115.42
Hong Kong Island	106.07	116.17	126.31	169.10	93.52	106.51	96.32	94.45	68.42	117.54
Sha Tau Kok	102.06	119.70	127.24	168.03	90.19	102.25	80.94	91.41	62.55	105.31
Lamma Island	108.65	117.96	131.18	175.11	97.42	110.17	107.41	110.42	76.12	122.86
Wanshan Islands	115.06	123.94	144.69	191.28	104.36	118.27	131.82	112.70	92.62	131.40
Dangan Islands	115.51	121.95	145.51	192.79	105.55	117.86	136.38	115.32	96.47	132.04
E Zhou Island	116.81	123.11	148.90	197.06	107.41	119.63	141.38	118.06	99.27	134.79
Jiapeng Islands	119.55	126.22	156.30	205.80	110.11	123.75	154.28	125.37	107.76	138.10
Lingao	88.24	95.06	98.24	130.88	76.39	85.38	62.27	72.63	46.02	94.09
Luohu	98.91	113.38	120.39	160.64	87.24	97.06	75.62	86.69	57.07	103.31
Sheku	67.67	108.53	114.82	153.66	85.76	95.53	78.17	83.93	56.22	104.33
Fanling	101.03	114.55	122.9	164.11	89.18	99.71	79.56	88.78	58.87	105.72
Gaotong	105.24	122.42	132.50	174.55	94.01	106.99	90.99	96.20	69.25	111.13
Heizei	101.00	111.50	119.05	158.87	88.94	100.36	86.72	88.01	61.39	109.20
Tuen Mun	100.21	110.72	118.80	159.12	88.89	99.87	85.39	87.51	59.75	109.50
Tsing Yi	102.11	113.13	120.96	162.07	89.65	101.90	86.59	88.97	61.57	112.25
Ma Wan	102.13	112.15	121.08	162.30	90.20	101.68	88.14	89.31	61.76	111.97
Tsin Yue Wan	108.35	118.13	130.48	173.64	96.48	110.26	107.74	99.99	76.33	121.51
Neilingding Island	101.61	112.87	120.54	159.85	89.49	101.03	88.22	89.58	63.56	109.39
Qiao Island	101.69	113.41	120.25	160.52	89.51	101.01	89.58	90.30	64.84	109.14
Xiangzhou	105.64	116.09	126.86	168.97	94.34	105.78	101.98	96.74	72.82	116.04
Modaomen	105.03	115.62	124.56	165.98	92.89	103.55	94.82	94.06	68.45	113.86
Gaolan Island	109.70	124.31	135.40	179.20	97.60	109.08	97.02	99.78	72.20	117.03

Table 7 - Intensity Values for 25 Sites from Different Attenuation Models (10% Exceedance in 50 Years)

Site	Equation 4.3 (Western U.S.A.)	Equation 4.4 (Southern China)	Equation 4.1 (Southern China)	Equation 4.2 (Southern China)
Guangzhou	6.14	6.44	6.60	6.82
Huangpu	6.07	6.36	6.55	6.78
Kowloon	6.52	6.82	6.98	7.11
Hong Kong Island	6.57	6.88	7.01	7.14
Sha Tau Kok	6.31	6.61	6.79	6.97
Lamma Island	6.71	7.04	7.12	7.24
Wanshan Islands	6.93	7.22	7.30	7.41
Dangan Islands	7.04	7.34	7.38	7.46
E Zhou Island	7.08	7.38	7.42	7.49
Jiapeng Island	7.17	7.49	7.51	7.56
Lingao	6.12	6.45	6.63	6.82
Luohu	6.24	6.56	6.73	6.92
Sheku	6.29	6.61	6.77	6.96
Fanling	6.31	6.62	6.79	6.98
Gaotang	6.46	6.76	6.91	7.06
Heizei	6.41	6.71	6.87	7.04
Tuen Mun	6.41	6.71	6.86	7.03
Tsing Yi	6.44	6.75	6.90	7.06
Ma Wan	6.47	6.76	6.91	7.07
Tsin Yue Wan	6.67	7.00	7.09	7.22
Neilingding Islands	6.42	6.72	6.88	7.04
Qiao Island	6.42	6.72	6.89	7.05
Xiangzhou	6.58	6.89	7.02	7.16
Modaomen	6.48	6.78	6.94	7.10
Gaolan Island	6.49	6.76	6.96	7.11

Table 8 - Bedrock PGA and Intensity Values for Selected Pearl River Delta Sites

Site	Zhou et al (1995)		Ding et al (1994)		Zhou et al (1996)		Ding et al (1987)		Zhang et al (1995)		Zhou et al (1987)		Huang et al (1989)		Wang et al (1989)		Hu et al (1993)		Seismic Intensity Zoning Map of China (1990)	Present Report	
	PGA (g)	I	PGA (g)	I	PGA (g)	I	PGA (g)	I	PGA (g)	I	PGA (g)	I	PGA (g)	I	PGA (g)	I	PGA (g)	I	Basic Inte	PGA (g)	I
Guangzhou	0.0866	6.94																	VII	0.0780	6.82
Huangpu			0.0887	6.936															VII	0.0725	6.78
Lingao					0.0608	6.8													VII	0.0635	6.82
Shenzhen							0.0587	6.4											VII	0.0771	6.92
Xinhui									0.0636										VI	0.0535	6.65
Zhuhai											0.092								VII	0.1040	7.16
Modaomen													0.099						VII	0.0967	7.10
Gaoland Island															0.132				VII	0.0989	7.11
Qiao Island																	0.0836	7.17	VII	0.0913	7.05
Neilingding Islands																	0.0839	7.18	VII	0.0899	7.04
Wanshan Islands																			VIII	0.1344	7.41
Dangan Islands																			VIII	0.1390	7.46
E Zhou Island																			VIII	0.1441	7.49
Jiapeng Island																			VIII	0.1573	7.56

Table 9 - Contributions to Bedrock PGA Values at Kowloon Site from Major Potential Source Zones

Zone No.		99	38	23	32	48
Potential Source Zone		Dangan Islands	Lantau	Shenzhen	Dapengwan	Pearl River Mouth
Bedrock PGA Value	20gal	40.1%	16.5%	22.6%	13.2%	7.7%
	75gal	62.6%	14.2%	14.1%	8.0%	1.2%
	150gal	83.9%	13.6%		2.5%	

Table 10 - Contributions to Intensity at Kowloon Site from Major Potential Source Zones

Zone No.		99	23	38	32	48	33	82	35	83
Potential Source Zone		Dangan Islands	Shenzhen	Lantau	Dapengwan	Pearl River Mouth	Huiyang	Honghai Bay	Zhong Shan	Outer Gaolan Islands
Seismic Intensity	VI	40.1%	14.9%	16.6%	11.8%	11.6%	2.7%	1.8%	0.3%	0.2%
	VII	85.3%	2.8%	11.6%	0.3%					
	VIII	100.0%								

Table 11 - Comparison of Results for Different Source Zoning and Different Weights

Combination Scheme #	Weight Matrix	Upper Bound Magnitude for Source Zone #99	Source Zones 38, 23, 32	PGA (gal)	I
1	W_1	7.0	separated	92.70	7.11
2	W_1	7.5	- ditto -	116.78	7.37
3	W_2	7.0	- ditto -	9.71	7.12
4	W_2	7.5	- ditto -	116.35	7.37
5	W_1	7.0	combined	86.14	7.07
6	W_1	7.5	- ditto -	112.87	7.35
7	W_2	7.0	- ditto -	88.32	7.09
8	W_2	7.5	- ditto -	114.62	7.36

Table 12 - Effect of b Value

Scheme	Outer Zone	Inner Zone	PGA (gal)	I
1	0.56	0.80	92.70	7.11
2	0.61	0.85	84.90	7.03
3	0.51	0.75	101.27	7.19

Table 13 - Effect of Annual Rate of Seismic Occurrence

Scheme	Outer Zone	Inner Zone	PGA (gal)	I
1	1.38	1.05	92.70	7.11
2	1.66	1.26	102.03	7.19
3	1.10	0.84	82.06	7.01

Table 14 - Effect of Orientation of Long Axis of Ellipse

Scheme	Orientation of Long Axis of Ellipse	PGA (gal)	I
1	Original Scheme	92.70	7.11
2	+ 15°	95.79	7.13
3	- 15°	93.63	7.11

LIST OF FIGURES

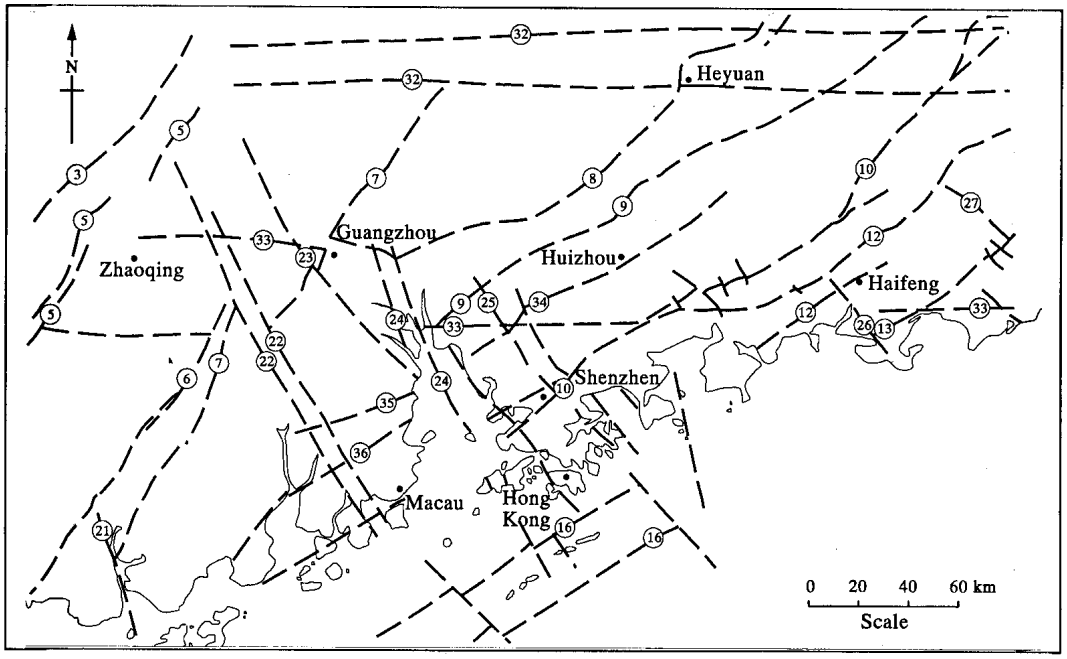

Figure 1 - Distribution of Main Faults in the Pearl River Delta

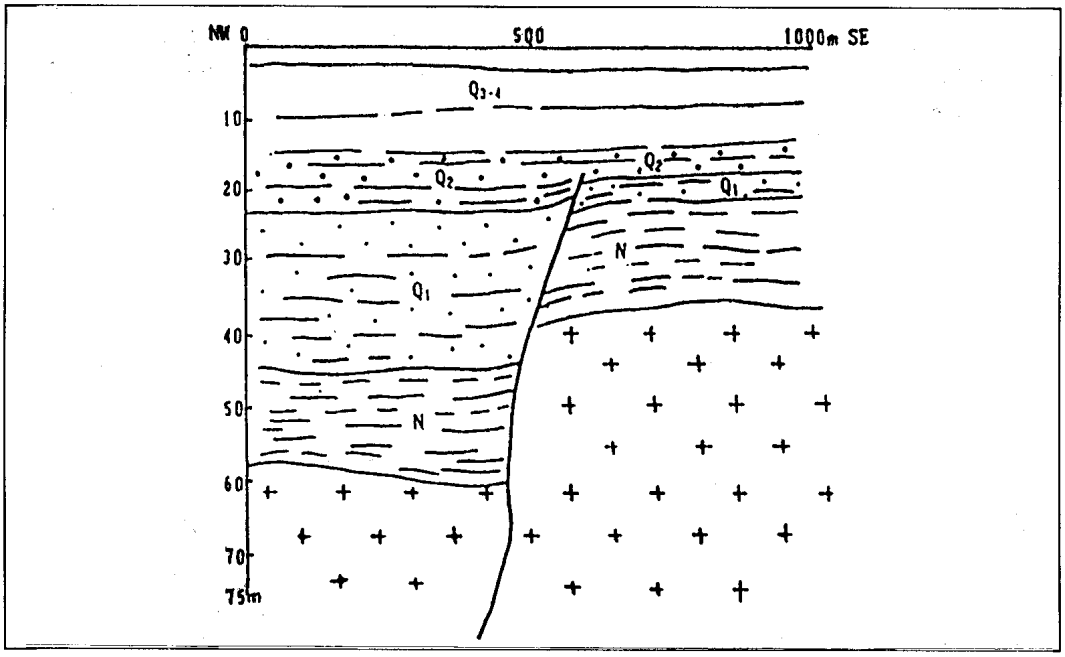

Figure 2 - Lower Quaternary Offsetted by Coastal Fault, as Indicated by Multichannel Seismic Survey Carried out South of Dangan Islands (Data from Guangzhou Marine Geology Bureau)

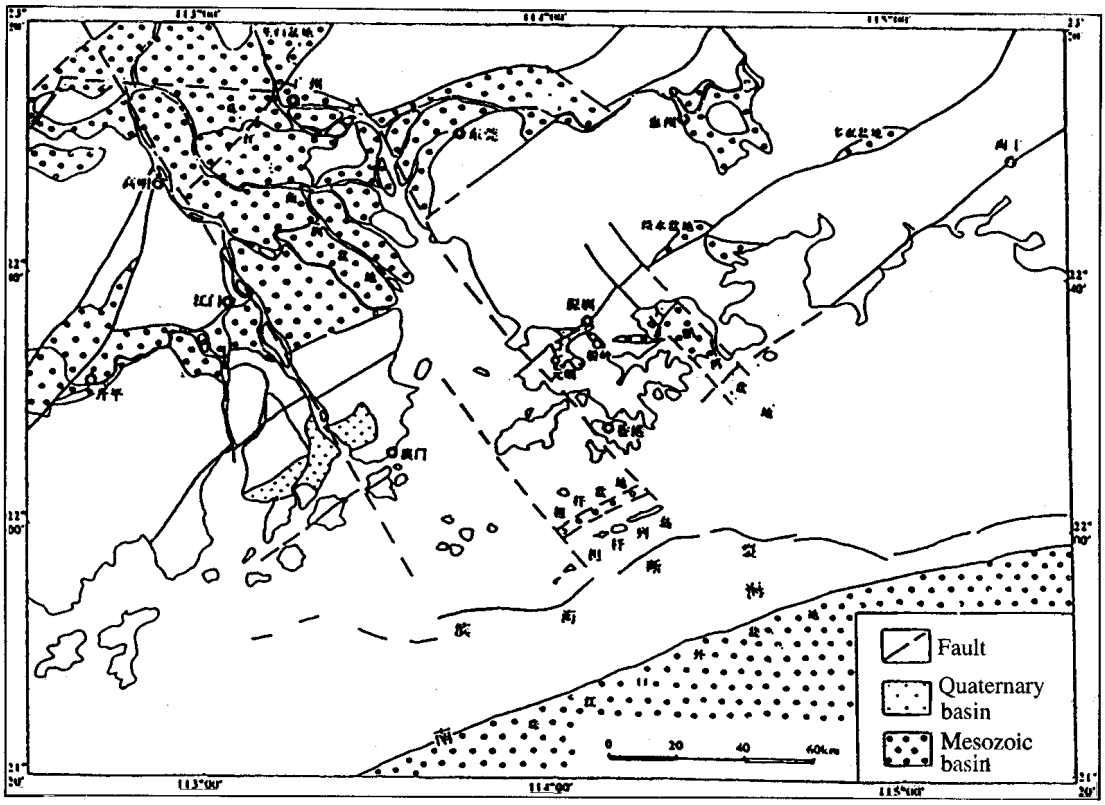

Figure 3 - Distribution of Main Tectonic Basins in Hong Kong and Vicinity

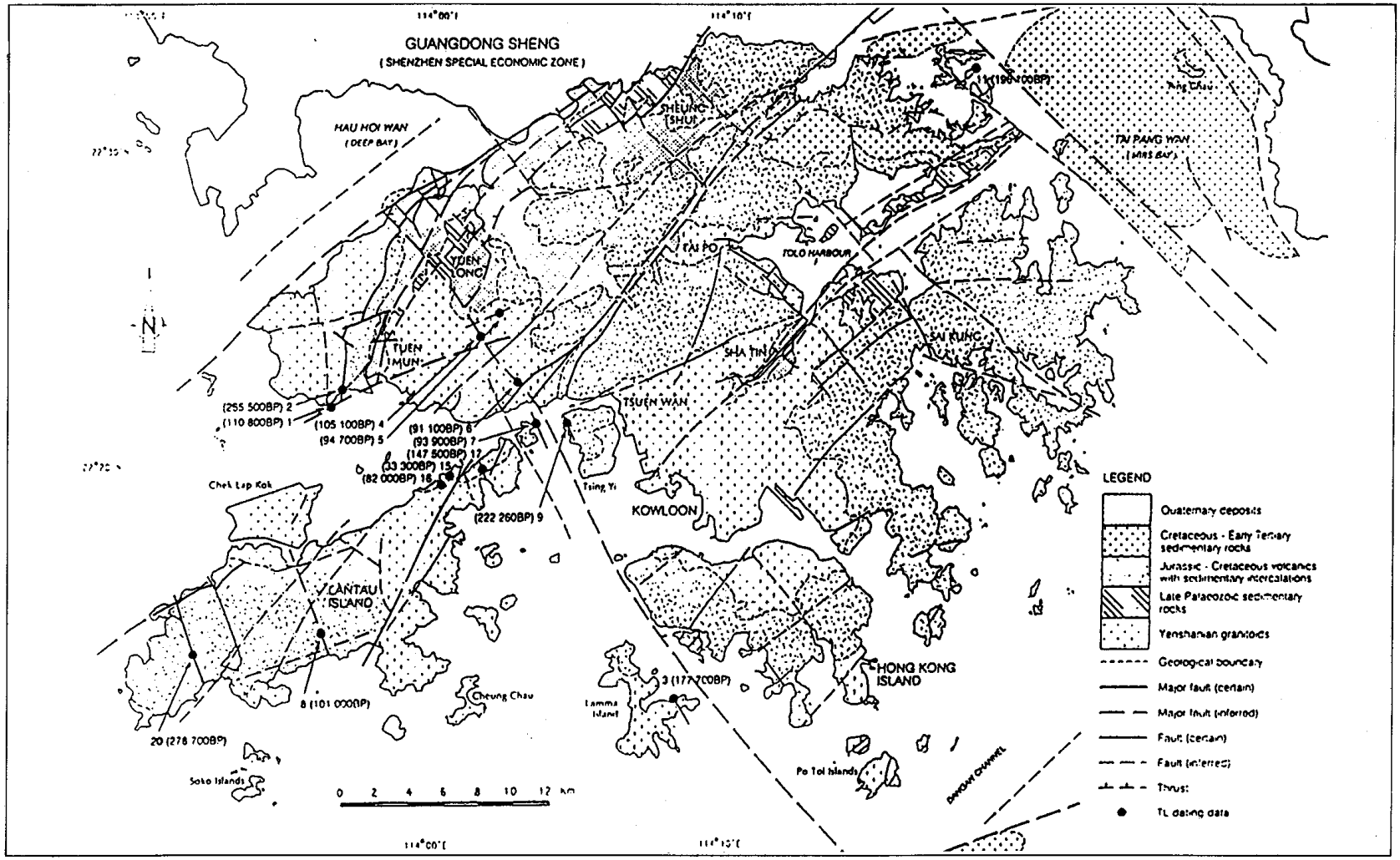

Figure 4 - TL Dating Data for Main Fault Systems in Hong Kong (Geological Data from the Hong Kong Geological Survey)

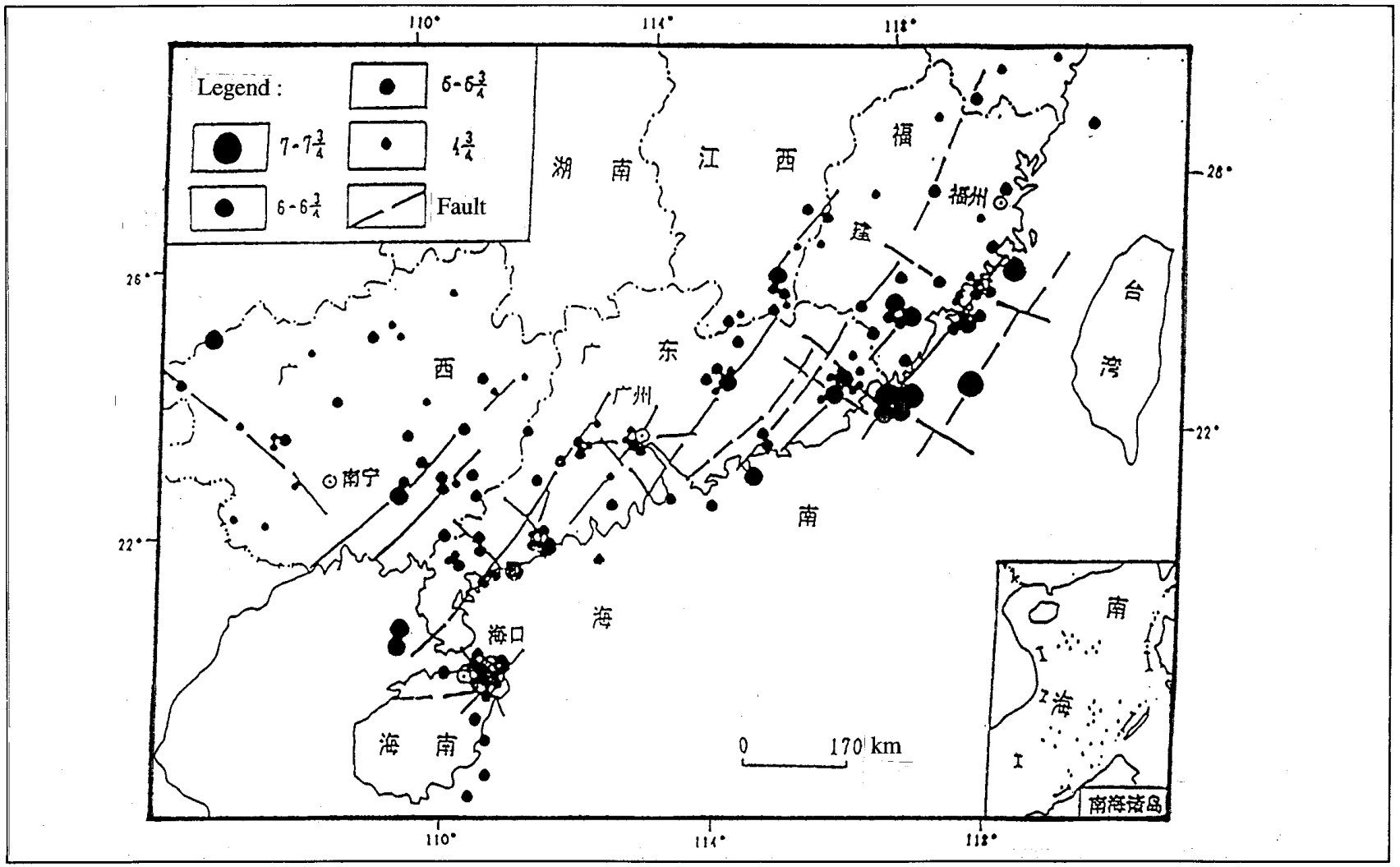

Figure 5 - Distribution of $M_s \geq 4¾$ Events along the Southeastern Coastal Seismic Belt, between 1067 and 1995

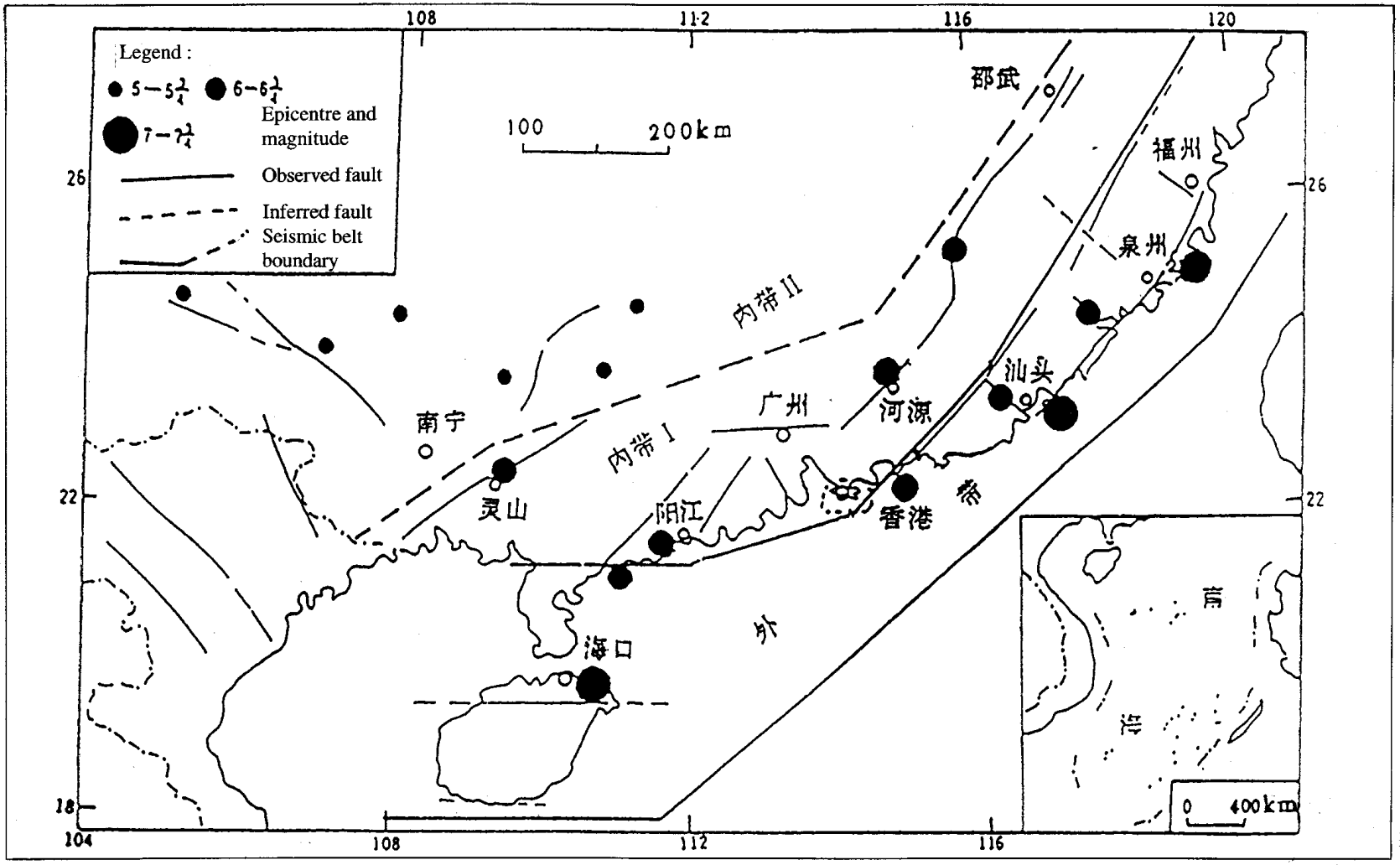

Figure 6 - Seismic Zoning of the Southeastern Coastal Region

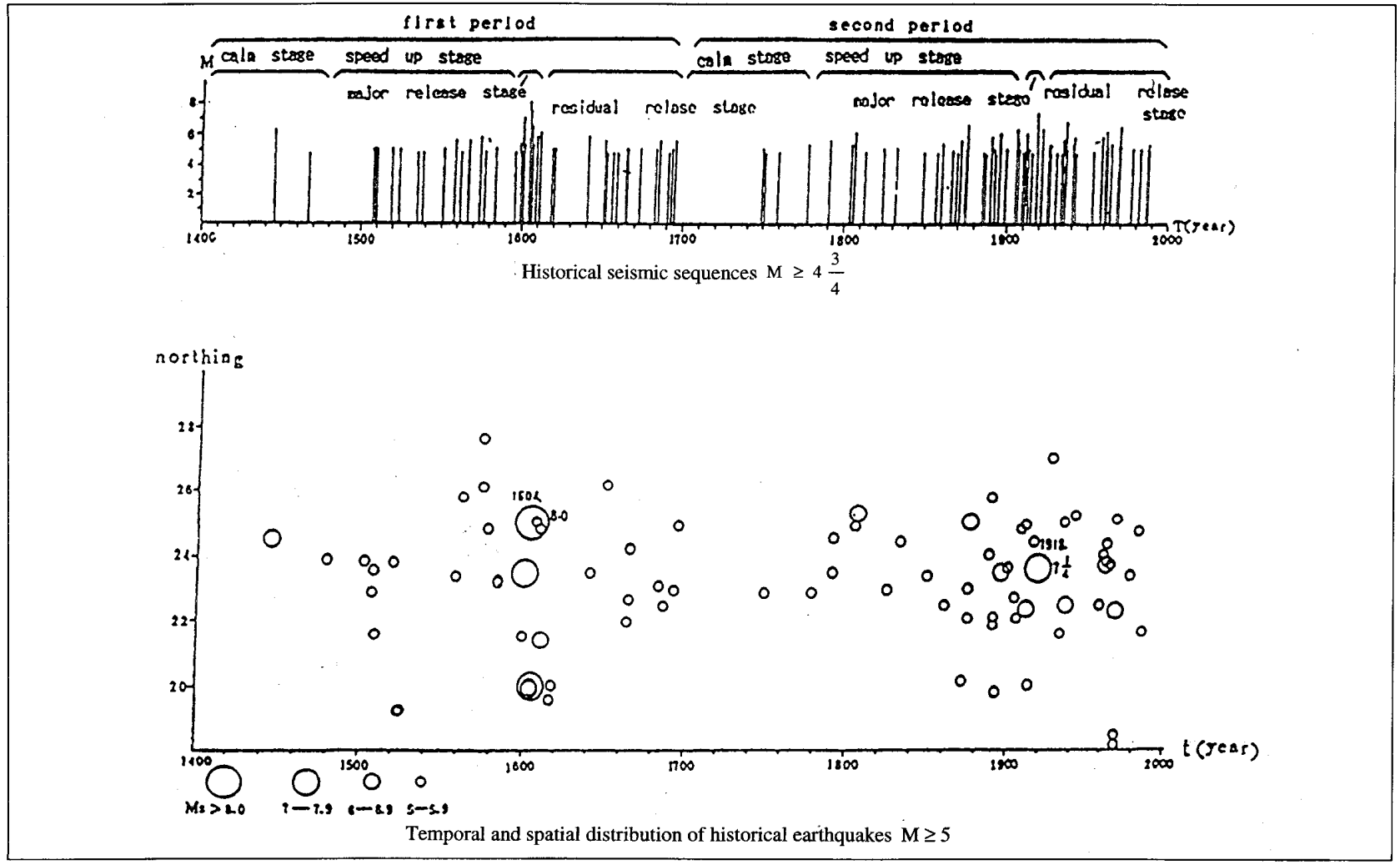

Figure 7 - Seismic Sequences for the Southeastern Coastal Seismic Belt

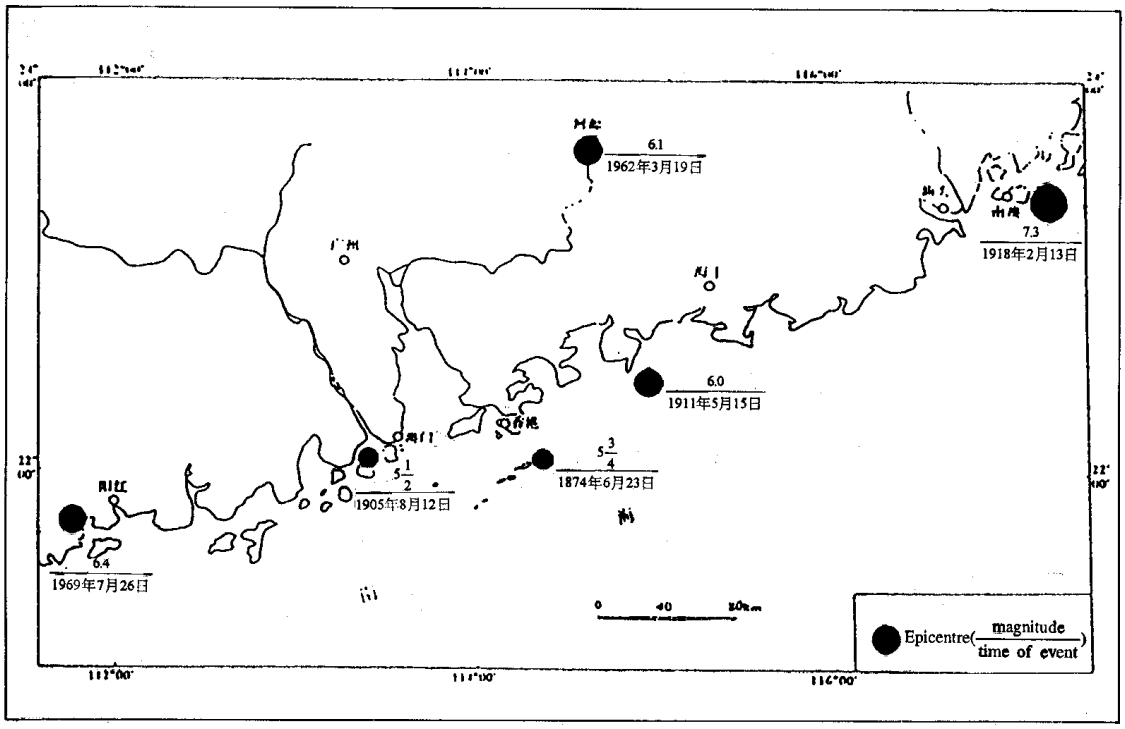

Figure 8 - Distribution of Historical Earthquakes in Hong Kong and Vicinities

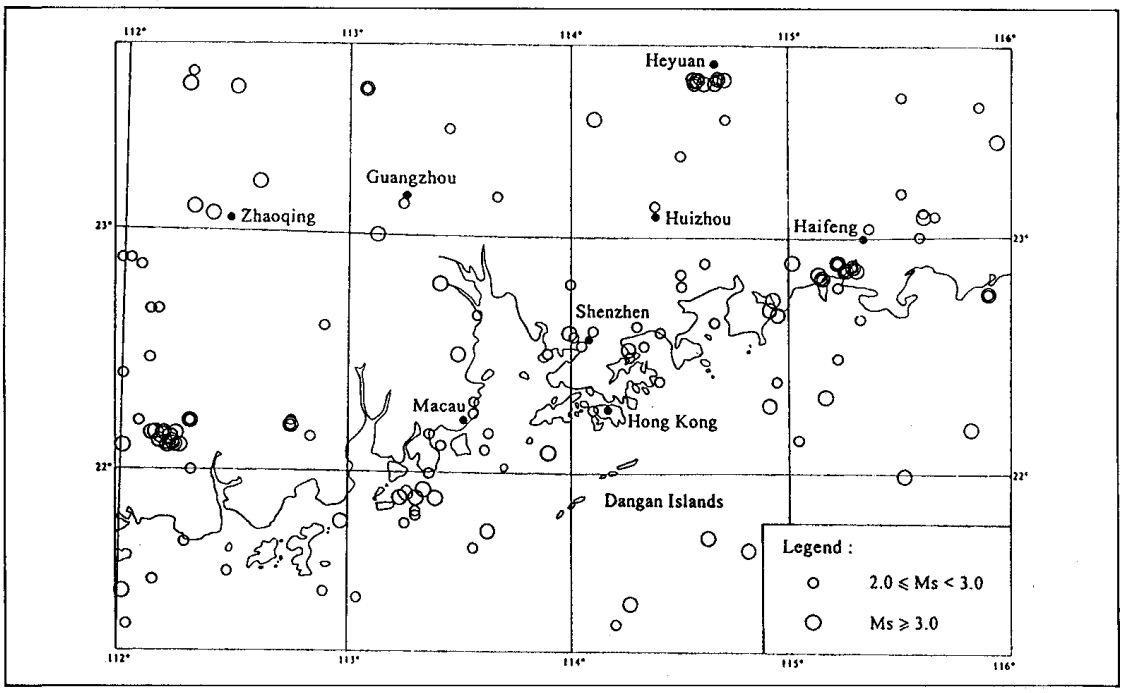

Figure 9 - Distribution of Earthquakes for $M_s \geq 2.0$ in the Pearl River Delta Area in the Period of 1970 to 1995

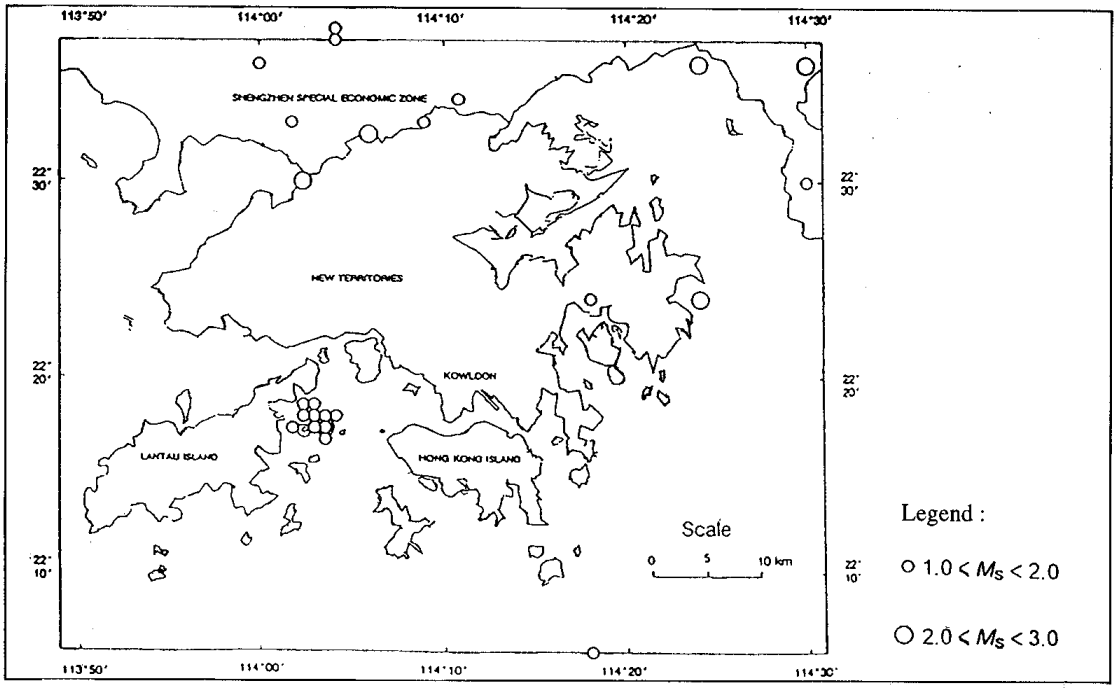

Figure 10 - Distribution of Earthquakes for $M_s \geq 1.0$ in Hong Kong and Vicinities in the Period 1972 to 1995

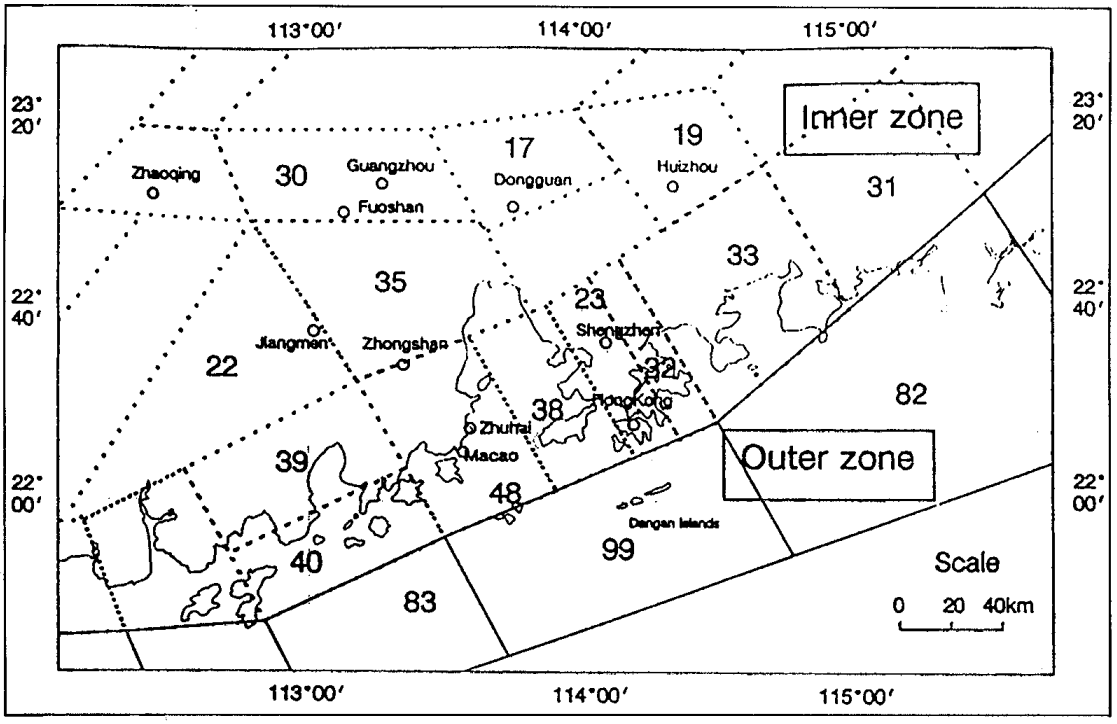

Figure 11 - Delineation of Potential Seismic Zones for Hong Kong and Its Surrounding Region

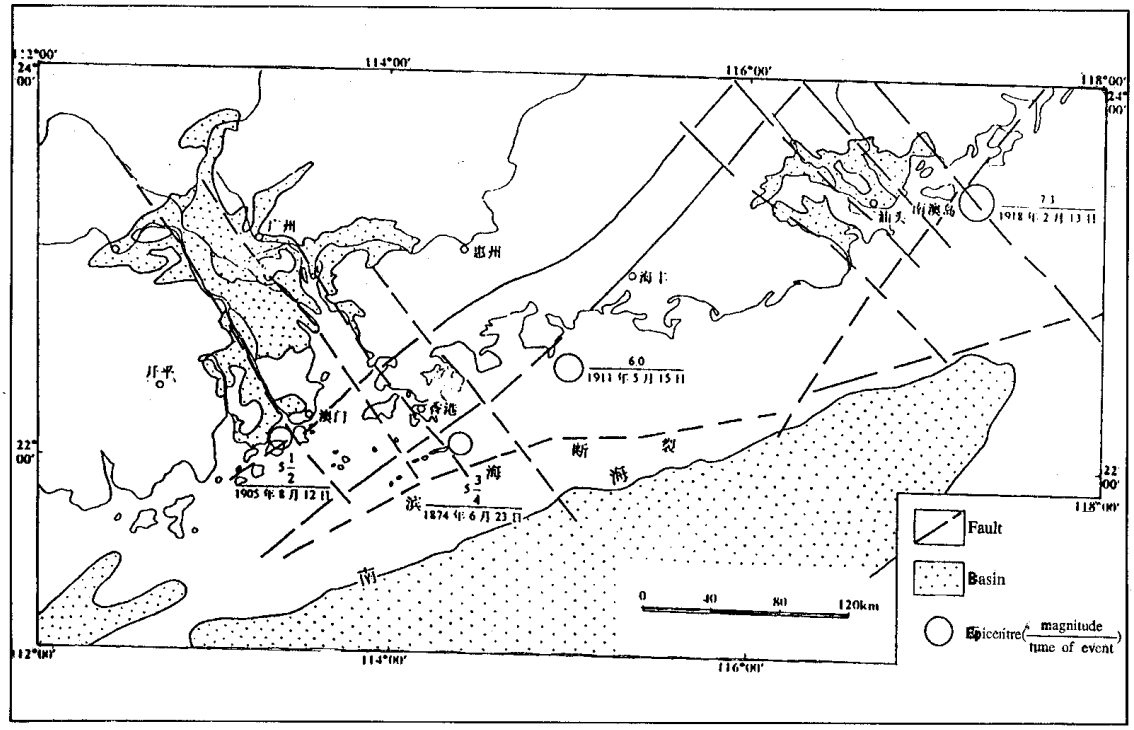

Figure 12 - Tectonic Setting of Nanao and Dangan Islands

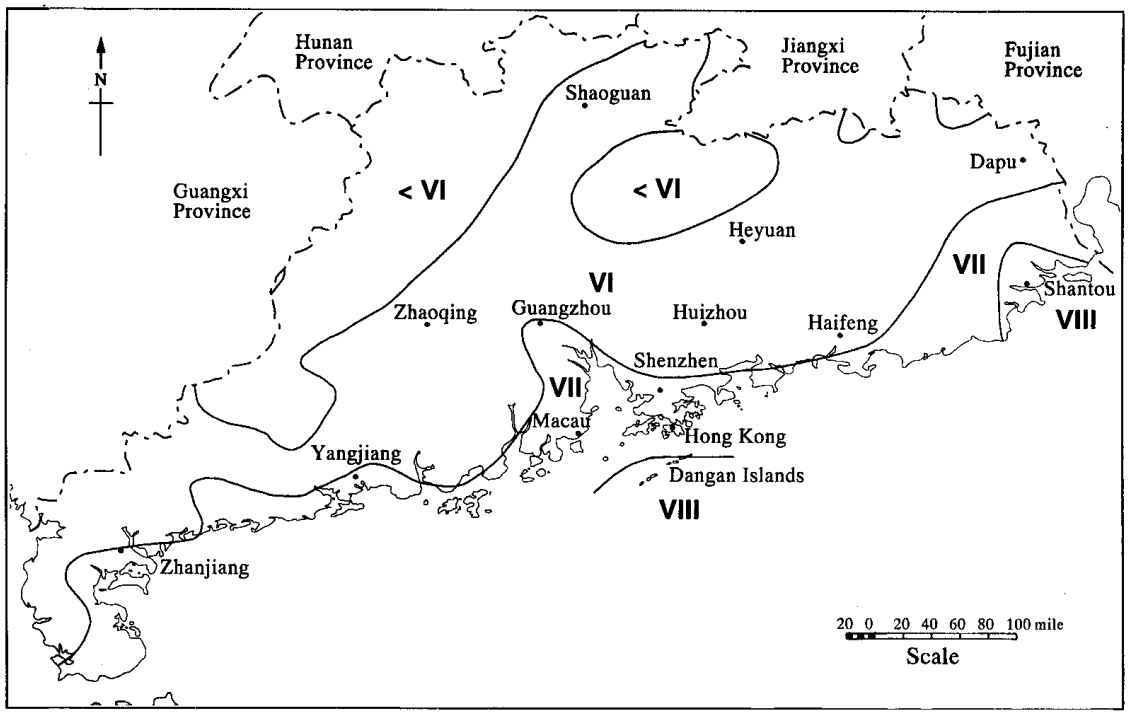

Figure 13 - Seismic Intensity Zonation of Guangdong Province
The Nanao-Shantou Area and Dangan Area Are Those Zones with Intensity VIII

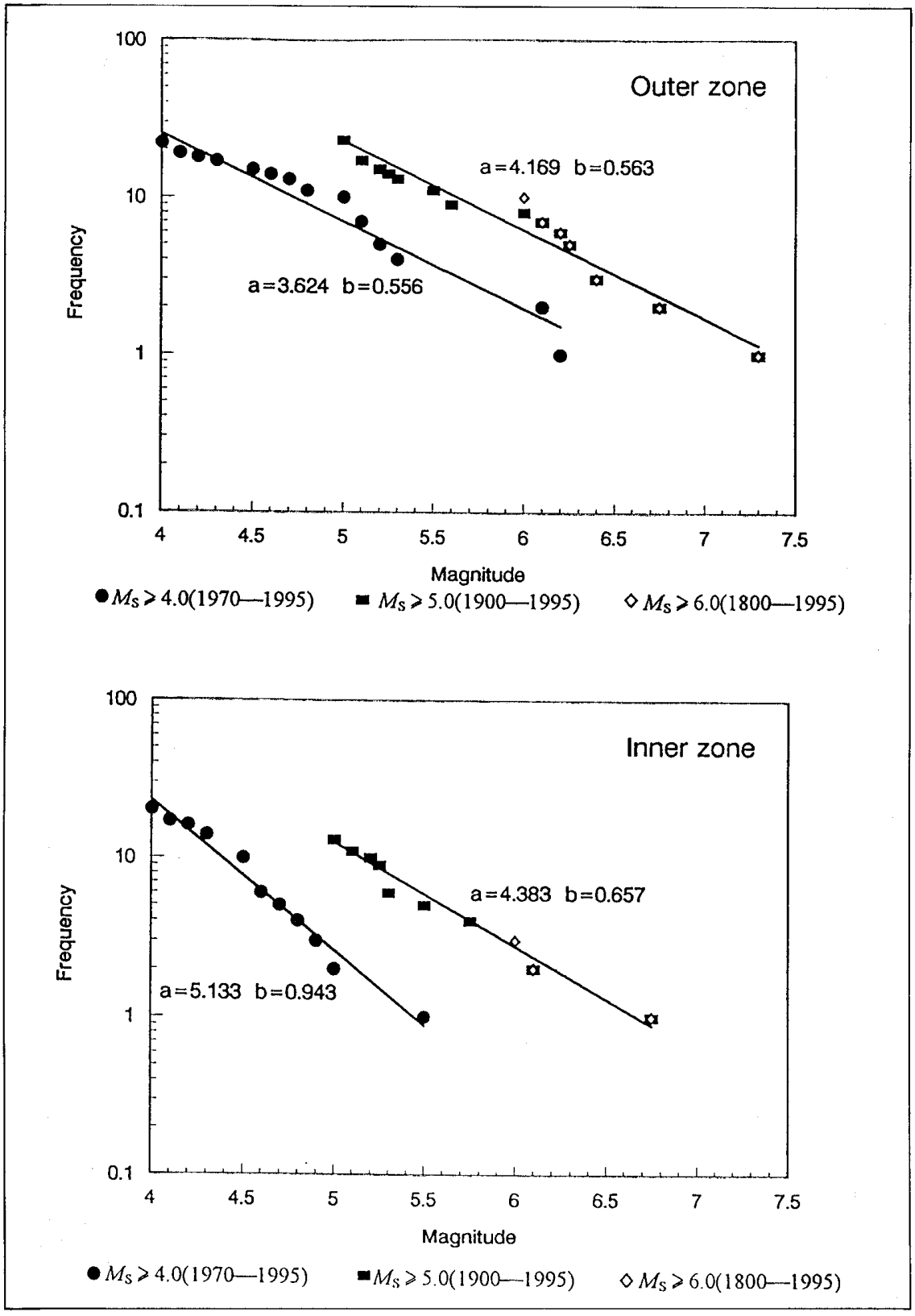

Figure 14 - b Values for the Southeastern Coastal Seismic Belt

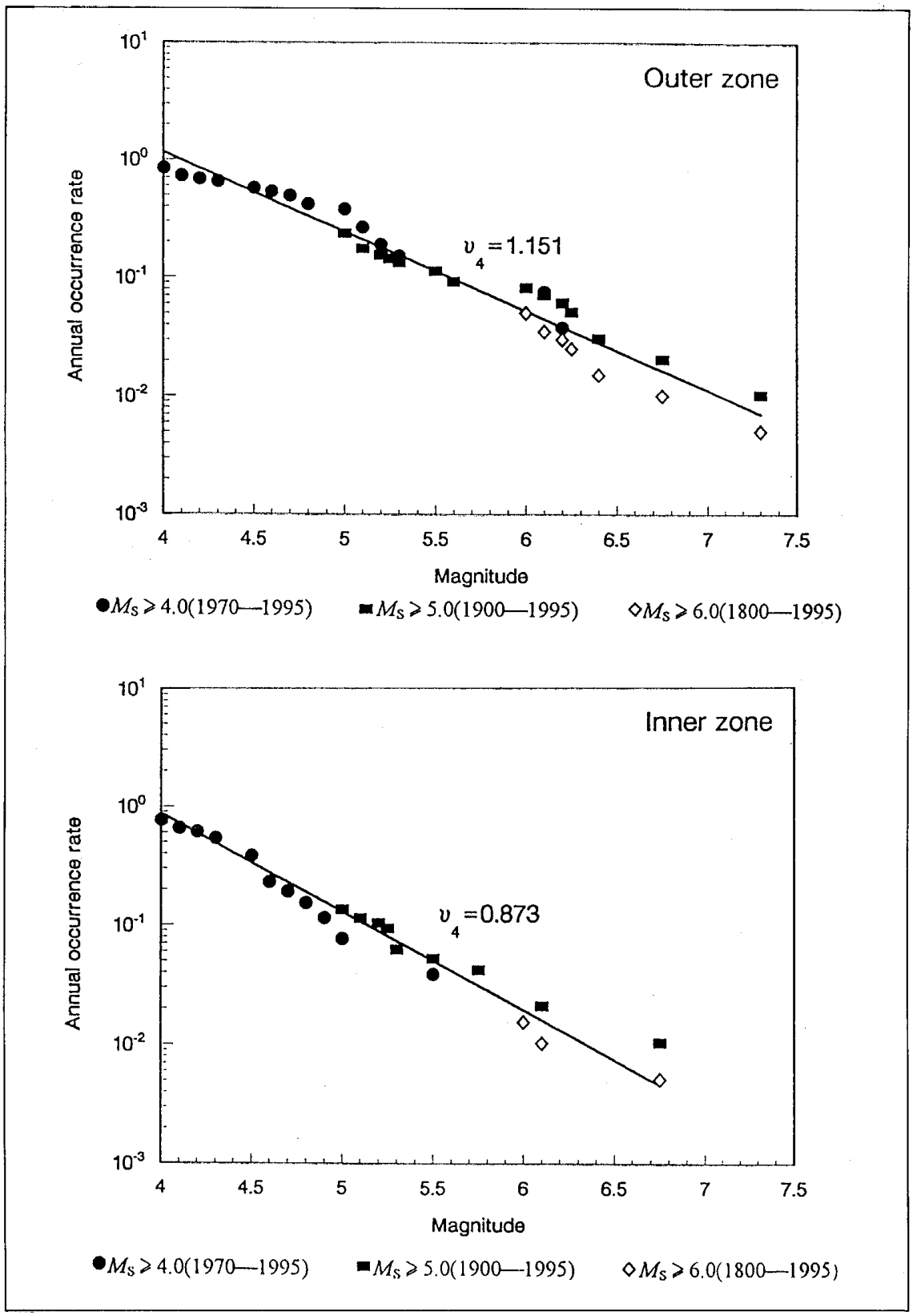

Figure 15 - Annual Occurrence Rate for the Southeastern Coastal Seismic Belt

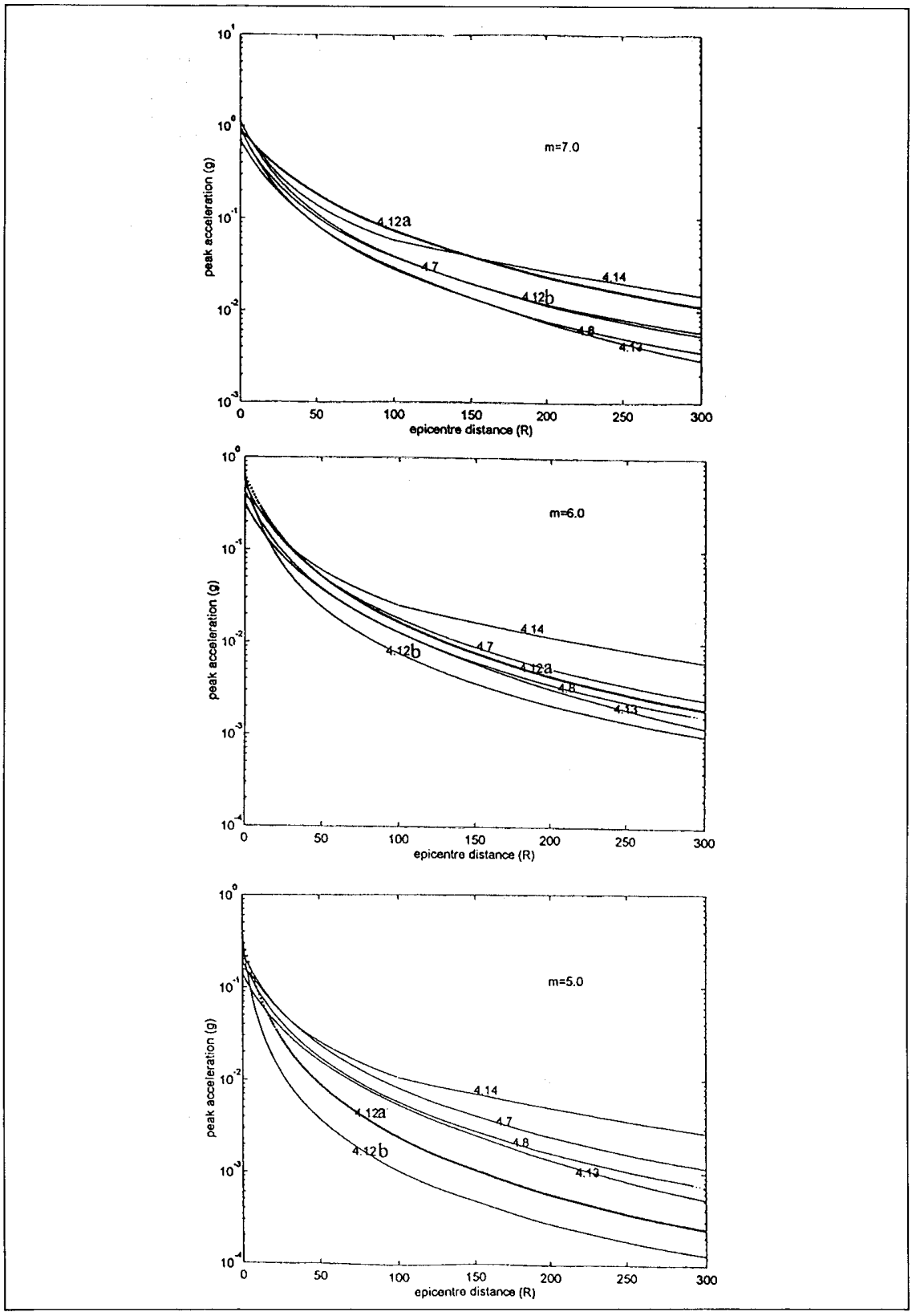

Figure 16 - Attenuation of PGA from Various Attenuation Relations

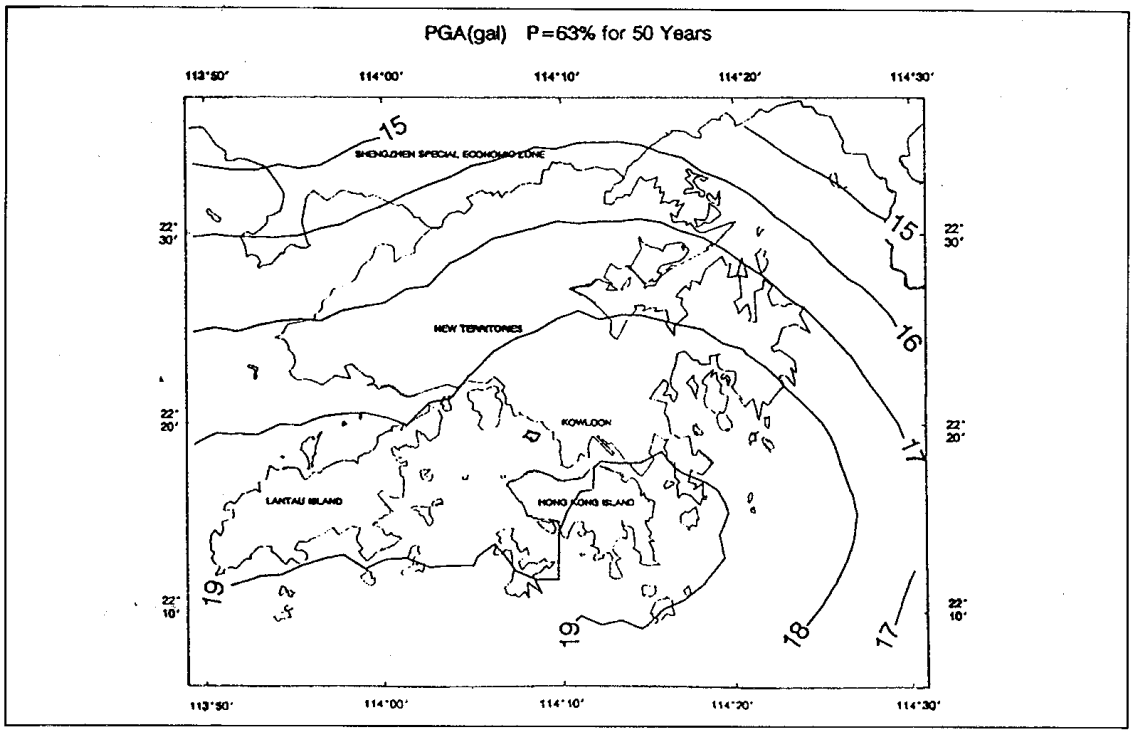

Figure 17 - 1 - Bedrock PGA Contours for 63% Exceedance in 50 Years

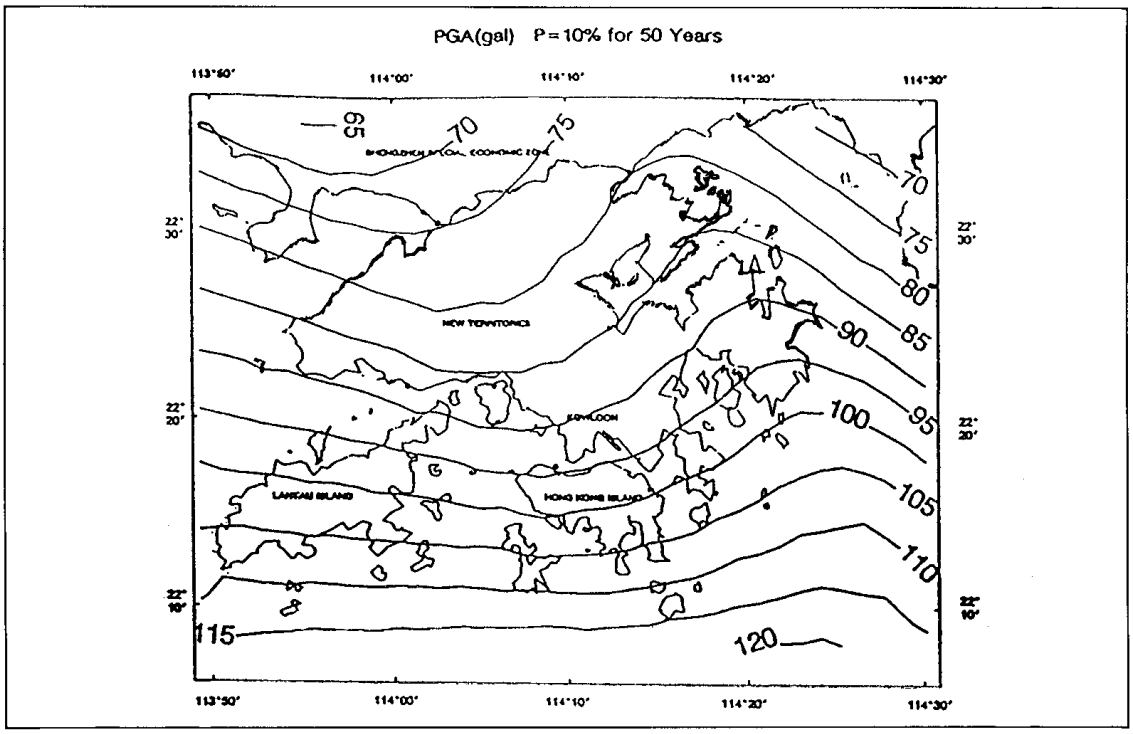

Figure 17 - 2 - Bedrock PGA Contours for 10% Exceedance in 50 Years

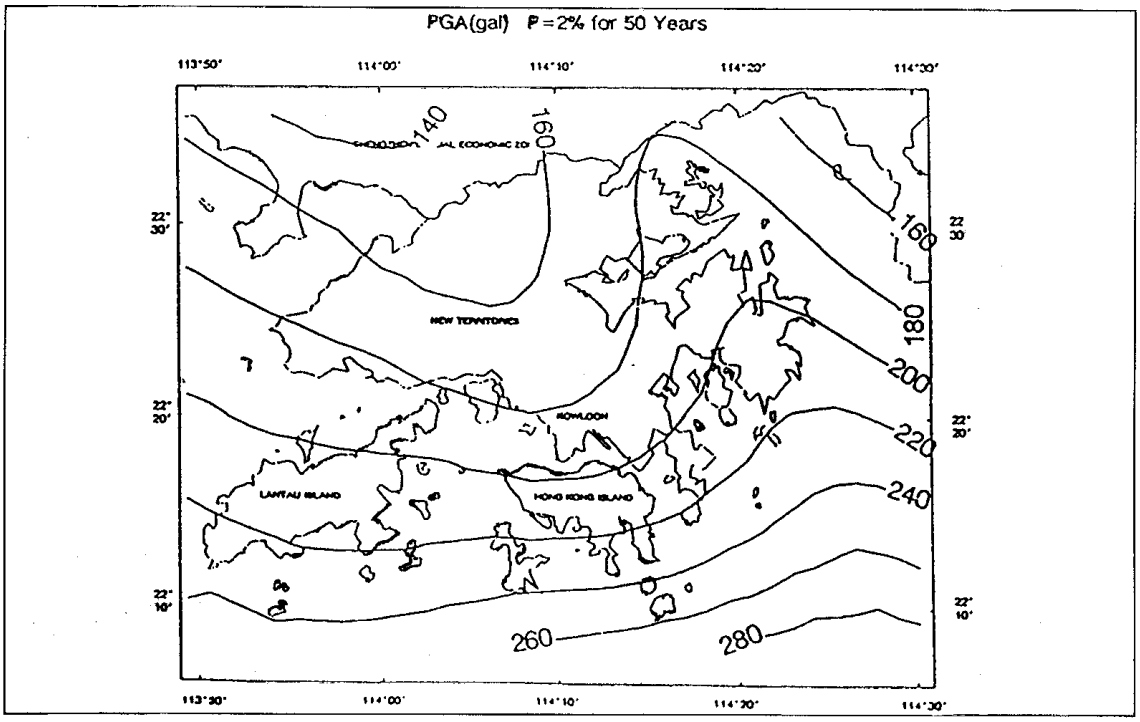

Figure 17 - 3 - Bedrock PGA Contours for 2% Exceedance in 50 Years

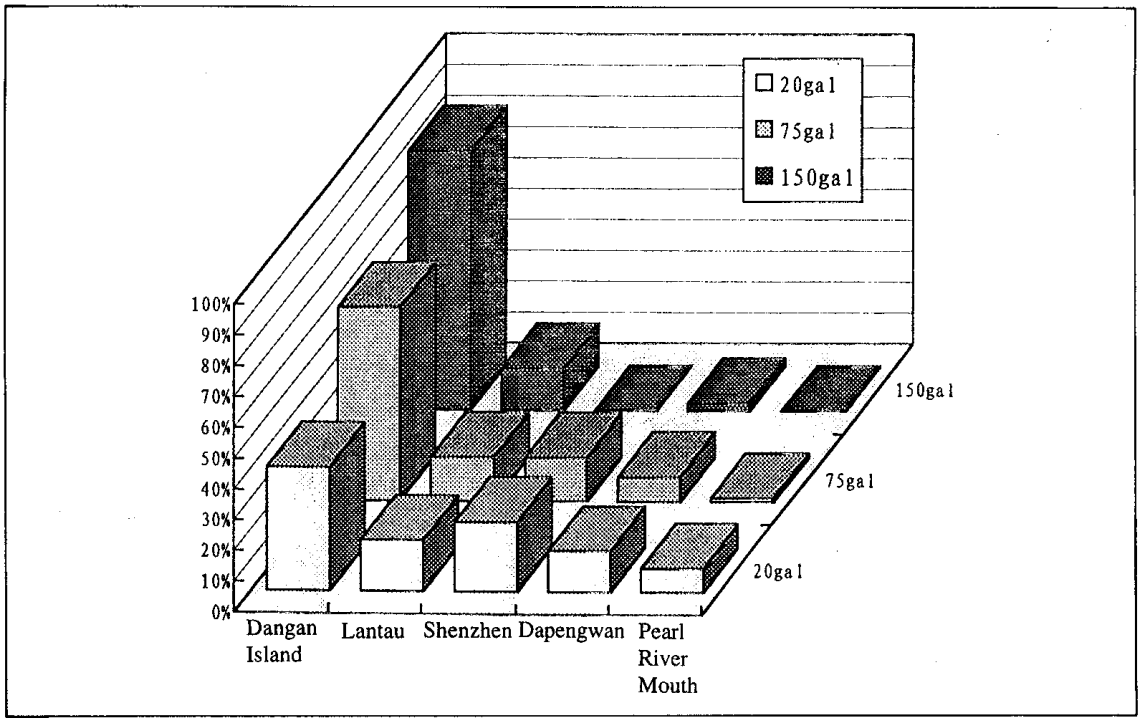

Figure 18 - Contributions to Bedrock PGA Values at Kowloon Site from Major Potential Source Zones

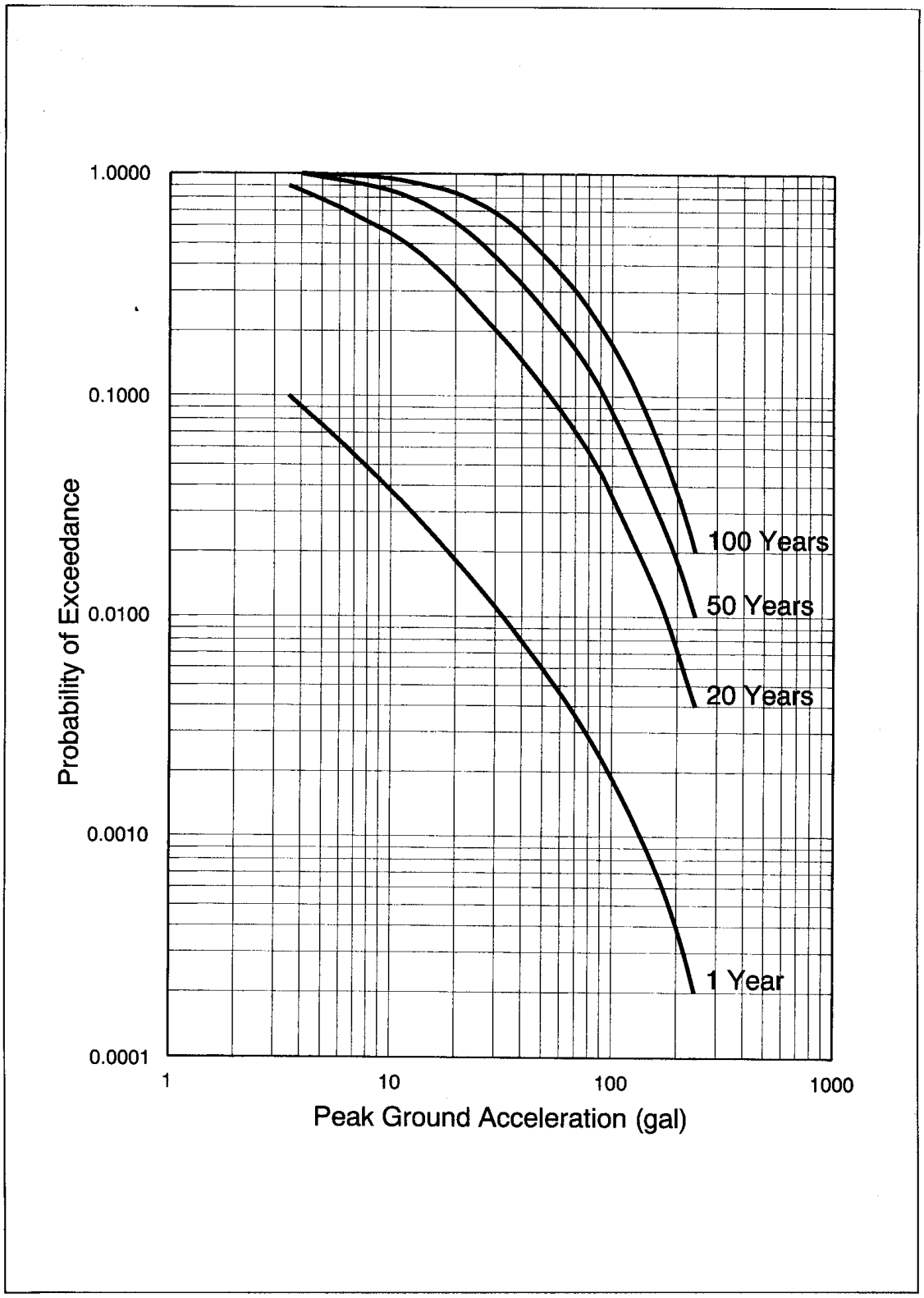

Figure 19 - Probability of Exceedance of PGA in 1, 20, 50 and 100 Years at Kowloon Site (114°10′ E, 22°19′ N)

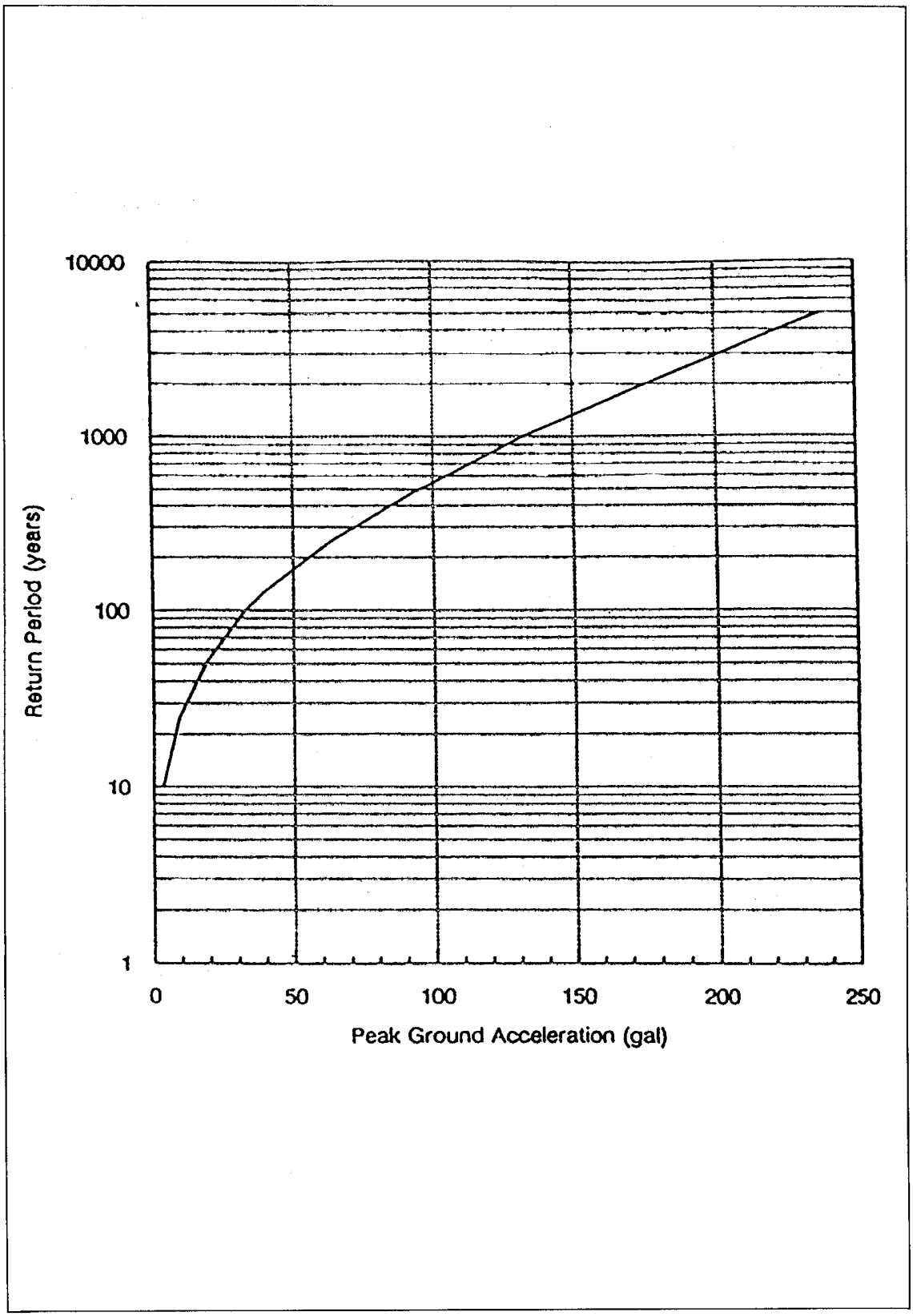

Figure 20 - Return Period of PGA at Kowloon

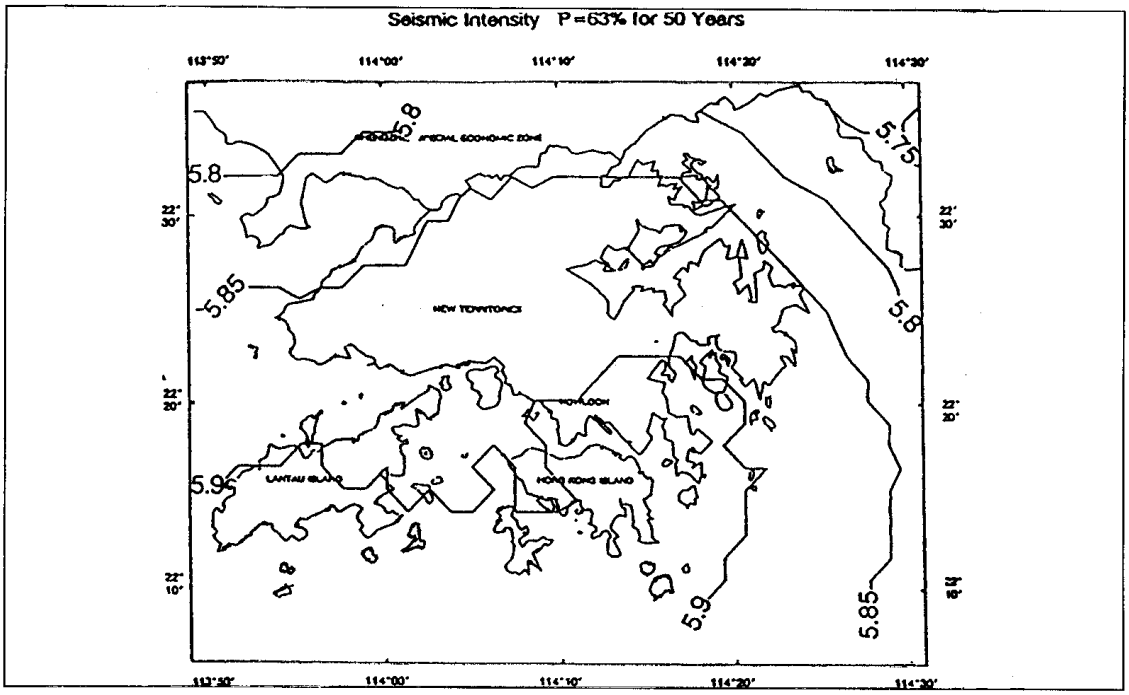

Figure 21 - 1 - Contour Map Showing the Regional Distribution of Seismic Intensity in Hong Kong

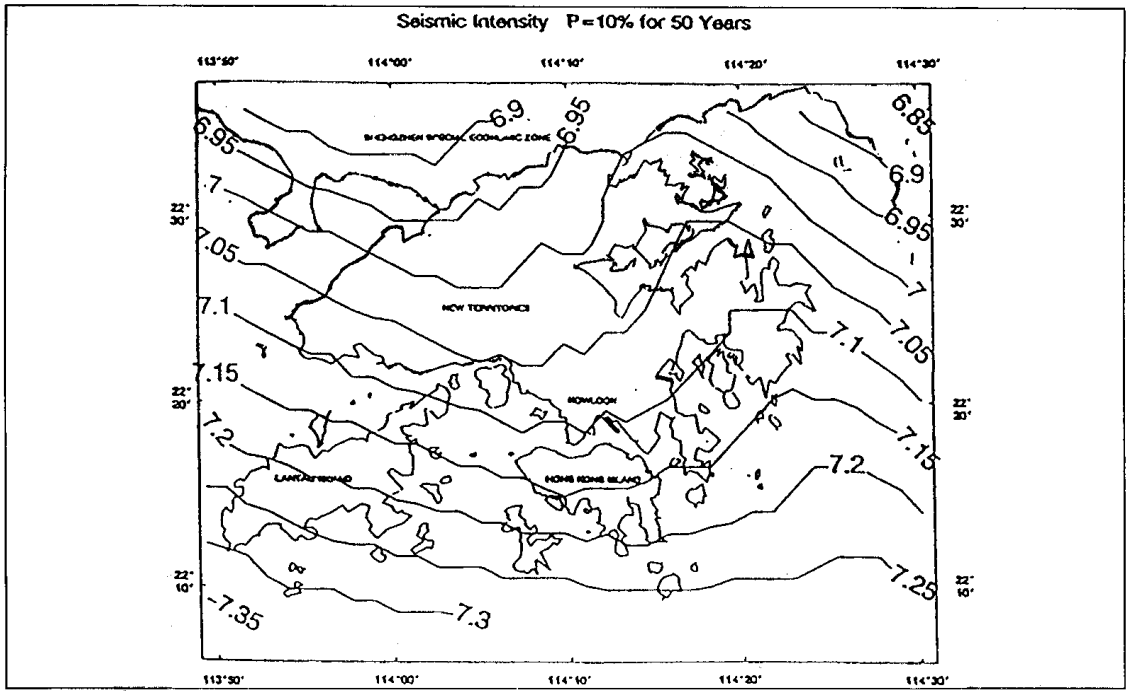

Figure 21 - 2 - Contour Map Showing the Regional Distribution of Seismic Intensity in Hong Kong

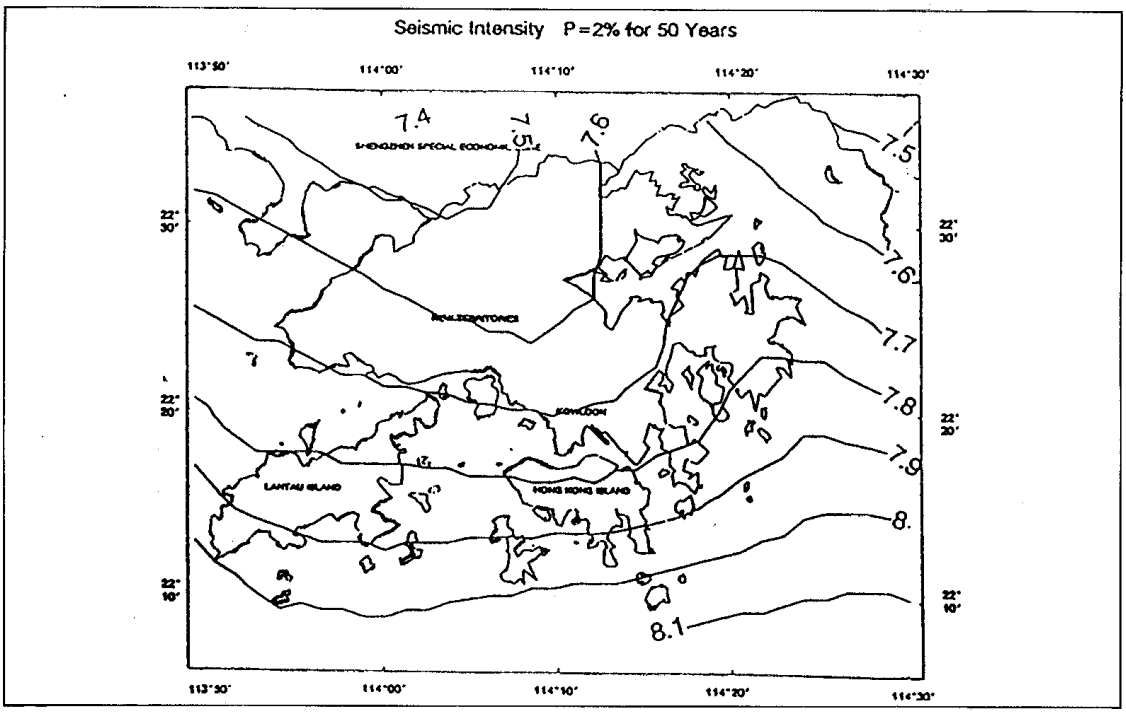

Figure 21 - 3 - Contour Map Showing the Regional Distribution of Seismic Intensity in Hong Kong

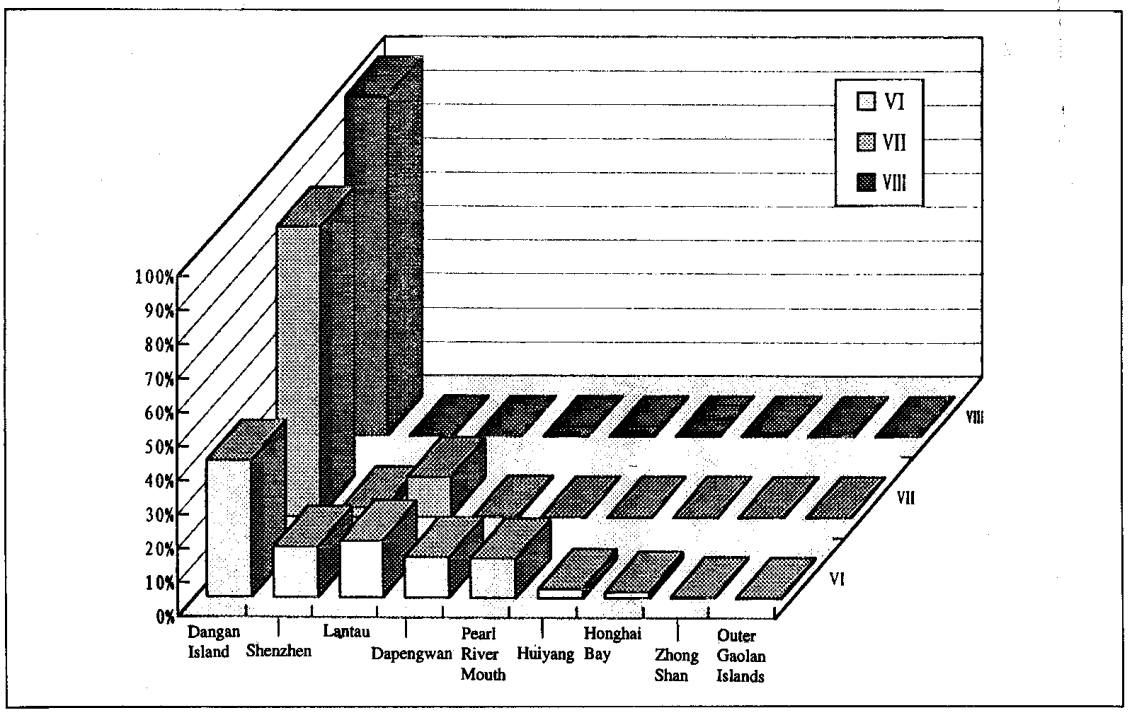

Figure 22 - Contributions to Intensity at Kowloon Site from Major Potential Source Zones

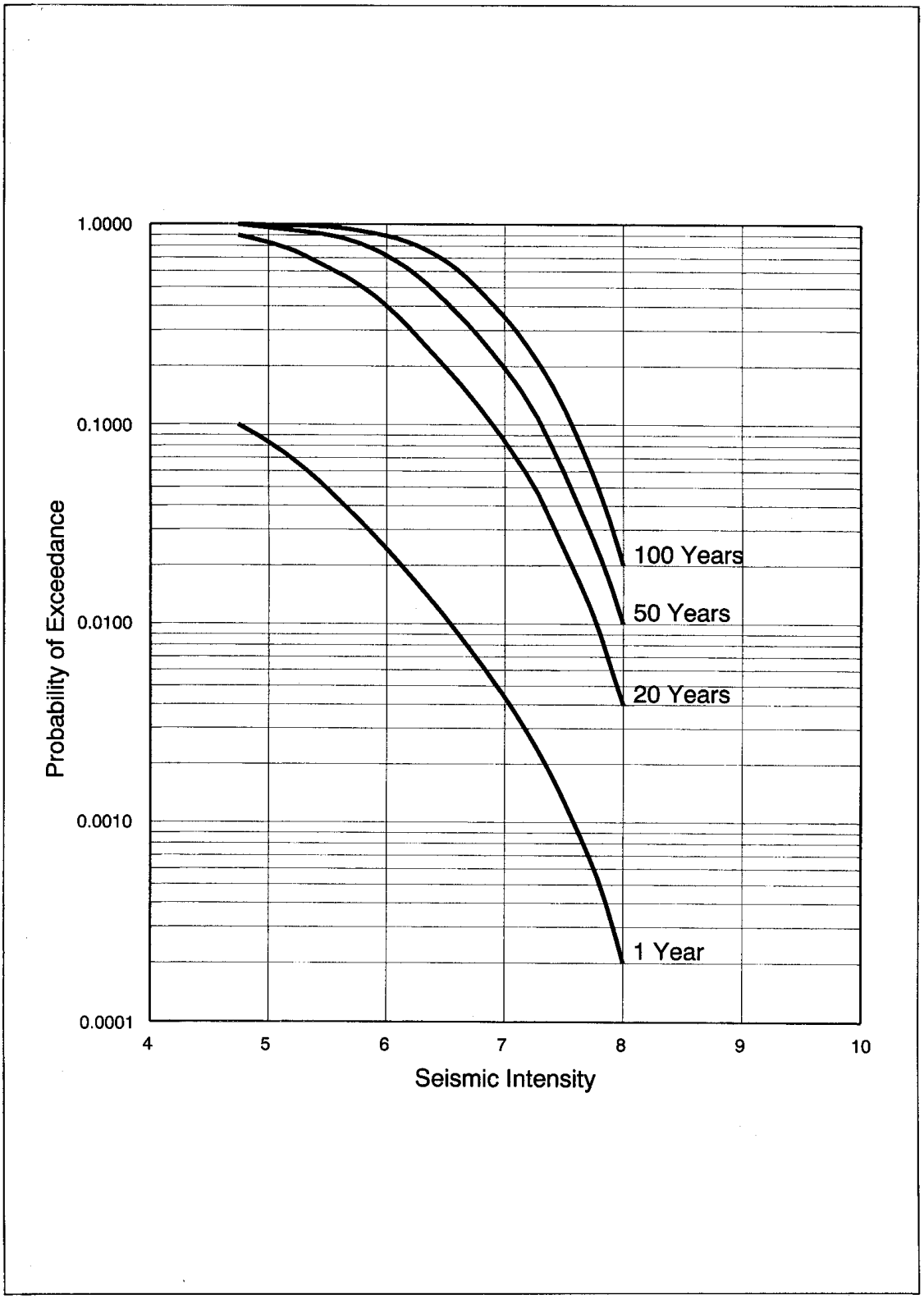

Figure 23 - Probability of Exceedance of Seismic Intensity in 1, 20, 50 and 100 Years at Kowloon Site (114°10′ E, 22°19′ N)

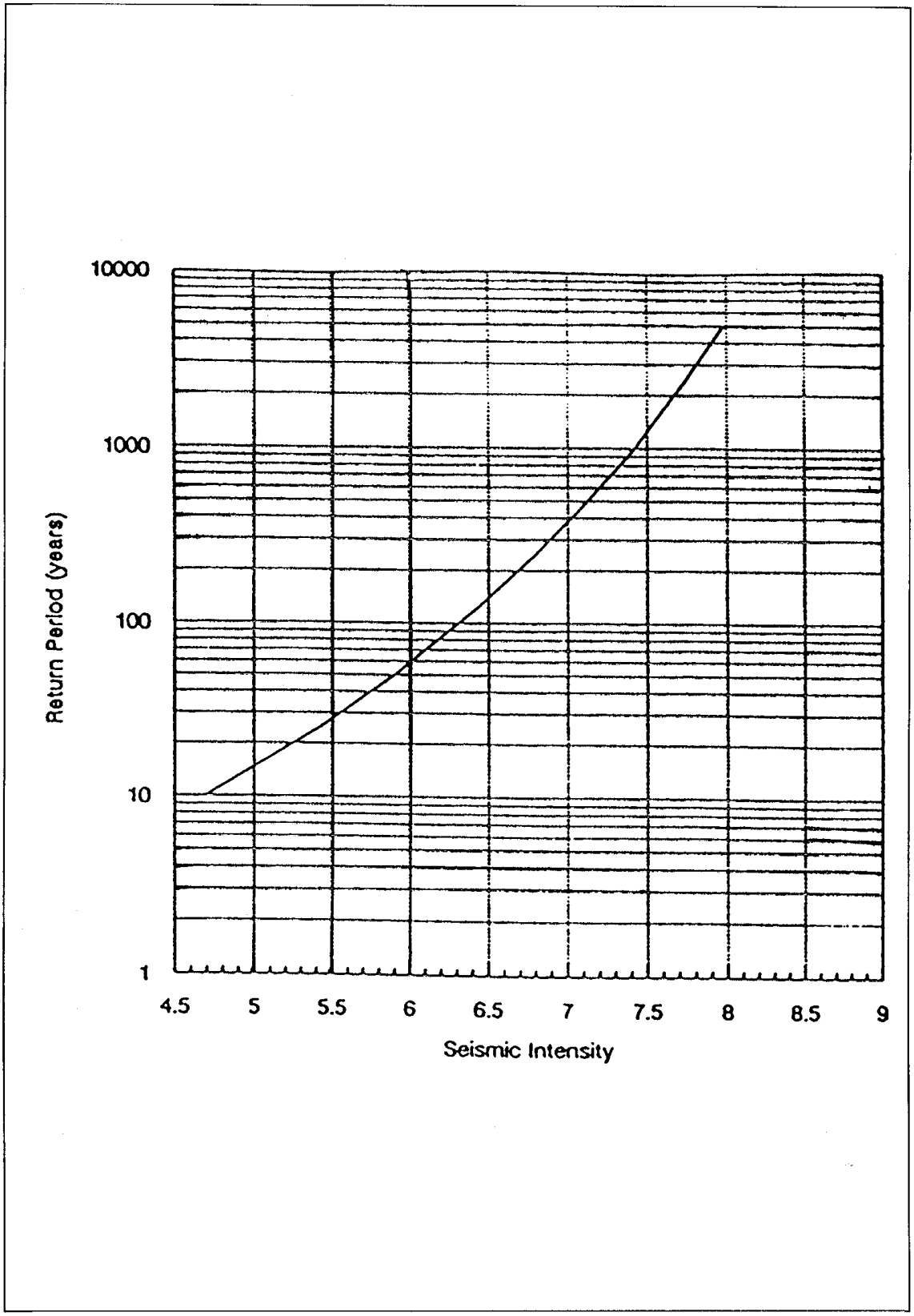

Figure 24 - Return Period of Seismic Intensity at Kowloon

香港地區地震危險性分析

李焯芬 丁原章 黃日恆
余演波 郭貴安 陳龐龍 及 黃新輝

序言

爲配合本處公開大眾感興趣的技術性文件的政策，我們將部份內部報告公開予公眾參考，並訂名爲土力工程處報告系列。這一系列報告是從本處僱員及我們委聘的顧問公司編寫的眾多報告中挑選出來，本報告也屬其中之一。報告的售價將用作補助印製成本。

土力工程處又出版指引文件，以及把大眾感興趣的研究結果編製成土力工程處刊物系列。政府新聞處負責銷售這些刊物和土力工程處報告系列，購買詳情載於本報告的末頁。

土力工程處處長
麥隆禮博士
一九九八年一月

前言

一九九五年六月，土力工程處批出了一份爲期一年的研究合約給香港大學（其分包合約顧問爲廣東省地震局），就香港地區的地震危險性進行分析。該項研究屬於土力工程處「工程地震」研究科目內的一個項目，於一九九五年七月展開，並由香港大學李焯芬教授與廣東省地震局丁原章教授共同領導。

一九九五年十二月，研究組人員向土力工程處提交了第一階段研究報告。該報告檢討及記錄了由廣東省地震局及其他來源提供的地震及地質相關資料。其後，研究組針對香港地區的情況進一步去深入研究。研究人員首先到現場進行了連串的地震地質考察，其後又研究了區內第四紀岩層的分佈、層位及岩土特徵。此外，又以分包合約形式，委託中國國家地震局地質研究所進行了熱釋光岩土年齡測定(20 項)、碳 14 岩土年齡測定(3 項)以及岩石薄片鑒定(22 項)。在研究過程中，又重新校核了從香港皇家天文台(於一九九七年七月改名爲香港天文台)取得的地震紀錄。研究組利用這些紀錄以及廣東地震局地震臺網的有關資料，編制成自一九七二年以來香港地區(東經 113°45′ - 114°45′；北緯 22°00′ - 23°00′) $M_L \geq 1.8$ 級的地震記錄。另外又對可能影響香港的潛在震源區及其地震活動性參數進行了分析，並且研究和比較了適用於本區的地震動衰減模型。最後，更對本區不同的地震動加速度峰值和地震烈度的超越概率和復發周期進行了計算分析。

香港天文台在整項研究期間提供了鼎力支持。黎權偉先生及潘偉強先生曾參與實地研究及協助研究組解決了許多有關的後勤問題。他們並聯同香港地質調查組的 Dr C.J.N. Fletcher 對本報告的初稿給予了很多寶貴的意見。

技術拓展部總土力工程師
彭沛來

摘要

在前人的研究基礎之上，本課題對香港周圍地區的潛在震源區及有關地震活動性參數作了研究和調整，對不同學者給出的衰減關系作了對比和分析。 經過初步計算后，以本課題的計算結果與近年不同學者在鄰近地區的工作成果作了比較，最后進行了不確定性分析。

本課題的主要結論是，香港地區 50 年超越概率 10% 的基岩水平加速度峰值界于 75 gal 和 115 gal 之間，九龍場點爲 92.7 gal ，本區各場點的地震基本烈度爲 VII 度。

目錄

第一章　區域地質構造背景

1.1 區域地質概況

珠江三角洲及其鄰近地區內出露了從震旦紀至第四紀各個時代地層，經歷了加里東旋迴、海西旋迴和印支—燕山旋迴等三個不同大地構造性質的發展階段，形成了褶皺基底、沉積蓋層和上迭盆地等三個基本構造層。其中燕山運動規模宏偉，活動强烈，影響深遠，出現大面積的中酸性岩漿侵入和噴發活動，形成頗爲壯觀的斷裂變質帶，產生一系列山間盆地，奠定了本區構造和地貌的基本輪廓。本區新構造運動是以斷裂繼承性活動和斷塊差异運動爲基本特征，以基性岩漿噴發活動爲特色。區內地殼厚度大部分地區爲30km以內，按照地震波速度和岩層密度，本區地殼結構由上而下可以分爲三層：第一層爲地殼表層，厚約1.4km，主要爲中—新生代陸相沉積層；第二層爲硅鋁層，厚約20km，由古生代地層、古老基底和花崗岩類組成；第三層爲硅鎂層，厚約11.1km，由玄武岩類岩石組成。第二層與第三層的界面爲康氏面，第三層與上地幔的界面爲莫氏面。

1.2 區域主要斷裂系統

區內斷裂構造發育，陸區主要有東西向、北東向和北西向三組(圖1)，南海北部近岸淺海區則有北東東向和北西向兩組。

東西向斷裂以高要—惠來斷裂帶爲代表，該斷裂帶分爲南、北二支㊀：北支爲鼎湖山—羅浮山斷裂，由西段廣利—三水斷裂㊀和東段瘦狗嶺—羅浮山斷裂組成。南支爲雲浮—惠來斷裂，由西而東可分爲四段：雲浮至高明段稱磉石—楊梅斷裂，主要表現爲燕山期黑雲母花崗岩和寒武系受其控制呈東西向分布；高明至東莞沙田段跨珠江三角洲被第四系復蓋，表現爲沿北江下游(順德水道、沙灣水道)呈東西向延

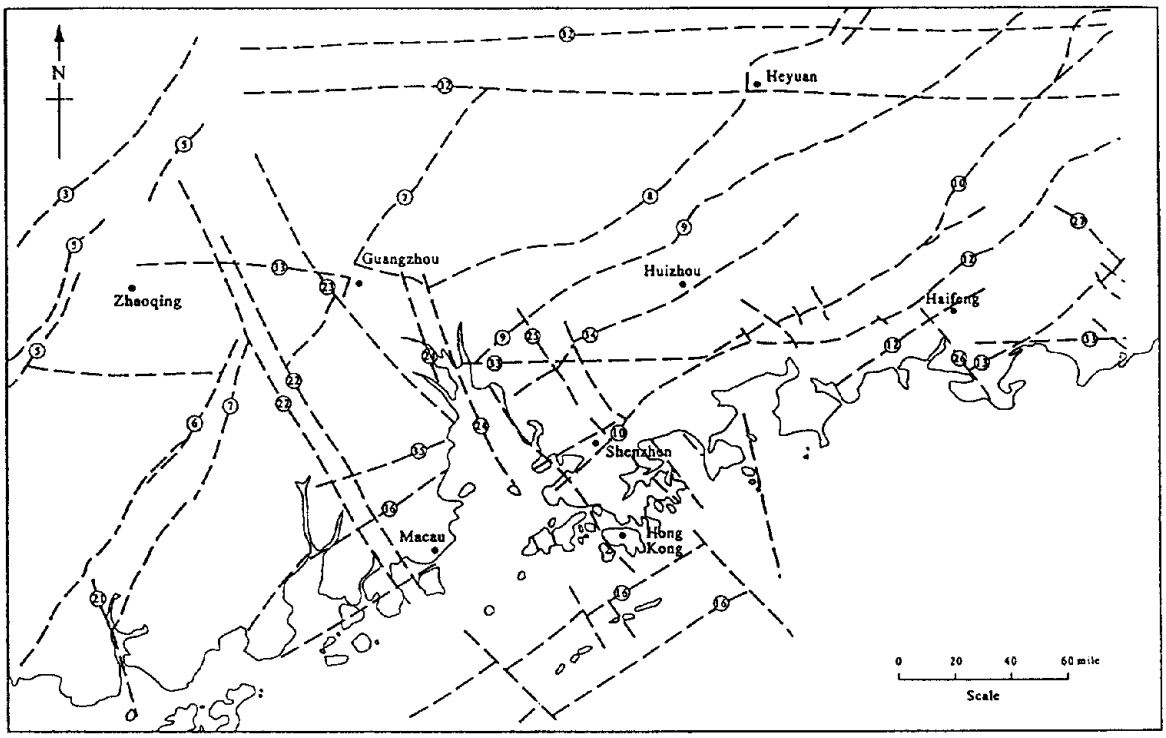

圖1　珠江三角洲地區主要斷裂分布圖

Fig.1　The Sketch showing the location of the faults in the Pearl River delta area

伸;東莞沙田至海豐長埔段稱樟木頭—長埔斷裂⑫,主要表現爲高基坪群火山岩沿斷裂呈東西向延伸;長埔至惠來段稱海豐—惠來斷裂⑬，它控制海豐—陸豐—惠來第四紀盆地呈東西向分布．高要—惠來斷裂帶的最新活動年代(據熱釋光測年資料)爲9萬—44萬年，即中更新世中期至晚更新世早期仍有明顯活動.

北東向斷裂由東而西主要有五華—深圳斷裂⑩、紫金—博羅斷裂⑨、河源—東莞斷裂⑧、從化—廣州斷裂⑦等．這組斷裂强烈活動于燕山期，沿斷裂帶形成一系列中—新生代半地塹盆地，如紫金—博羅斷裂的古竹盆地，河源—東莞斷裂的河源—楊村盆地，從化—廣州斷裂的太平盆地、龍歸盆地．第四紀時期斷裂活動有所減弱.

北西向斷裂由東而西有東莞—深圳斷裂㉓、珠江口斷裂㉔、白坭—沙灣斷裂㉕、西江斷裂㉖等．這組斷裂形成較晚、活動較新，控制水系、港灣和第四系的發育，如珠江三角洲斷陷盆地的東西兩側就受控于珠江口斷裂和西江斷裂。沿西江斷裂出現多個第四紀沉降中心，第四系等厚綫呈北西向展布。北西向斷裂的最新活動年代，據熱釋光等測年資料結果，一般爲10萬年左右，即在晚更新世早期有明顯活動，局部地段在晚更新世中晚期仍有活動，故此北西向斷裂是活動斷裂.

北東東向斷裂以濱海斷裂⑫爲代表，該斷裂控制了珠江口外盆地的發生和發展，使其接受了厚達7000m的上第三系和厚約250m的第四系沉積，地層等厚綫呈北東東向分布．海洋地球物理勘探資料(廣州海洋地質局，1992年)表明，該斷裂切割了第四系(圖2)，應是第四紀有過活動的斷裂。

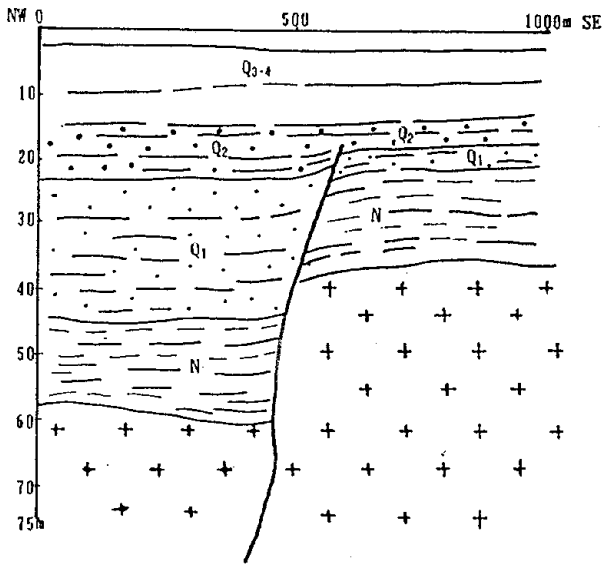

圖2　多道地震顯示濱海斷裂切斷第四系下部

(在擔杆列島以南)　(據廣州海洋地質局資料)

Fig.2　Quaternary system cut by fault showing from multichannel seismic survey at the south of Dangan Islands(by the data of Ocean-Geology Bureau of Guangzhou)

1.3 香港及鄰近地區的構造盆地

由于斷塊差异運動，形成若干山間盆地或谷地，這些盆地主要受斷裂控制，故爲斷陷盆地。最主要的盆地有以下幾個(圖3):

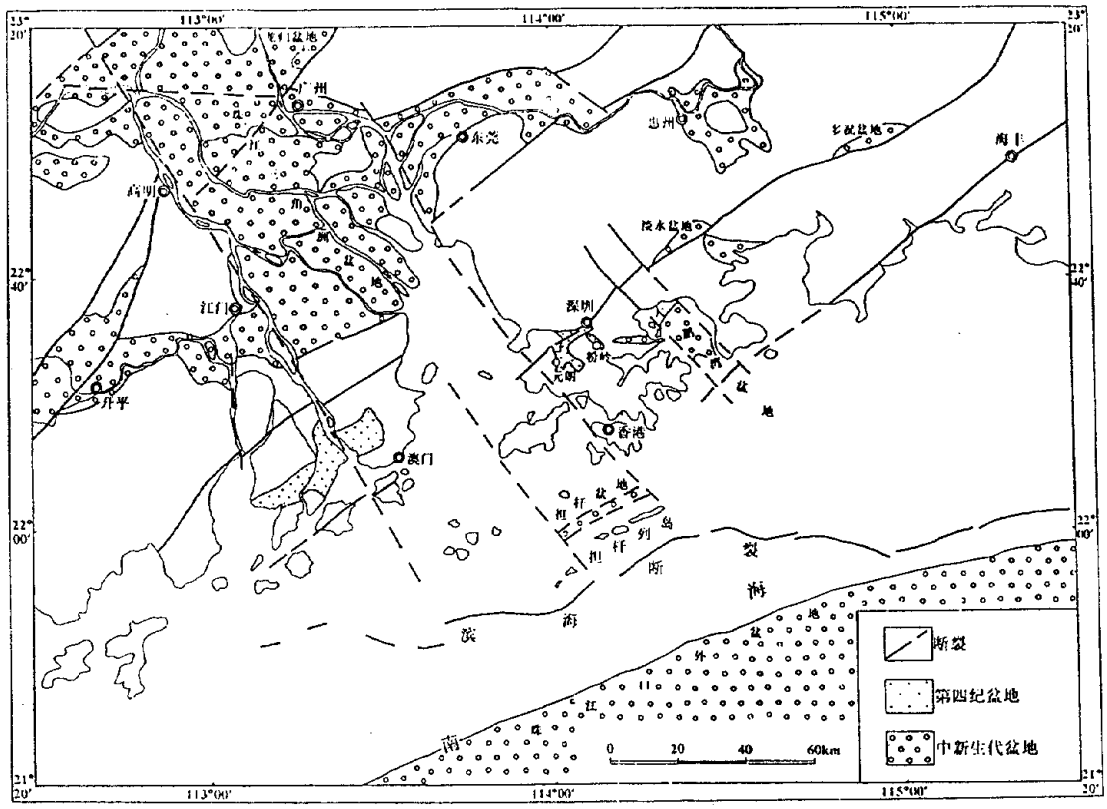

圖3　香港及鄰近地區的主要構造盆地分布圖

Fig.3　The map showing the location of the main basins in Hong Kong and vicinities

多祝盆地和淡水盆地：受控于北東向五華—深圳斷裂，爲半地塹式的斷裂盆地，主要由上白堊統組成。

龍歸盆地：受控于北東向從化—廣州斷裂，爲半地塹式的斷裂盆地，主要由下第三系組成。

珠江三角洲盆地：該盆地是在三水、東莞和新會三個白堊紀—第三紀紅色盆地的基礎上發展起來的第四紀盆地，發育六個第四紀凹陷：1、東莞凹陷，繼承了白堊紀至第三紀的東莞盆地，沉積中心第四系厚約35—45m；2、三水凹陷，繼承了白堊紀至第三紀的三水盆地，

沉積中心第四系厚約30—40m; 3、順德凹陷，繼承了早白堊紀的紅色盆地，沉積中心第四系厚約30—40m; 4、中山凹陷，是喜馬拉雅山期運動所形成的新凹陷，沉積中心第四系厚約40—60m; 5、新會凹陷，繼承了白堊紀至第三紀的新會盆地，沉積中心第四系厚約30—35m; 6、斗門凹陷，是一個第四紀新生的沉降幅度最大的凹陷，第四系最厚達64m。

大鵬灣盆地：是一個中—新生代的斷陷盆地，東部受控于葵涌—西涌斷裂，西部受控于吉澳洲—赤洲斷裂，由上白堊統赤洲組礫岩和粗砂岩夾粉砂岩以及下第三系平洲組深灰色薄層粉砂岩和白雲質粉砂岩夾泥岩組成。

擔杆盆地：位于擔杆島北面，受北東東向擔杆島斷裂控制，由下第三系類磨拉石建造組成。

珠江口外盆地：位于珠江口外海域，受北東東向濱海斷裂控制，是在第三紀斷陷盆地的基礎上發展起來的新生代盆地，沉積了厚達8000—10000m的碎屑岩層夾含油層。本盆地在第四紀期間仍然不斷沉降，其北側則爲萬山群島隆起區，反映差异升降運動明顯。

此外，在粉嶺和元朗有比較發育的第四紀河流冲積層，^{14}C和熱釋光測年均證明它們爲距今16298±831—32500±490年的産物。

1.4 香港地區的斷裂活動性

香港地區斷裂十分發育，主要有北東向、北西向和北東東向三組斷裂(圖4)。

1. 北東向斷裂

這組斷裂主要有4條斷裂帶，它們是蓮花山斷裂帶的組成部分，由南東而北西，依次排列爲：

(1)蒲臺(Po Toi)斷裂帶

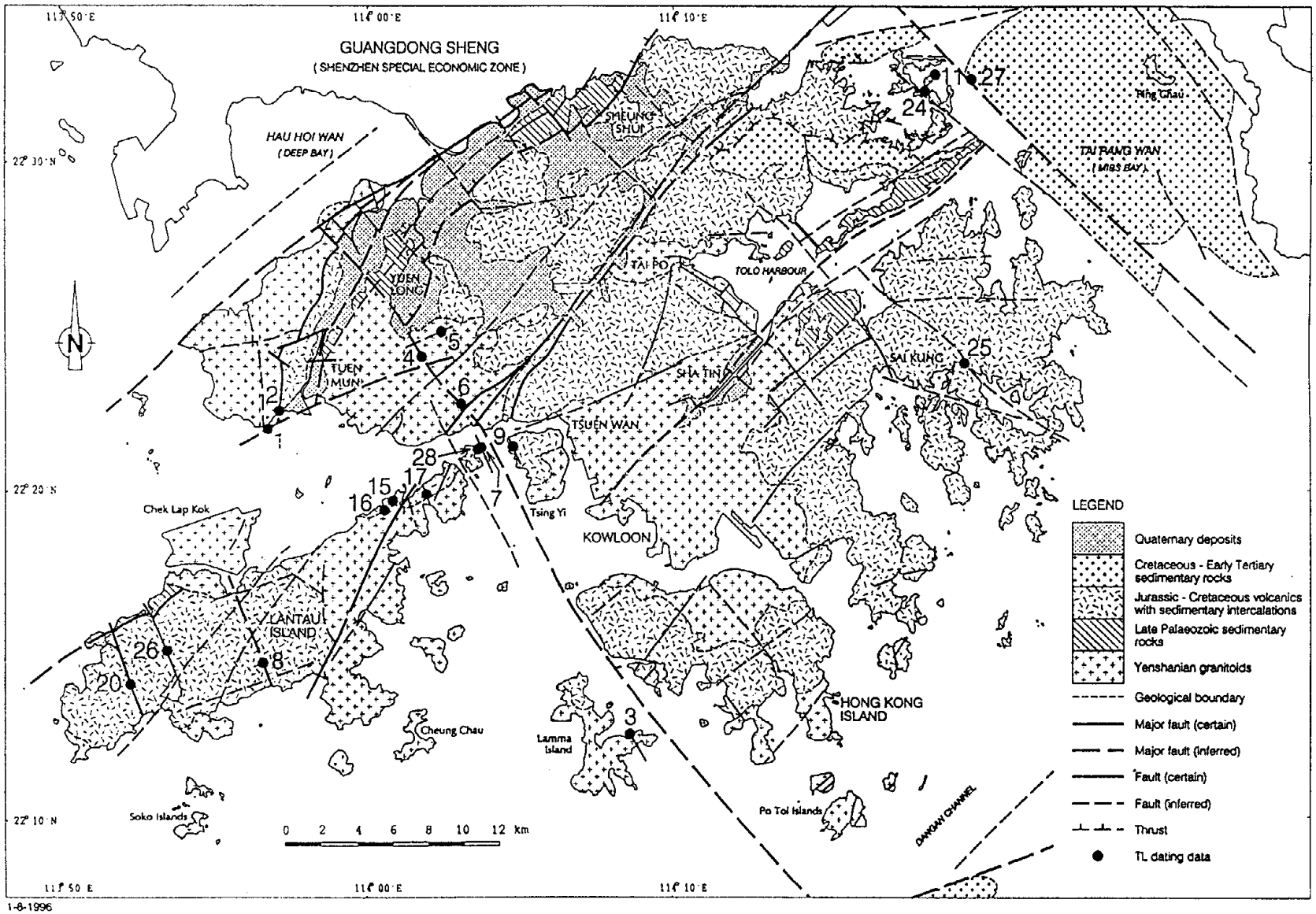

圖 4　香港主要斷裂的熱釋光測年資料　　地質資料據香港土力工程處

Fig.4　TL dating data of fault Syetems in Hong Kong　　Geological data from Hong Kong Geological Survey

本斷裂在擔杆島和蒲臺島之間的海峽通過，往東北延伸經惠東平海半島南、海豐至大埔，組成蓮花山斷裂帶的東南分支斷裂束。斷裂走向北東50°，傾向南東，傾角60°—70°，斷裂的西南段被北東東向擔杆島斷裂切斷。

(2)荔枝角(Lai Chi Kok)——赤門海峽(Tolo Channel)斷裂帶

本斷裂西南起于九龍荔枝角，往東北經沙田延入沙田海，被北西向斷裂錯動，往西南延入東博寮海峽被北西向流浮山—東博寮海峽斷裂所截。斷裂走向北東40°—50°，傾向南東，傾角75°—80°。

(3)沙頭角(Sha Tau Kok)—貝澳灣(Pui O Wan)斷裂帶

這條斷裂帶走向北東30°—50°，傾向北西，傾角60°—70°，控制海峽和谷地發育。主要由四條斷裂組成。

a 沙頭角(Sha Tau Kok)—深井(Sham Tseng)斷裂：由沙頭角向西南延伸經林村河谷至深井。

b 麻雀嶺(Ma Tseuk Leng)—小欖(Shiu Lam)斷裂：北起麻雀嶺向西南經和合石、大欖涌水塘至小欖。

c 陰澳灣(Yam O Wan)—貝澳灣(Pui O Wan)斷裂：北起大嶼山北側陰澳灣，往西南經梅窩至大嶼山南側貝澳灣。

d 東涌(Tung Chung)—石壁(Shek Pik)斷裂：北起大嶼山北側的東涌往西南經木魚山至大嶼山南面的石壁。

(4)羅湖(Lo Wu)—屯門(Tuen Mun)斷裂帶

位于新界西北部、深圳灣東南岸，往北東經五華延至梅縣，往南西延伸到澳門南至高欄島，組成蓮花山斷裂帶的西北分支斷裂束。斷裂束由五條斷層組成。

a 新田(San Tin)斷裂：走向北東40°，傾向北西，傾角35°—50°。

b 羅湖(Lo Wu)斷裂：由屯門經元朗至羅湖，由一系列次級平行斷層組成，如橫洲(Wang Chau)—山下村(Shan Ha Tsuen)斷層、豬黃嶺(Chu

Wong Leng)—欖口(Lam Kau)斷層。它控制后海灣(Deep Bay)，元朗(Yuen Long)平原和屯門(Tuen Mun)河谷的發育。

c 屯門(Tuen Mun)斷裂：由屯門延伸到深圳河口，走向由西南段的北東15°到東北段北東40°。

d 青山(Tsing Shan)斷裂：起于屯門西面Pak Kok，經青山東側延伸至深圳河口，斷裂西南段走向北東10°—20°，傾向北西，傾角40°—50°，東北段走向北東50°—55°，傾角50°—67°。在蝴蝶灣西側海灘(1316 2552)取得的斷裂物質經熱釋光測年爲26.55萬 ± 2.1萬年(表1)[1][注]。

e 流浮山(Lau Fau Shan)斷裂：走向北東60°，傾向北西，傾角51°—67°，在流浮山至尖嘴咀沿斷層出現一條寬20m，長4km的石英脈。

2. 北東東向斷裂

這組斷帶有兩條斷裂帶，由北而南爲：

(1)青山灣(Tsing Shan Wan)—大埔海(Tai Po Hoi)斷裂帶

主要由兩條斷裂組成。

a 青山灣(Tsing Shan Wan)—河背水塘(Ho Pui Reservoir)斷裂

該斷裂由屯門南面以北東65°—70°方向經大欖涌水塘到河背水塘。斷裂西段錯斷北東向青山斷裂和屯門斷裂。在元朗南坑排南900m處(2170　3016)，一條NEE向斷裂取得的斷層物質經熱釋光測年爲9.47萬 ± 0.81萬年。在蝴蝶灣西側海灘(1316　2552)取得斷裂物質經熱釋光測年爲11.08萬年。

b 東涌(Tung Chung)—大埔海(Tai Po Hoi)斷裂

斷裂西起大嶼山島東涌，往東沿大嶼山北邊經荃灣延入大埔海。在大嶼山島北側陰澳篤(Yim O Tuk)(1960　2072)其中一條平行的小斷裂采樣，經熱釋光測年，斷裂最新一期强烈活動距今爲8.2萬 ± 0.68萬年。

---

[1] 注：学者们对用热释光方法测定断层的活动年代尚有不同意见，请引用本数据时注意。

Thermoluminescnce Dating Result

1.08.96

No.	Field No.	Location	Coordinates		Depth m	Elevation mPD	Landform	Soil Type	Laboratory Code	TL age Year BP	Fault Type
			Easting	Northing							
1	TM 01	West of Wu Tip Wan	13160	25520	0.1	3	Seashore	Quartz Vein ,Fault material	LG 225	110,800	NEE
2	TM 02	West of Wu Tip Wan	13160	25540	0.1	3	Seashore	Fault material	LG 226	265,500 ± 21,000	NNE
3	MT 06	Mo Tat Wan,Lamma Island	33140	07860	0.1	4	Seashore	Fault material	LG 227	177,700 ± 15,100	NW
4	TT 09	1.5 km south of Tai Tong	21000	29420	0.1	30	Stream	Fault breccia	LG 228	105,100 ± 8,700	NW
5	NH 10	900m south of Nam Hang Pai	21700	30160	0.1	100	Stream	Fault material	LG 229	94,700 ± 8,100	NEE
6	TL 012	Tsing Lung Tau	23560	25940	0.1	110	Stream	Fault breccia	LG 230	91,100 ± 7,500	NW
7	MW 16	Cheung Tsui, Ma Wan	24650	23700	0.1	5	Seashore	Fault material	LG 231	93,900 ± 7,900	NW
8	TC 17	Milestone 4, Tung Chung Road	12430	11740	0.1	220	Gully	Fault material	LG 232	101,000 ± 8,600	NW
9	TY 20	Tsing Yi	26360	23760		20	Bridge pier	Calcite vein	LG 233	222,260 ± 17,800	NW
10	FX 22	Fei Shue Ngam	50400	45450	0.1	5	Wave eroded cave	Fault breccia	LG 234	>1,000,000	NW
11	WN 24	Wong Nai Chau	50160	44660	0.1	4	Wave eroded cave	Fault gouge	LG 235	196,100 ± 16,900	NW
12	YL 26	Shan Ha Tsuen	19180	32100			Terraced alluvium	Upper layer silty fine sand	LG 236	23,800 ± 2,000	
13	YL 28	Shan Ha Tsuen	19180	32100			Terraced alluvium	Lower layer silty fine sand	LG 237	29,300 ± 2,300	
14	YL 29	400m west of Shan Ha Tsuen	18940	32000			Terraced alluvium	Upper layer silty fine sand	LG 238	20,500 ± 1,700	
15	YO 31	Yim O Tuk	19700	20720	0.1	40	Slope	Fault material of quartz vein	LG 239	33,300 ± 2,700	NW
16	YO 32	Yim O Tuk	19600	20720	0.1	40	Slope	Fault gouge	LG 240	82,000 ± 6,800	NEE
17	CK 34	Ngong Shuen Au	21380	21240	0.1	50	Gully	Fault material	LG 241	147,500 ± 11,800	NW
18	TO 36	Po Chue Tam, Tai O	04140	13440	1	3	Terraced alluvium	Upper layer silty sand with cobbles	LG 242	24,400 ± 20,000	
19	TO 37	Po Chue Tam, Tai O	04140	13440	4	0.2	Terraced alluvium	Lower layer silty sand with gravel	LG 243	126,100 ± 10,100	
20	TO 38	Ngau Kwo Tin	05240	11060	0.1	130	Gully	Fault material	LG 244	278,700 ± 23,100	NW
21	FX39	Fei Shue Ngam	50400	45450	0.1	5	Wave eroded cave	Fault breccia	LG466	190,600 ± 15,800	NW
22	FX40	Fei Shue Ngam	50400	45450	0.1	5	Wave eroded cave	Fault breccia	LG467	201,800 ± 16,100	NW
23	FX41	Fei Shue Ngam	50400	45450	0.1	5	Wave eroded cave	Fault breccia	LG468	177,500 ± 13,300	NW
24	WM42	Wang Mun Hoi	49500	43900	0.1	6	Wave eroded cave	Fault breccia	LG469	254,500 ± 20,400	NW
25	PT44	Pak Tam Chung	51780	28660	0.1	30	Stream	Fault breccia	LG470	118,700 ± 9,700	NW
26	SW45	Shum Wat Wan	07285	12585	0.1	230	Stream	Fault breccia	LG471	196,800 ± 16,300	NW
27	PS46	Pak Sha Chau	52150	44560	0.1	6	Wave eroded cave	Fault breccia	LG472	188,500 ± 15,400	NW
28	MW50	Ma Wan	24580	23860	0.1	5	Seashore	Fault breccia	LG473	126,200 ±10,300	NW

Notes: Samples collected by Guangdong Seismological Bureau
Test by thermolumuiescence laboratory, Institute of Geology, State Seismological Bureau,Beijing, China
TL Thermoluminescence dating

(2)擔杆島斷裂帶

位于擔杆島北面，這條斷裂屬于濱海斷裂的一部分．沿北東70°延伸．它控制擔杆海峽沉積盆地。

3．北西向斷裂

本區北西向斷裂非常發育，分布頗廣，主要有三條斷裂帶，分別位于九龍半島東部和西部。

(1)吉澳洲(Kat O Chau)—赤洲(Chek Chau)斷裂帶

位于大鵬灣西側，主要由兩條斷裂組成:

a 鷄公頭(Kai Kung Tau)—羊角頭(Yeung Kok Tau)斷裂

自吉澳洲鷄公頭至赤洲羊角頭一帶，該斷裂呈北西310°展布，斷裂的東北盤下降，形成大鵬灣中新生代沉積盆地。

b 吉澳(Kat O)—弓洲(Kung Chau)斷裂

北起于吉澳洲深涌，往南東穿過橫門海、直門頭、黄竹角咀、赤洲口至沙排。

在黄泥洲(5016　4466)采樣經熱釋光測年得知，斷裂最新一次活動距今爲19.6萬 ± 1.69萬年。

(2)流浮山(Lau Fau Shan)—東博寮海峽(East Lamma Channel)斷裂帶

位于流浮山、深井、南丫島一帶，由一系列平行排列的斷層組成。

在元朗大棠(2100　2942)所取樣品的熱釋光測年，數據爲10.51萬 ± 0.87萬年; 在深井青龍頭(2356　2594)所取得斷層樣品的熱釋光測年數據爲9.11萬 ± 0.75萬年; 在馬灣島長咀(2465　2370)所取斷層的熱釋光測年數據爲9.39萬 ± 0.79萬年; 在青衣島西端(2636　2376)所取斷層的熱釋光測年數據爲22.22萬 ± 1.78萬年; 在大嶼山島昂船洲(2138　2124)所取斷層物質的熱釋光測年數據爲14.75萬 ± 1.18萬年; 在南丫島模達灣(3314　0786)所取樣品的熱釋光測年數據爲17.77萬 ± 1.51萬

年; 在大嶼山島陰澳篤(1970　2072)所取斷層物質的熱釋光測年數據爲3.33萬 ± 0.27萬年。

(3)珠江口—大嶼山斷裂帶

在工作區内出露于大嶼山島東涌以西，由三條平行的斷裂組成。

a 東涌(Tung Chung)—長沙海灘(Cheung Sha Beach)斷裂：北起東涌往南經伯公坳至長沙海灘。

在東涌路上4英里路碑冲溝處(1243　1174)所取樣品的熱釋光測年數據爲10.1萬 ± 0.86萬年。

b 深屈灣(Sham Wat Wan)—獅子頭山(Sz Tsz Tau Shan)斷裂：位于大嶼山島深屈灣至籮箕灣一帶。

c 大澳(Tai O)—大浪灣(Tai Long Wan)斷裂：位于大嶼山大澳至大浪灣一帶。

在牛過田(0524　1106)所取斷層物質的熱釋光測年，數據爲27.87萬 ± 2.3萬年。

4. 斷裂活動的主要特征

本文以距今10萬年有過活動的斷裂劃爲活動斷裂，在上述三組斷裂中，香港地區最主要的活動斷裂爲北西向和北東東向兩組．它們的主要構造特征如下。

(1)北東東向斷裂主要分布于大嶼山島至赤門海峽和擔杆島一帶; 北西向斷裂主要位于九龍半島的東西兩側，形成頗具規模的北西向斷裂密集帶．北西向斷裂規模稍遜于北東東向斷裂，每條北西向斷裂長度一般爲數km至數十km。

(2)在地貌上往往形成負地形—海峽、溝谷，控制水系的發育．

(3)在現今構造應力場的作用下，北西向斷裂和北東東向斷裂組成共軛斷裂系統，即北西向斷裂顯示左旋壓剪性，北東東向斷裂具右旋

張剪性特征．野外觀察證明了這種性質，如見到大棠北西向斷裂有左旋滑動擦痕，同時看到北東向石英脈被北西向破裂面左旋錯移．

(4)北東東向和北西向斷裂都具有多次活動特征，尤其是北西向斷裂，多次活動迹象明顯，一般都有兩期方解石脈或石英脈侵人。

(5)斷裂物質的熱釋光測年資料揭示，斷裂最新活動年代爲距今8萬—10萬年左右，即活動持續到晚更新世早期．

第二章　香港地區的地震活動性

2.1 東南沿海地震帶的地震活動

1. 歷史地震($M_S \geqslant 4\frac{3}{4}$)的空間分布

本區屬于東南沿海地震帶的中段. 自1067年以來至今，該地震帶範圍內共記載了$M_S \geqslant 4\frac{3}{4}$級地震119次(圖5)，其中$4\frac{3}{4}$—$5\frac{1}{4}$級(烈度Ⅵ度)84次，$5\frac{1}{2}$—$5\frac{3}{4}$級(烈度Ⅶ度)21次，6—$6\frac{1}{2}$級(烈度Ⅷ度)7次，$6\frac{3}{4}$—7級(烈度Ⅸ度)4次，7.3—$7\frac{1}{2}$級(烈度Ⅹ度)3次. 這些地震主要呈北東—北東東向，分布于內陸的會昌—河源—廣州一帶和濱海的泉州—汕頭—陽江一帶，分別組成東南沿海地震帶的內帶和外帶(圖6). 外帶地震活動較强，內帶相對較弱. 數百年來，7級以上地震只發生于外帶，并有多次6級地震，內帶最大地震爲$6\frac{3}{4}$級，而且6級地震爲數較少. 不論在外帶抑或內帶，地震的分布與北東向—北東東向和北西向的活動斷裂都有密切的關系.

2. 地震活動的時間序列

在時間發展的進程上，東南沿海地震帶的地震活動呈現時强時弱的周期性變化特點. 地震史料記載表明，自1400年以來至今，經歷了兩個地震活動周期，即第Ⅰ活動周期爲1400年至1710年，第Ⅱ活動周期爲1711年至今(尚未結束). 每個周期大約爲320年(圖7). 進一步分析地震應變積累與釋放的全過程，每一個地震活動期又可分爲四個發展階段：第1階段爲應變積累階段，延續時間73—112年，發生若干$M<6$級地震；第2階段爲前兆釋放階段，延續時間112—155年，可發生$6 \leqslant M<7$級地震；第3階段爲大釋放階段，延續時間4—6年，有$M \geqslant 7$級地震.

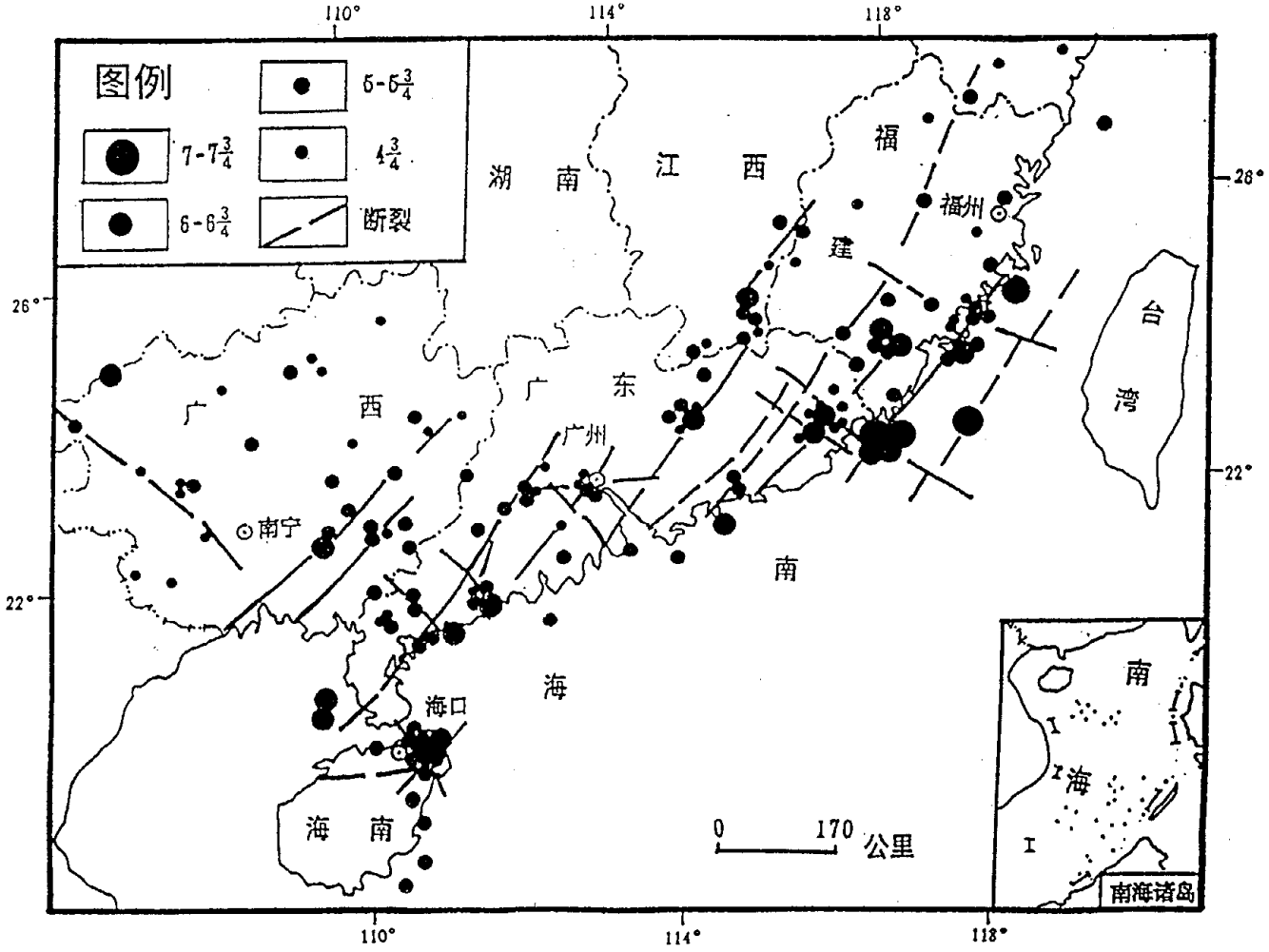

圖 5　東南沿海地震帶 $M_S \geq 4\frac{3}{4}$ 級地震分布圖(1067—1995)

Fig.5　The sketch showing the distribution of earthquakes for $M_S \geq 4\frac{3}{4}$ in the period 1067 to 1995

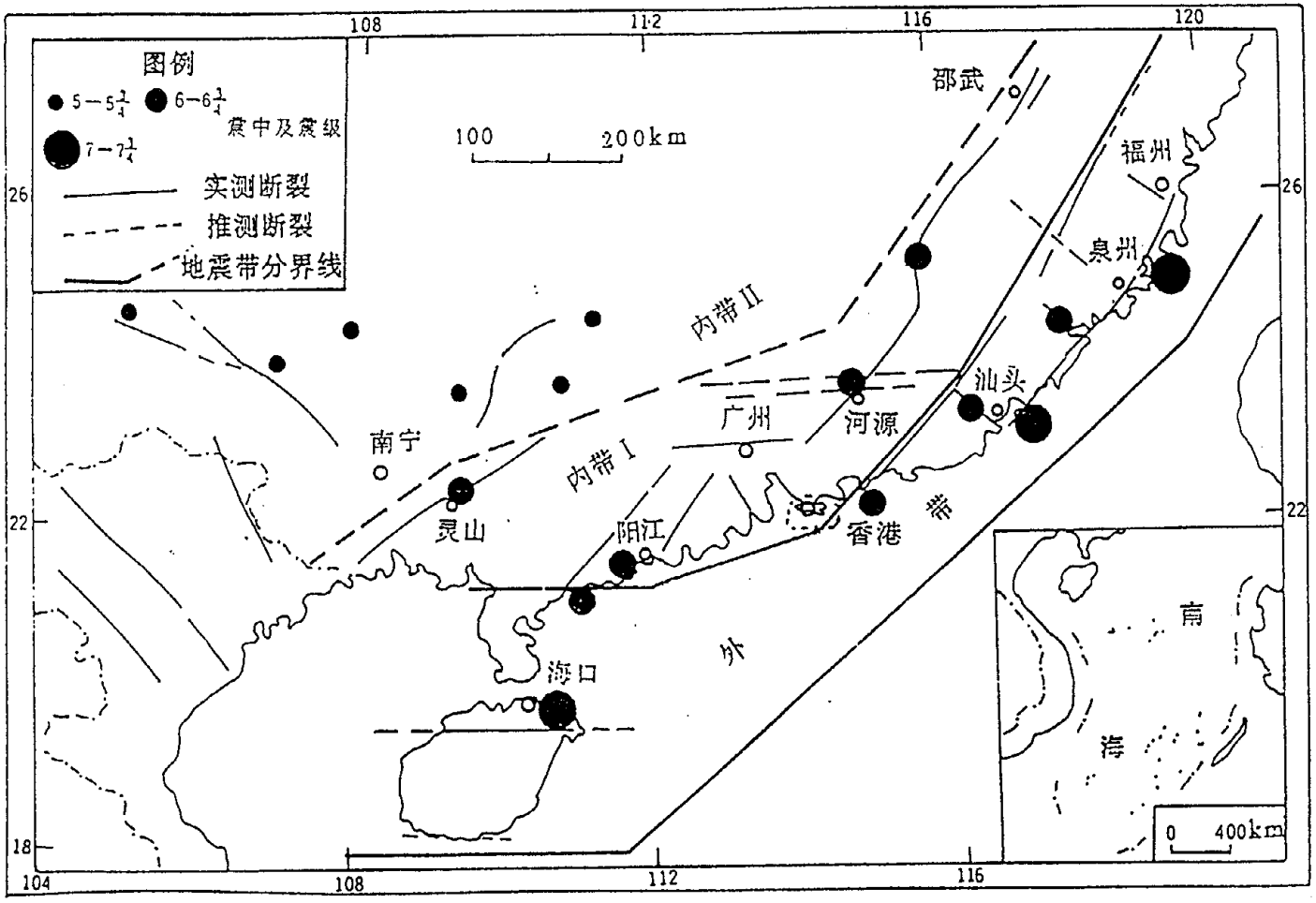

圖 6　東南沿海地區地震帶劃分

Fig.6　The location of the southeast coastal seismic zone

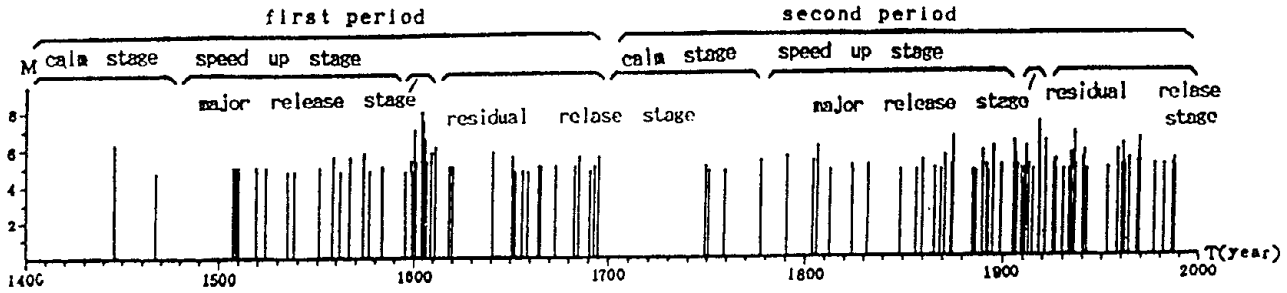

Historical seismic sequences

时间序列 $M \geqslant 4\frac{3}{4}$

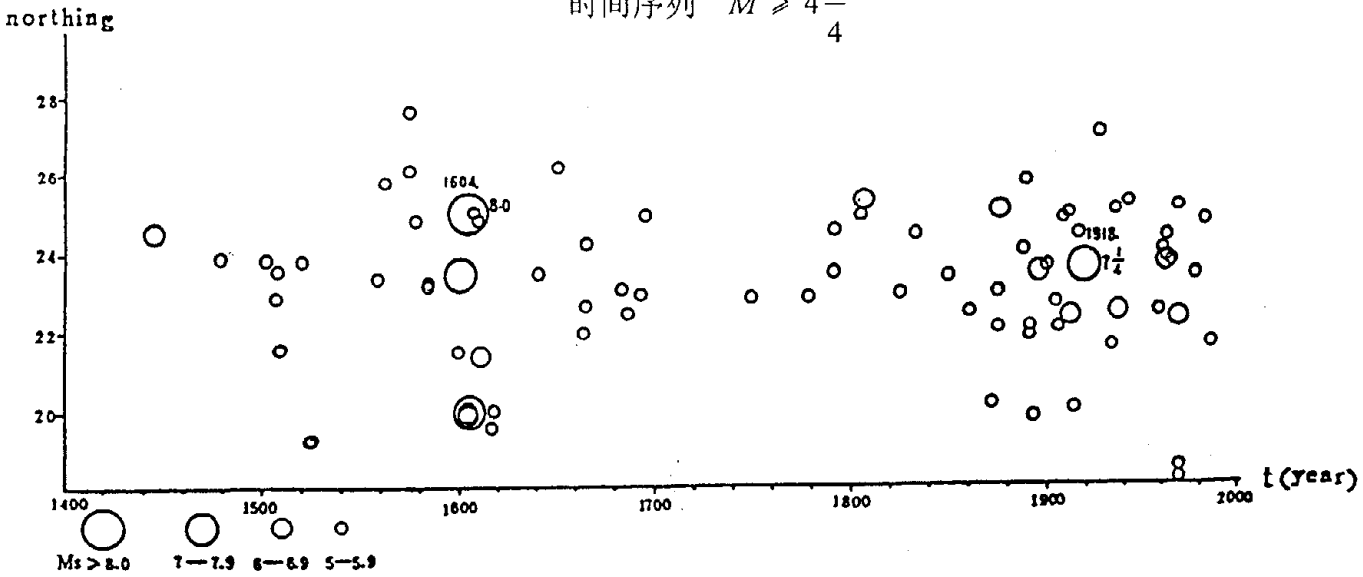

Tempora and spatial distribution of historical earthquakes

时空分布 $M \geqslant 5$

圖 7 東南沿海地震帶時間序列圖 (據林紀曾)

Fig.7 Seismic sequences in southeast coastal seismic zone in China

發生；第4階段爲剩余釋放階段，延續時間88—94年，可發生6—$6\frac{3}{4}$級地震。目前本地震帶處于第II活動周期的剩余釋放階段，預計本活動周期將延續到2015年前后，然后進入第III活動周期的應變積累階段。

2.2 香港地區的地震活動

1. 本區外圍幾次較大地震的影響場(圖8)

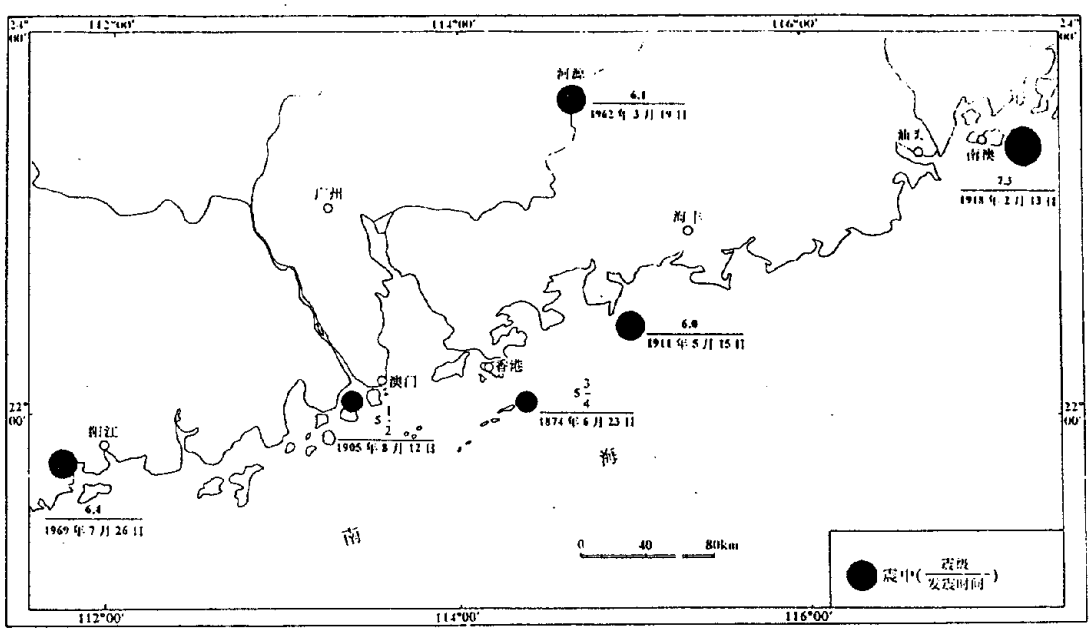

圖8　香港外圍地區幾個歷史地震的位置

Fig.8　Distribution of historical earthquakes in Hong Kong and vicinities

a 1874年6月23日擔杆島$5\frac{3}{4}$級地震

1874年6月23日即清穆宗同治十三年五月初十日在南海北部發生一次破壞性地震，震中在擔杆列島東端海域。有感範圍波及到惠州、河源、龍川、連平等地，在《惠州府志》(光緒年版)及《廣東通志稿·災變》(民國二十四年)都曾記載此次地震，香港報紙詳細報導了此次地震對香港的影響。據1874年7月1日(即同治十三年五月十八日)香港《申報》記載:

“初十日早九點鐘時逾一刻。地忽大震。自東北西南殊足令人駭异。是處之人皆惶遽不知所措。房内窗户皆叮當有聲，幾被折毁，地板也搖動，而牆壁勢皆欹側……公堂院内地勢如回風逐浪，見者無不色駭，沿海灘屋檐之石，半多墜落。……火警大鐘乃自鳴數響，各房内之小鐘亦皆叮當而附和焉。皮器路間一西房幾致傾倒，房中器皿盡搖動，即最重之鐵櫃亦爲震力所移。……查此地震共計五秒之久。……又得本港外村之電報，謂地震勢猛，已將西屋涼臺，震動散裂，有傾覆之狀，幸旋即如舊耳。”又據次日《申報》記載，“港内曾有華屋兩間震倒，其屋中人皆所壓，幸即救起，不致受重傷也。”從上述描述可知，香港地區的此次地震烈度可達VI度。

b 1905年8月12日磨刀門$5\frac{1}{2}$級地震

此地震在中國地震目錄上原定爲澳門5級地震，后來在對廣東大亞灣核電站的烈度復核過程中，重新校核史料記載，認爲震中應在磨刀門海域，震級定爲$5\frac{1}{2}$級。此地震使澳門受到地震烈度VI度破壞，香港地區明顯有感。

c 1911年5月15日紅海灣6級地震

據史料記載推測，地震震中大致位于北緯22.5°，東經115.0°海域。該地震使海豐公平受到地震烈度爲VII度的破壞，估計該地震使香港地區受到V度的影響。該區至今還時常記錄到2—3級地震。

d 1918年2月13日南澳7.3級地震

該地震是廣東省内近百年來最大的地震，震中烈度達X度。它使遠離震中四百多km的廣州産生明顯的震感，香港也受到VI度影響。

此外，1962年河源6.1級地震和1969年陽江6.4級地震時，香港地區都有明顯感覺，屬烈度IV—V度範圍。總之，一百多年來，香港地區多次受到外圍地震的波及，有的還造成輕微破壞。地震影響最大可達

VI度．本區較大地震頻度和地震影響程度均與廣東省沿海地區大致相當。

2．香港地區的現今地震活動

在珠江三角洲及其鄰近地區，自1970年有地震臺網記錄以來至1995年共記錄$M_S \geq 2.0$級地震212次(圖9)，其分布特點是，除內陸區河源因水庫誘發地震較爲密集外，主要分布于濱海區，即海豐—深圳—澳門—恩平一綫及其以南地區．此地震密集區略呈北東東方向展布．香港位于此區之內，所以香港地區的微震活動略高于珠江三角洲的多數市縣，地震强度則無區別。

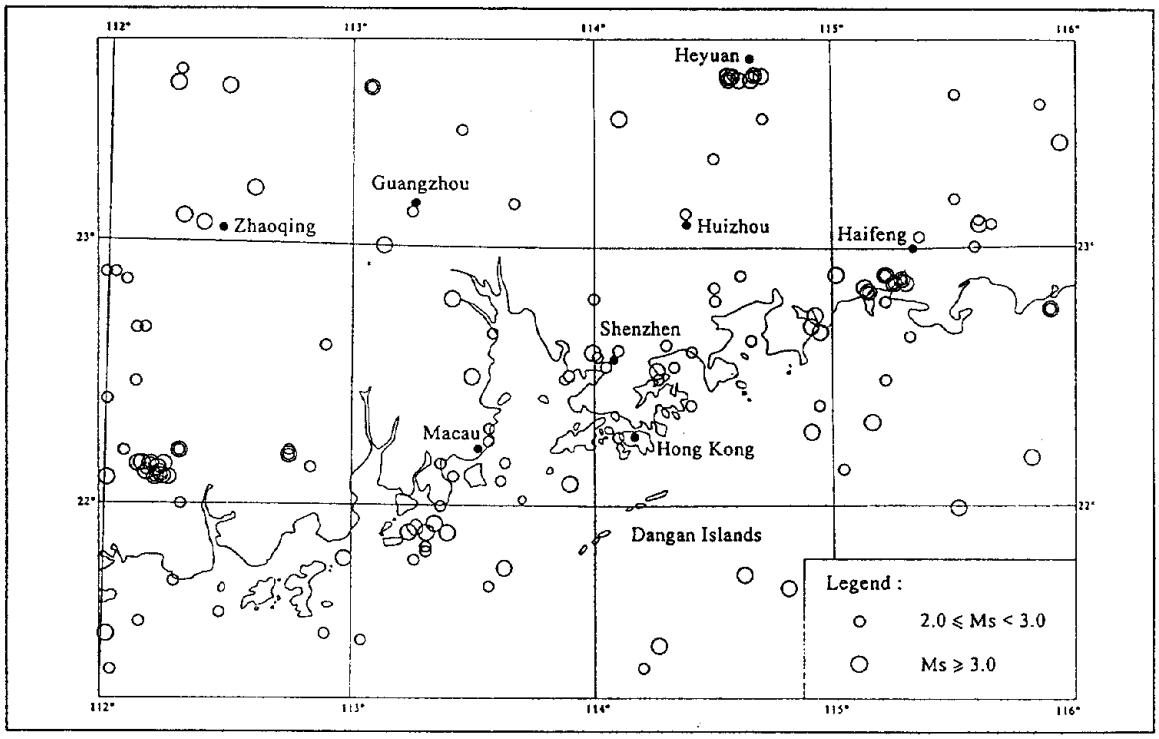

圖9　珠江三角洲及其鄰區地震分布圖($M_S \geq 2.0$,1970—1995)

Fig.9　Distribution of earthquakes for $M_S \geq 2.0$ in the Pearl River delta area in the period 1970 to 1995

爲了準確地厘定香港近場微震震中的位置，本課題組利用廣東省地震臺網和香港皇家天文臺地震臺網的資料，剔除了人工爆破造成的影響，重新校核了1972年以來在北緯22°00′—23°00′，東經113°45′—

114°45′的地震目錄. 1972—1995年期間在上述地區內發生$M_L \geqslant 1.8$級地震53次(包括兩次較小微震)(表2). 其中1972—1978年共19次，平均每年2.7次；1979—1989年11次，平均每年1次；1990—1995年23次，平均每年3.8次. 1990年以來，香港地區微震活動的頻度略有增强，强度的變化則不大. 這種變化與大區域的地震活動自1989年以來進人相對活躍期一致. 不過本區的地震活動相對分散全區，目前没有集中于一個點或一個條帶的迹象. 微震活動主要分布于深圳、大嶼山島周圍海域和大鵬灣附近(圖10). 這些地區是北西向和北東東向斷裂比較發育的地段，表明這兩組斷裂與微震活動有關，這與前面提到的斷裂年代學資料是完全吻合的.

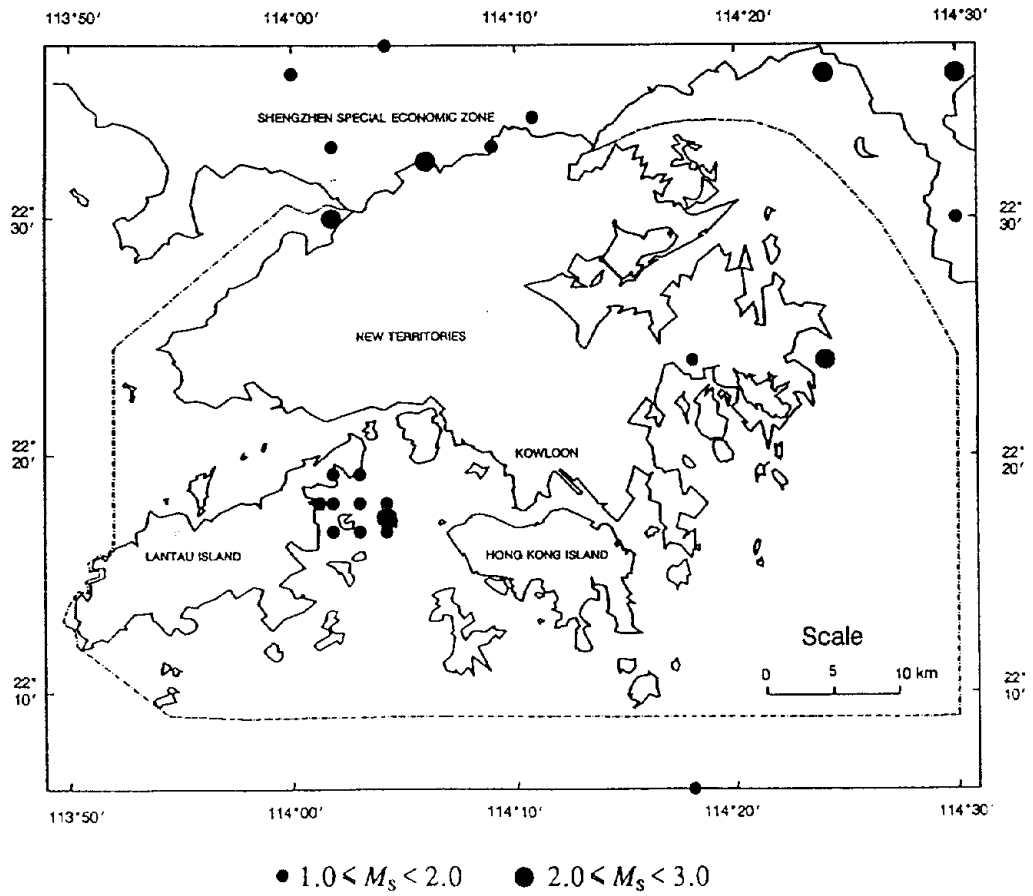

圖10　香港及其鄰區地震震中分布圖($M_S \geqslant 1.0$, 1972—1995)

Fig. 10　Distribution of earthquakes for $M_S \geqslant 1.0$ in Hong Kong and vicinities in the period 1972 to 1995

表2 香港地區地震目錄

編號	時間	震中		震級		備注
	年 月 日	北緯	東經	M_L	M_S	
1	1972 02 20	22°48′	114°30′	2.7	2.0	
2	1972 02 20	22°48′	114°30′	2.6	1.9	
3	1972 04 05	22°54′	114°36′	2.9	2.2	
4	1972 04 05	22°54′	114°36′	2.9	2.2	
5	1972 04 05	22°46′	114°39′	2.4	1.6	
6	1972 12 31	22°05′	113°54′	3.3	2.6	
7	1973 06 02	22°18′	114°54′	3.2	2.5	
8	1973 07 05	23°00′	113°54′	3.3	2.6	
9	1973 12 16	22°48′	114°00′	2.8	2.1	
10	1975 05 15	22°24′	114°18′	2.6	1.9	
11	1976 06 14	22°24′	114°24′	2.7	2.0	
12	1976 06 17	22°57′	114°27′	2.5	1.7	
13	1976 06 21	22°42′	114°18′	2.4	1.6	
14	1976 08 20	23°06′	114°18′	1.8	1.0	
15	1976 10 08	23°06′	114°18′	2.5	1.7	
16	1977 05 06	22°48′	114°24′	2.0	1.2	
17	1977 06 17	22°36′	114°00′	2.3	1.5	
18	1977 10 22	22°36′	114°30′	3.1	2.4	
19	1978 05 27	22°30′	114°30′	2.1	1.3	
20	1982 01 22	22°46′	114°36′	2.3	1.5	
21	1982 08 29	22°18′	114°01′	1.5	0.6	**
22	1982 10 07	22°18′	114°01′	1.5	0.6	**
23	1983 07 22	22°32′	114°06′	2.8	2.1	*
24	1983 07 28	22°33′	114°02′	1.8	1.0	
25	1983 10 01	22°33′	114°09′	1.5	0.6	
26	1983 12 06	22°30′	114°02′	2.8	2.1	*
27	1984 03 15	22°50′	113°59′	2.2	1.4	

接下頁

接上頁

28	1985 06 04	22°15′	113°34′	2.4	1.6	
29	1986 11 09	22°42′	114°54′	3.0	2.3	
30	1987 06 09	22°37′	114°04′	1.6	0.7	
31	1987 07 18	22°38′	114°04′	1.2	0.3	
32	1988 01 24	22°34′	114°11′	2.3	1.5	
33	1990 01 13	22°24′	114°56′	3.0	2.3	
34	1990 06 11	22°41′	114°56′	3.3	2.6	
35	1990 06 11	22°45′	114°55′	3.0	2.3	
36	1990 06 29	22°35′	114°35′	1.8	1.0	
37	1993 03 01	22°36′	114°24′	2.8	2.1	
38	1995 05 11	22°17′	114°04′	3.1	2.4	
39	1995 05 11	22°19′	114°02′	2.4	1.6	**
40	1995 05 12	22°17′	114°04′	2.1	1.3	**
41	1995 05 12	22°17′	114°03′	2.2	1.4	**
42	1995 05 13	22°19′	114°02′	2.2	1.4	**
43	1995 05 13	22°19′	114°03′	2.4	1.6	**
44	1995 05 16	22°18′	114°03′	2.2	1.4	**
45	1995 05 18	22°17′	114°03′	2.0	1.2	**
46	1995 05 23	22°17′	114°02′	2.3	1.5	**
47	1995 05 26	22°18′	114°03′	2.3	1.5	**
48	1995 05 28	22°18′	114°03′	2.3	1.5	**
49	1995 05 29	22°18′	114°03′	2.4	1.6	**
50	1995 05 29	22°18′	114°04′	2.2	1.4	**
51	1995 05 29	22°18′	114°02′	2.2	1.4	**
52	1995 05 29	22°17′	114°03′	2.4	1.6	**
53	1995 06 23	22°17′	114°04′	2.2	1.4	**
54	1995 08 15	22°18′	114°02′	2.3	1.5	**
55	1995 11 20	22°18′	114°04′	2.1	1.3	**

注: * 震中是用香港皇家天文臺地震臺網資料確定的.

**震中是用香港皇家天文臺地震臺網資料確定的, 震級是用長洲臺資料確定的.

2.3 對東南沿海地震帶未來地震趨勢的基本估計

目前東南沿海地震帶處在第II活動周期的剩余釋放階段，預計本階段將延續到2015年前后。今后地震活動雖然仍有起伏變化，但總體水平應與本世紀20年代以來的情況相似，在今后數十年内可能發生最大地震爲6—$6\frac{3}{4}$級。本剩余釋放階段的地震活動有時强時弱的變化，可以分出三個地震活動相對活躍的活動幕。1989年以后進入第三個活動幕。從前兩個活動幕得知，每個活動幕都有兩次6級地震發生在不同地點，例如前一個活動幕在河源(1962年)和陽江(1969年)分別發生兩次(6.1級和6.4級)地震。1994年底和1995年初在外帶的北部灣連續發生雙震型的6級地震(6.1級和6.2級)，今后數年内在本地震帶的其他地點還可能發生另一次6級地震。但是在剩余釋放階段本地震帶内不大可能發生7級或更大的地震，至于5級左右地震則不論外帶和内帶都可能有多次。

第三章　香港及鄰近地區的潛在震源區

所謂潛在震源區，是指今后可能發生破壞性地震的地區，它是通過對地質構造、地球物理、地殼形變、地震活動等信息的分析綜合確定，劃分潛在震源區有兩條最基本的原則：1.曾經發生過地震的地區，還可能重演同樣强度的地震；2.地質條件相同的地區，其地震活動性也可能相同．在劃分不同震級的潛在震源區時，還應考慮具體的構造條件．一般以歷史地震的最大震級作爲潛在震源區的震級上限。當認爲此震級不能代表未來地震活動趨勢時，則加$\frac{1}{2}$—1級作爲震級上限。根據上述原則，在編制《中國地震烈度區劃圖(1990)》時，在東南沿海地震帶內劃分出一百余個潛在震源區，本課題仍然沿用其劃分方案，不過對香港地區的潛在震源區作了調整和修改，茲對香港有較大影響的潛在震源區(圖11)簡述如下。

3.1 香港及鄰區的潛在震源區

1．廣州潛在震源區(30)

位于東西向高要—惠來斷裂帶上呈近東西向分布．近東西向的廣利—三水斷裂、瘦狗嶺斷裂横貫全區．此外，尚有北東向的從化—廣州斷裂和北西向的白坭—沙灣斷裂．這些斷裂在第四紀時期仍有活動，尤其是北西向斷裂活動更新，局部地段至晚更新世晚期還有活動。區內的三水盆地沉積了近3km厚的中新生界，第四紀仍然是沉降中心，發育厚約40m的第四系。垂直形變資料表明本區近年來仍然爲沉降區．在1372年、1683年、1824年、1915年分別在廣州、南海、番禺等地發生4$\frac{3}{4}$—5級地震4次，近期本區也時常有微震活動。本潛在震源區的震級上限定爲6級。

2．東莞潛在震源區(17)

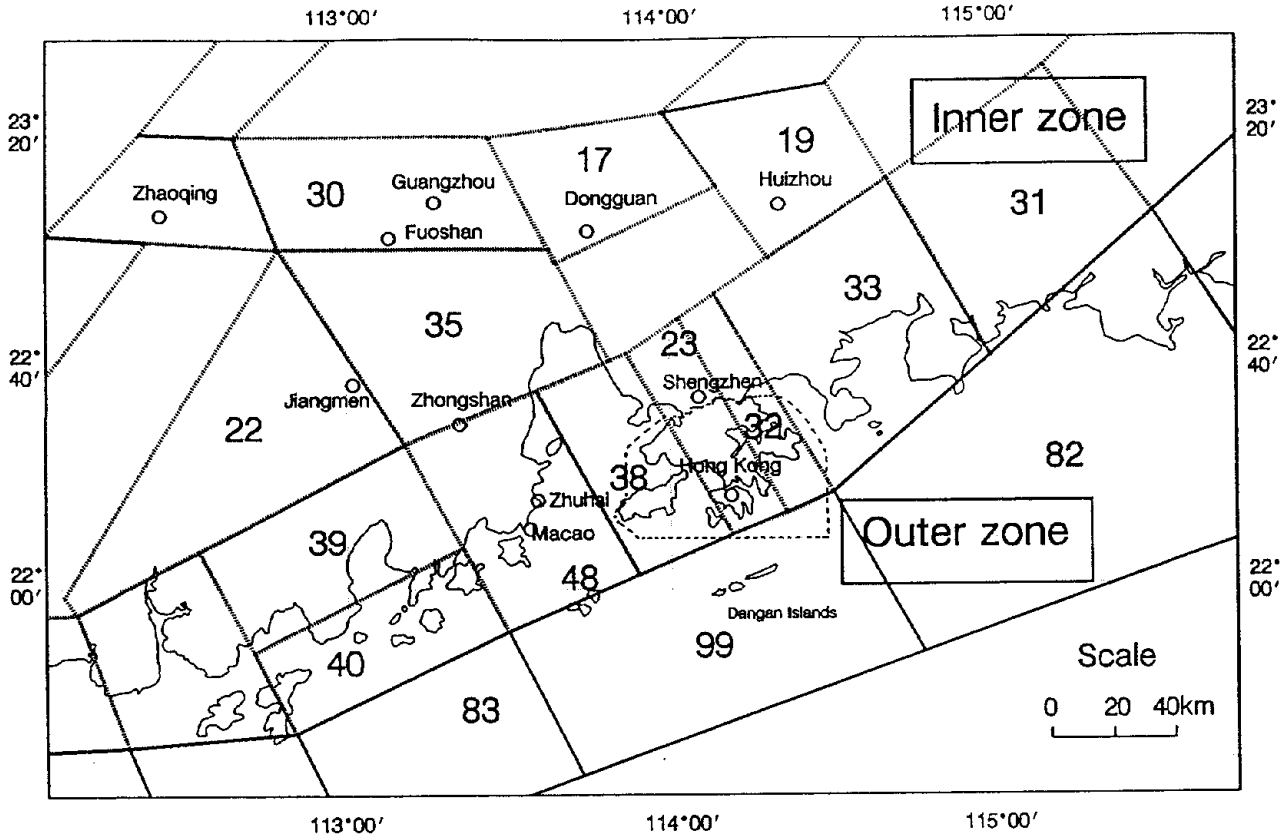

圖11 香港周圍的主要潛在震源區分布圖(實綫區爲外帶,虛綫區爲内帶)

Fig.11 Delineation of potential seismic zones for Hong Kong and its surrounding region

位于受北東向邵武—河源斷裂、北東東向瘦狗嶺—羅浮山斷裂和北西向珠江口斷裂控制的東莞盆地内，沉積了厚約35m的第四系。東莞盆地實際上是受控于前兩斷裂的尾端張性盆地。本區歷史上未記載過破壞性地震，近期小震活動也不多。本潛在震源區震級上限定爲5.5級。

3. 惠州潛在震源區(19)

位于廣東博羅、惠州、惠東一帶，呈北西向。北西向惠州—鹽洲深斷裂縱貫全區，北東向紫金—博羅斷裂横穿本區，南面有北東向五華—深圳斷裂。惠州爲一中新生代盆地。歷史上未發生過破壞性地震，近期時有小震活動。本潛在震源區震級上限定爲5.5級。

4. 海豐潛在震源區(31)

北東向的蓮花山斷裂帶、東西向的樟木頭—長埔斷裂和北東東向的大亞灣—惠來深斷裂都通過本區。海豐、陸豐一帶爲東西向的第四紀槽地，第四系最厚可達50m。海豐于1963年和1874年先后發生$4\frac{3}{4}$級地震，近期在梅隴、后門一帶發生一系列小震或震群。本潛在震源區震級上限定爲6級。

5. 惠陽潛在震源區(33)

位于廣東惠陽、惠東一帶，呈北西向。北有北東向五華—深圳斷裂，南爲北東東向濱海斷裂，東抵北西向惠州—鹽洲斷裂與海豐潛源區相接，西止于北西向葵冲—西冲斷裂。區内尚有北北西向大亞灣斷裂和北東東向大亞灣—惠來深斷裂。沿五華—深圳斷裂發育中—新生代多祝盆地和淡水盆地。歷史上未記錄過破壞性地震。自地震臺站建立以來，在白花、霞涌、大亞灣等地出現一系列小震活動。本潛在震源區震級上限定爲6.0級。

6. 大鵬灣潛在震源區(32)

東以北西向大鵬灣斷裂爲界與惠陽潛源區相鄰，西止于羅湖—西貢斷裂，中部有北西向簡頭圍—萬宜水庫斷裂帶通過，大鵬灣斷裂與東部葵冲—西冲斷裂共同控制了中新生代大鵬灣盆地的發育，使之沉積了厚達數km的上白堊統赤洲組和下第三系平洲組。區内近期時有小震活動。本潛在震源區震級上限定爲6.0級。

7. 深圳潛在震源區(23)

位于深圳至香港島一帶，呈北西向。東以北西向羅湖—西貢斷裂爲界與大鵬灣潛源區接壤，西達珠江口斷裂帶東支：蘿崗—太平斷裂和流浮山—東博寮海峽斷裂，北爲五華—深圳斷裂，南爲大埔—海豐斷裂。歷史上未發生過破壞性地震，近年來在深圳西部、九龍西部常有小地震出現。本潛在震源區震級上限定爲5.5級。

在編制《中國地震烈度區劃圖(1990)》時，把大鵬灣潛在震源區(32)與深圳潛在震源區(23)合并爲一個潛在震源區，震級上限定爲5.5級。本課題經過研究認爲，活動的北西向斷裂和現今小震活動都主要分布于大鵬灣附近，較少見于九龍半島中部。故此，把上述兩個潛源分開，震級上限分別定爲6.0級(32)和5.5級(23)。

8. 大嶼山潛在震源區(38)

位于珠江口、大嶼山及其附近海域，呈北西向。東以北西向蘿崗—太平斷裂、流浮山—東博寮海峽斷裂爲界與深圳潛源區交界，西止于北西向淇澳島—桂山島斷裂，北爲北東向五華—深圳斷裂向西延伸部分，在大嶼山北側有北東東向青山灣—大埔海斷裂。此外，在大嶼山還有一系列北西向斷裂。如竹篙灣斷裂、東涌—長沙海灘斷裂、深屈灣—獅子頭山斷裂、大澳—大浪灣斷裂等。據熱釋光測年資料，這些斷裂的最新活動年代爲距今9萬—27萬年，即在中更新世晚期至晚更新世早期仍有活動。區內近期有一些小震活動。本潛在震源區震級上限定爲6.0級。

9. 珠江口潛在震源區(48)

位于珠海、萬山群島一帶，呈北西向。東以淇澳島—桂山島斷裂爲界與大嶼山潛源區毗鄰，西界爲北西向西江斷裂，北抵北東向的翠亨—田頭斷裂(又稱五桂山南麓斷裂)，中部尚有北東東向的橫琴島—上川島斷裂。區內北西向和北東東向斷裂均活動較新，即在晚更新世中晚期仍有活動。1905年在磨刀門發生過5.5級地震，近期時常有小地震發生。本潛在震源區震級上限定爲6.5級。

編制《中國地震烈度區劃圖(1990)》時，把大嶼山潛在震源區(38)與珠江口潛在震源區(48)合并爲一個潛源，震級上限定爲6.5級。本課題經過研究認爲，大嶼山潛源(38)與大鵬灣潛源(32)的地質構造特征和

小震活動相當，震級上限定爲6級爲妥。故此把珠江口潛源(48)與大嶼山潛源(38)分爲兩個潛源區。

10. 中山潛在震源區(35)

位于廣東中山、順德一帶，東以蘿崗－太平斷裂爲界，西以西江斷裂爲界，北爲東西向磋石－楊梅斷裂向東延伸部分，與廣州潛源區相接，南爲翠亨－田頭斷裂。區內發育第四紀凹陷—中山凹陷，沉積中心第四系厚約35m。歷史上有感地震較多，近期小震較少。本潛在震源區震級上限定爲6.0級。

11. 江門潛在震源區(22)

位于廣東江門、新會、開平、臺山一帶，呈北東向三角形。東界爲西江斷裂，西界爲蒼城－海陵斷裂。1656年在鶴城發生$4\frac{3}{4}$級地震。本潛在震源區震級上限定爲5.5級。

12. 廣海潛在震源區(39)

位于廣海—崖門－磨刀門一帶，呈北東東向。北有翠亨－田頭斷裂，南爲橫琴島－上川島斷裂，前者活動于7萬年前(晚更新世早期)，后者活動于17萬年前(中更新世晚期)。近期在崖門口、廣海灣一帶有小震活動。本潛在震源區震級上限定爲6級。

13. 高欄島潛在震源區(40)

位于上川島、高欄島及其附近海域，呈北東東向。北以橫琴島—上川島斷裂爲界與廣海潛源區接壤，東界爲西江斷裂，南界頻臨濱海斷裂帶。上述斷裂在第四紀時均有活動。近期在高欄島、三竈島附近有一些小震活動。本潛在震源區震級上限定爲6.0級。

14. 高欄島外潛在震源區(83)

位于高欄島以南海域，呈北東東向。處在濱海斷裂帶上，該斷裂帶在第四紀有明顯活動，控制海、陸分界綫，東面止于西江斷裂。沿濱海斷裂帶有一些小震活動。本潛在震源區震級上限定爲6.5級。

15. 擔杆島潛在震源區(99)

北東東向濱海斷裂横貫全區。濱海斷裂不僅是第四紀以來有過活動的斷裂，而且是新構造分區界綫，北側爲萬山群島隆起區，海蝕崖上升到180m高程，南側爲珠江口外盆地沉降區，堆積了近7000m的上第三系和250m第四系。由此可見，本區爲新構造運動差异變化明顯的地帶。同時，本區爲北東東向濱海斷裂帶與北西向斷裂交匯地區，這種構造格局頗類似于南澳—汕頭地區(已經發生過7.3級地震)的構造格局(圖12)，而且這兩區均位于東南沿海地震帶外帶。《中國地震烈度區劃圖(1990)》把這兩個地區劃Ⅷ度區，是廣東省地震烈度最高的兩個地區(圖13)。1874年擔杆島東端發生$5\frac{3}{4}$級地震，使香港造成地震烈度Ⅵ度的破壞。近年來沿濱海斷裂仍然時常有地震活動。過去的研究工作認爲擔杆島潛在震源區的震級上限應爲7.5級。本課題雖然認爲本區確實具備發生7級地震的構造條件，可是震級上限定爲7.5級可能偏高。本區相鄰的外帶的潛在震源(如紅海灣(82)，高欄島外(83))的震級上限爲6.5級。擔杆島潛在震源比它們高出0.5級爲宜。因此，擔杆島潛在震源的震級上限定爲7.0級。

16. 紅海灣潛在震源區(82)

位于大亞灣、紅海灣南面海域，呈北東東向。也處在濱海斷裂帶上，西面以大鵬灣斷裂爲界與擔杆島潛源區相鄰。1911年在紅海灣發生過6級地震，近期也有小震活動。本潛在震源區震級上限定爲6.5級。

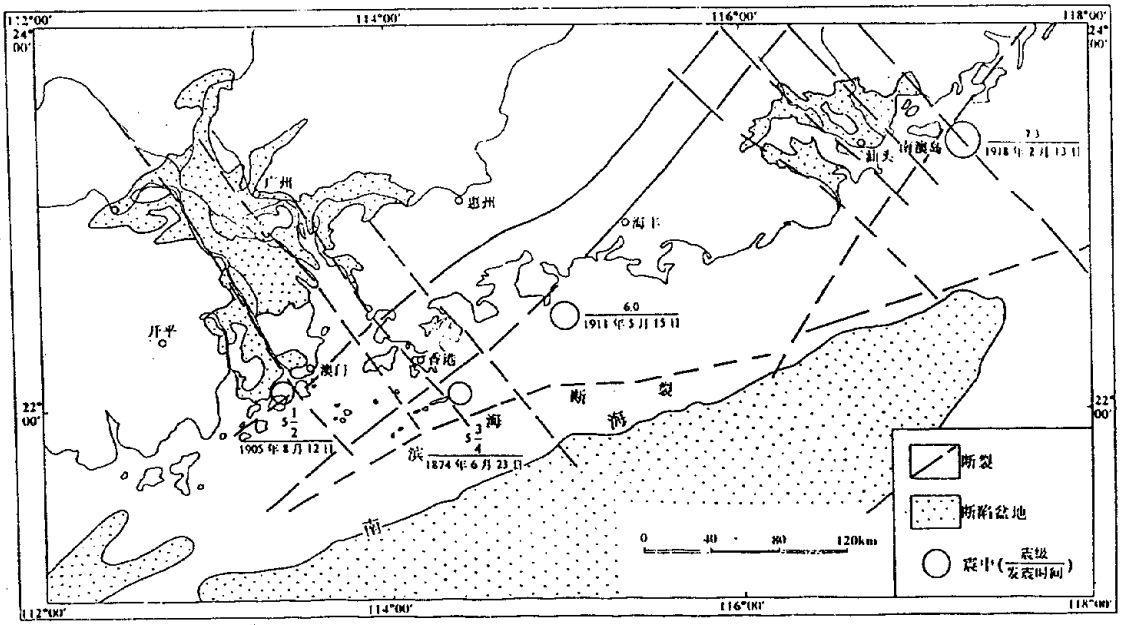

圖12　南澳島及擔杆島構造格局示意圖

Fig.12　The sketch showing the main tectonics in Nanao and Dangan Islands

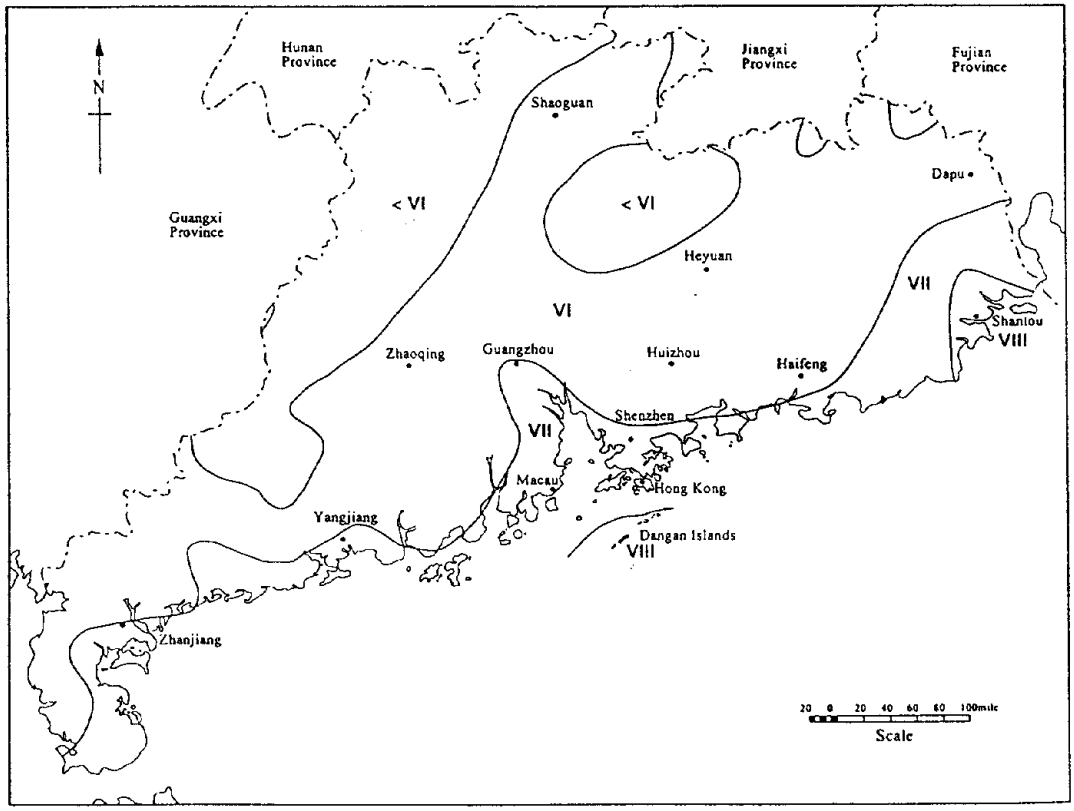

圖13　廣東省的地震區劃圖

(南澳—汕頭地區和擔杆島地區地震烈度均爲Ⅷ度)

Fig.13　Seismic intensity zonation of Guangdong Province

Nanao-Shantou area and Dangan area are the zones with intensity Ⅷ

3.2 潛在震源區的地震活動性參數

在地震危險性分析中，需要劃分地震帶和潛在震源區，并確定其地震活動性參數。香港地區屬于東南沿海地震帶的一部分。按照地震活動與區域地質構造特征，可以把該地震帶進一步劃分爲外帶和内帶。香港地區位于内帶，鄰近外帶。外帶地震活動性相對較强，歷史上有過數次7級以上地震和多次6級以上地震，外帶位于沿海或近岸海域，不論歷史地震記錄抑或現代地震，遺漏小地震的可能性均較大。内帶的地震活動相對較弱，地震頻度和强度都遜于外帶，歷史上没有發生過7級以上地震，只有6級左右地震。另外，内帶的地震記錄較豐富，現代地震監測能力較强，遺漏地震的可能性較小。

在進行香港地區地震危險性計算時，針對上述情況，對有關地震帶和潛在震源的地震活動參數做了如下確定。

1. 起算震級

起算震級是對本區有明顯地震影響的最小震級。本區地震均爲淺源地震，歷史上有一些4級地震曾經造成輕微破壞。爲了提高地震危險性分析的精確度，所以，本課題在進行地震危險性計算時，選擇4級地震爲起算震級，在統計b值和年發生率時，也都以4級地震爲起算震級。

2. 本底地震

本底地震爲潛在震源區以外的地區可能發生的最大地震。本區内帶的本底地震定爲5級，外帶的本底地震爲5.5級。換言之，内帶和外帶的任何地區都分别有發生5級和5.5級地震的可能性。

3. 震級—頻度關系中的b值

b值反映本地震帶内大小地震頻數的比例關系，而且和未來發生地震的概率大小有關。目前多根據自某個時期以來的歷史地震，按照震級—頻度關系公式（$\log N=a-bM$），求得a、b值。由于歷史時期記載的中、小地震往往有遺漏，大震所占比重偏大，b值偏小。現代儀器測

定的地震記錄比歷史時期完整，但記錄時間太短，往往缺少中一强地震事件，仍然不能反映本區地震活動的特征。爲此，本課題采用不同時段各級不被遺漏的地震，分時段分震級統計，即1800年以來$M_S \geqslant 6$級地震，1900年以來$M_S \geqslant 5$級地震(以上爲歷史地震)和1970年以來$M_S \geqslant 4$級地震(儀器測定的現代地震)(表3)。按歷史地震和現代地震分別擬合，求得外帶和内帶各兩個b值(圖14),然后取其平均數，得到外帶b值爲0.56，内帶b值爲0.80。潘偉强(1992)在分析香港地震危險性時，給出基本上包括全部廣東省陸地及南海北部海域的廣大地區(約43萬km^2)的b值爲0.75。該區包括本文所指内帶和外帶各一部分。

4. 地震年平均發生率

這是指外帶或内帶平均每年發生$M_S \geqslant 4$級地震的數值。此值對地震危險性計算結果有較大影響。本課題采用與確定b值一樣的分時段分震級統計的辦法，再擬合得到外帶4級以上地震年平均發生率爲1.151，内帶4級以上地震年平均發生率爲0.873(圖15)。考慮到目前本區地震活動的趨勢特點，今后一定時期内，本區正處于地震相對活躍時期，外帶和内帶的地震活動均可能比多年平均數值略高，爲此把上述兩個數值分别增加20%，求得外帶的4級以上地震年平均發生率爲1.38，内帶爲1.05(圖15)。東南沿海地震帶各震級地震的年平均發生率和復發周期見表4。

表3　東南沿海地震帶不同時段各級地震的發生次數

1970—1995　$M \geqslant 4$

震級	4.0	4.1	4.2	4.3	4.5	4.6	4.7	4.75	4.8	4.9	5	5.1	5.2	5.25	5.3	5.5	5.6	5.75	6	6.1	6.2	6.25	6.4	6.5	6.75	7	7.3	7.5	總計
內帶	3	1	2	4	4	1	1		1	1	1					1													20
外帶	3	1	1	2	1	1	2		1		3	2	1		2					1	1								22
全部	6	2	3	6	5	2	3		2	1	4	2	1		2	1				1	1								42

1900—1995　$M \geqslant 5$

震級		5	5.1	5.2	5.25	5.3	5.5	5.6	5.75	6	6.1	6.2	6.25	6.4	6.5	6.75	7	7.3	7.5	總計
內帶		2	1	1	3	1	1		2							1				13
外帶		6	2	1	1	2	2	1		1	1	1	2	1		1		1		23
全部		8	3	2	4	3	3	1	2	1	1	1	2	1		2		1		36

1800—1995　$M \geqslant 6$

震級		6	6.1	6.2	6.25	6.4	6.5	6.75	7	7.3	7.5	總計
內帶		1	1					1				3
外帶		3	1	1	2	1		1		1		10
全部		4	2	1	2	1		2		1		13

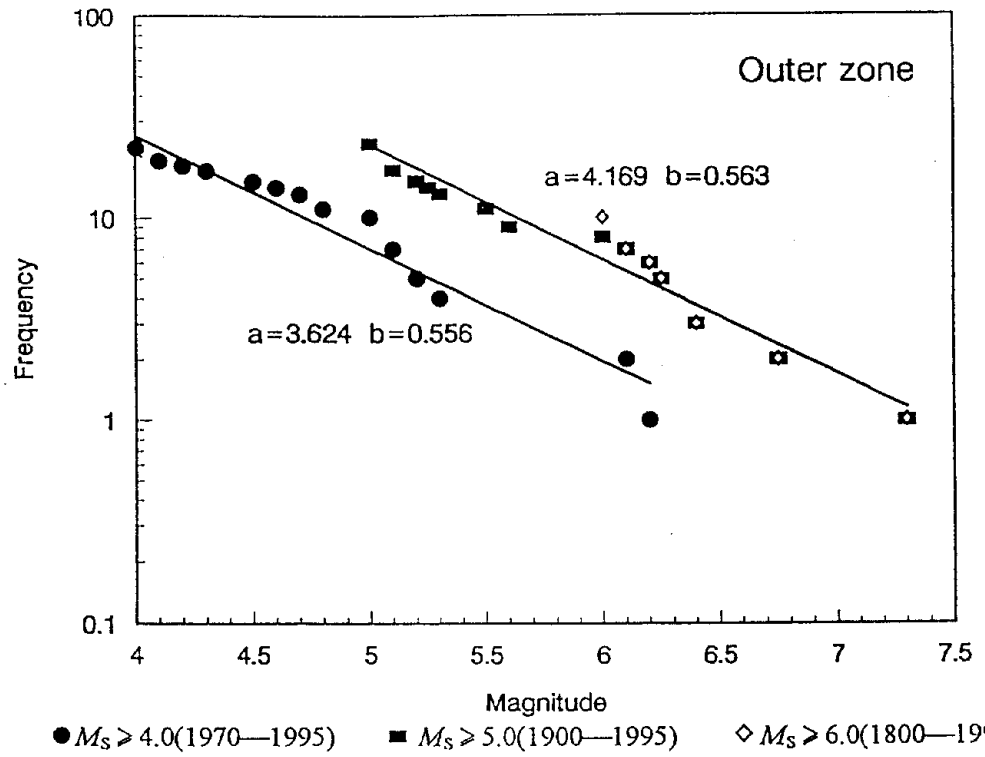

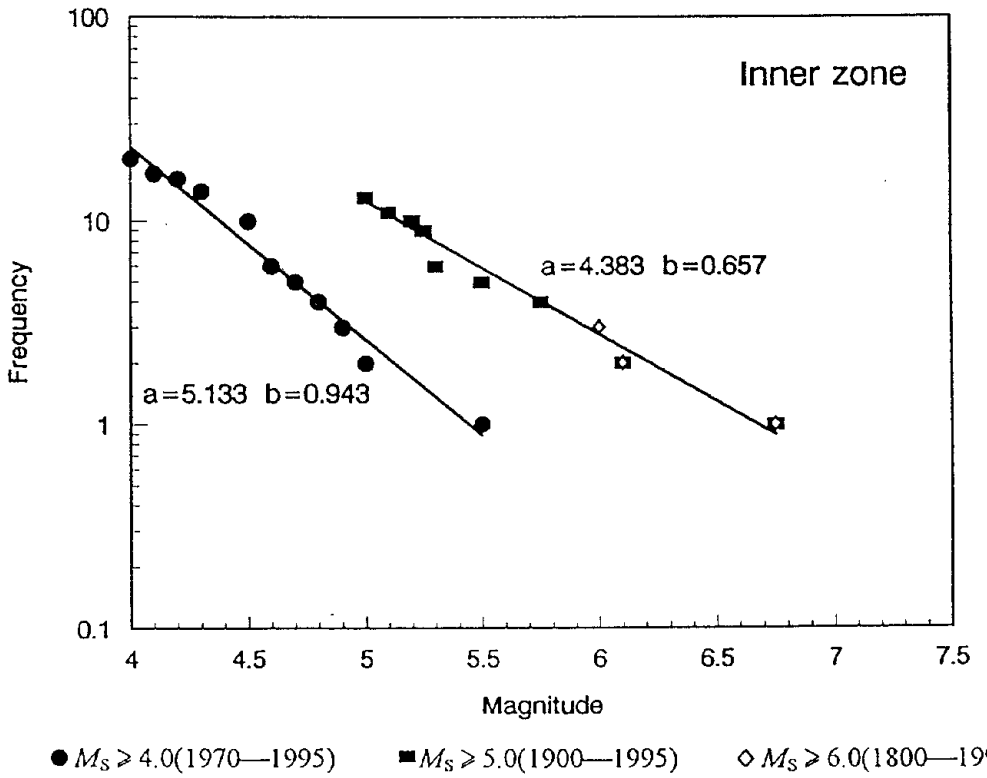

圖14 東南沿海地震帶的*b*值(上圖爲外帶，下圖爲內帶)

Fig.14 *b* values of the southeast coastal seismic zone in China

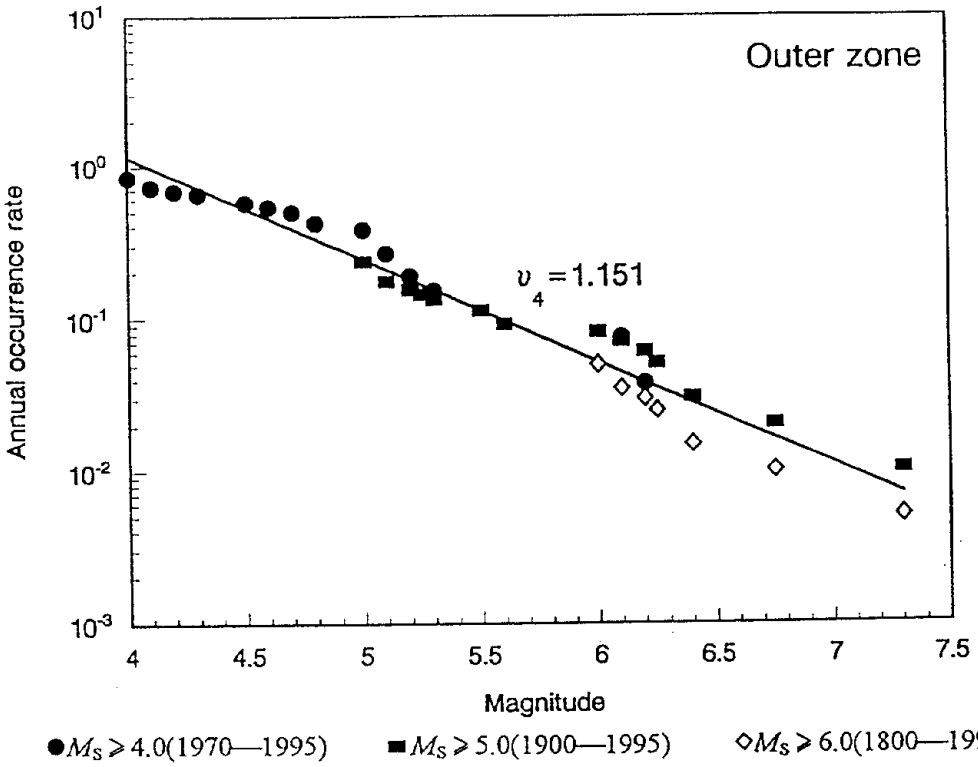

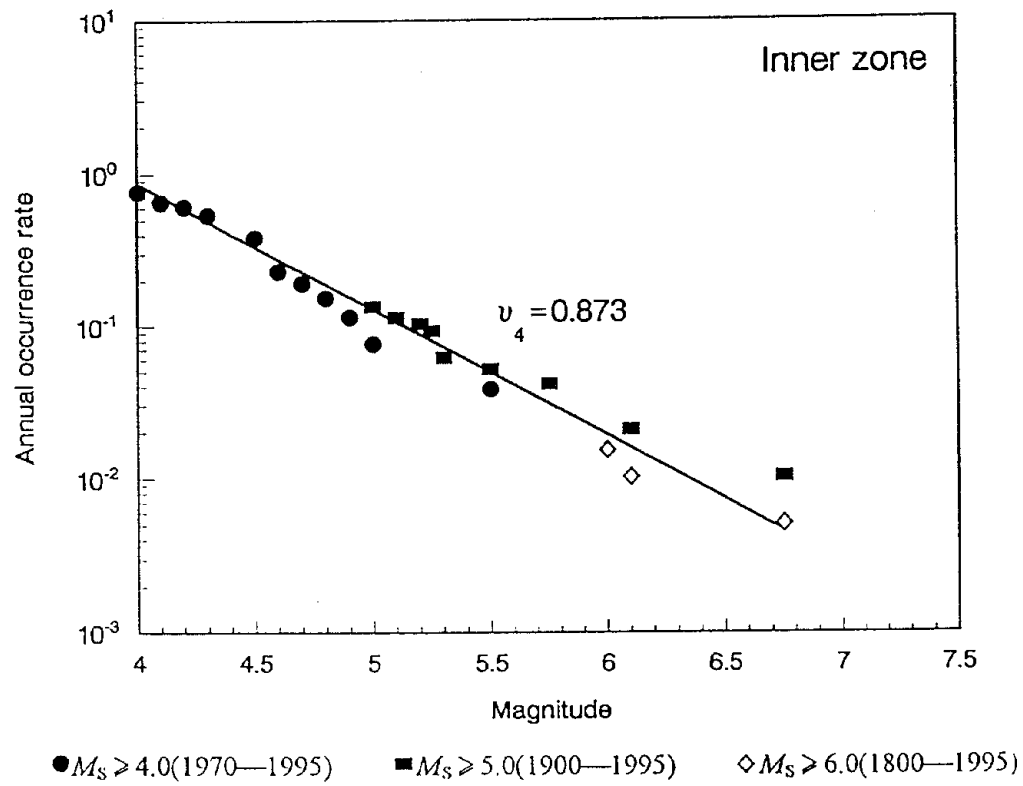

圖15　東南沿海地震帶的地震年平均發生率(上圖爲外帶，下圖爲內帶)

Fig.15　Annual occurrence rate of the southeast coastal seismic zone in China

表4　東南沿海地震帶不同震級地震的年平均發生率和復發周期

震級 M_S	内帶		外帶	
	年平均發生率(次/年)	復發周期(年)	年平均發生率(次/年)	復發周期(年)
4.0	1.05	0.95	1.38	0.72
4.5	0.44	2.29	0.65	1.55
5.0	0.18	5.59	0.30	3.33
5.5	0.073	13.6	0.14	7.15
6.0	0.030	33.2	0.065	15.3
6.5	0.012	80.9	0.031	33.0
7.0	——	——	0.014	70.8

5. 潛在震源區震級分布的空間權重

各潛在震源區的地震活動是不均勻的，爲此計算了各潛在震源區不同震級地震的權重分布(其意義見5.1節)。判別各震級的權重是基于①潛在震源區的可靠程度,②中長期地震預報成果，③地震活動的區域特征，④面積因素，同時還考慮到該潛在震源區可能發震斷裂的走向和權重。根據上述因素，給出了東南沿海地震帶各潛在震源空間權重矩陣。對本區地震危險性分析影響相對較明顯的潛在震源區震級分布的空間權重矩陣如表5。

表5　本區主要潛在震源區震級分布的空間權重矩陣(W_1)

地震帶	編號	潛源名稱	4.0—5.5	5.6—6.0	6.1—6.5	6.6—7.0	θ_1	W_{θ_1}	θ_2	W_{θ_2}
內	17	東　莞	0.0165				0	1.0	0	0
	19	惠　州	0.0127				20	1.0	0	0
	22	江　門	0.0277				120	0.7	40	0.3
	23	深　圳	0.0155				120	0.7	40	0.3
	29	肇　慶	0.0287	0.0573			120	0.5	10	0.5
	30	廣　州	0.0304	0.0593			120	0.5	10	0.5
	31	海　豐	0.0280	0.0454			120	0.5	30	0.5
	32	大鵬灣	0.0166	0.0271			120	1	0	0
	33	惠　陽	0.0235	0.0332			120	0.5	30	0.5
帶	35	中　山	0.0282	0.0531			120	0.7	40	0.3
	38	大嶼山	0.0182	0.0289			120	0.8	20	0.2
	39	廣　海	0.0261	0.0468			120	1	0	0
	40	高欄島	0.0253	0.0458			120	0.5	20	0.5
	48	珠江口	0.0212	0.0335	0.0939		120	0.7	40	0.3
外	82	紅海灣	0.0298	0.0341	0.0405		120	0.5	20	0.5
	83	高欄島外	0.0232	0.0256	0.0398		20	0.6	120	0.4
	84	下川島外	0.0273	0.0338	0.0379		20	0.6	120	0.4
帶	99	擔杆島	0.0266	0.0366	0.0558	0.0947	120	0.5	20	0.5

第四章　地震動的衰減模型

4.1 地震動的衰減

發生一次地震時，地震波從震源向外傳播擴展，距離能量釋放處(即震源)愈遠，地震波的能量愈小，即所謂衰減。確定地震動的衰減模型是地震危險性分析的重要環節之一。我國(包括華南地區在內)積累了豐富的歷史地震資料，可以從歷史地震和現代强震影響場取得地震烈度的衰減關系，可是華南地區已經布設的强震儀爲數不多，只有極少量的强震記錄，不能依據强震記錄直接給出華南地區的地震加速度的衰減關系。故此，本區的基岩地震動衰減模型都是用推導的方法(胡聿賢，1984年)求得的，即利用歷史地震的記載和近代强震的宏觀資料，從地震加速度記錄比較豐富的美國西部地區的衰減關系轉換成適合華南地區實際情況的地震動衰減模型。

4.2 地震烈度的衰減

不同地區的震源特性、傳播介質和場地條件有很大差別，所以不論是地震動峰值，還是地震烈度的衰減規律都有一定區別。

過去有不少學者對華南地區的歷史地震做了分析研究，給出了爲數可觀的等震綫資料。根據已知等震綫圖，采用圓形衰減模型或橢圓形衰減模型，求得華南地區的烈度衰減規律。

以黃日恒歸納的歷史地震資料爲基礎，余演波采用圓形衰減模型，得到

$$I = 41839 + 14372M - 16099\ln(R+14) \qquad \sigma_I = 0515 \qquad (4.1)$$

同樣以黃日恒提供的資料爲基礎，黃新輝按橢圓形衰減模型，求得華南地區地震烈度的衰減關系爲

長軸　$I_l = 485474 + 131271M - 149944\ln(R+15)$　　$\sigma_{I_l} = 0556$　　$(4.2a)$

短軸　$I_s = 320975 + 131271M - 124136\ln(R+7)$　　$\sigma_{I_s} = 0556$　　$(4.2b)$

Joyner—Boore(1984)給出美國西部的地震烈度衰減公式爲

$$I = 5.876 + 1.500M - 2.100\ln(R+25) \qquad \sigma_I = 0.274 \qquad (4.3)$$

周克森(1985)根據華南地區16個地震等震綫作了統計分析，得出該區的地震烈度圓形衰減關系爲

$$I = 5.8520 + 1.4899M - 1.9986\ln(R+25) \qquad \sigma_I = 0.210 \qquad (4.4)$$

4.3 加速度峰值的衰減

W.K.Pun(1990年)進行香港地震危險性分析時，直接引用Ambraseys給出的衰減關系

$$\lg a = -0.789 + 0.2128M - \lg R - 0.00255R + 0.25P \qquad (4.5a)$$

Ambrasseys和Bommer還給出另外一組衰減關系，即

$$\lg a = -1.00 + 0.251M - \lg R - 0.00268R \qquad \sigma_{\lg a} = 0.26 \qquad (4.5b)$$

$$R^2 = D^2 + H^2 \quad (H < 25\text{km})$$

Joyner—Boore(1981年)給出美國西部基岩與硬土的衰減模型爲

$$\ln a = -2.349 + 0.573M - \ln R - 0.00587R \qquad \sigma_{\ln a} = 0.60 \qquad (4.6)$$

$$R^2 = D^2 + 7.3^2$$

在廣東地區進行地震危險性分析時，時常以美國西部地區的地震動衰減模型爲參考，該區的基岩加速度峰值衰減關系爲

$$\ln a = 8.250 + 0.790M - 2.167\ln(R+25) \qquad \sigma_{\ln a} = 0.649 \qquad (4.7)$$

周克森(1986年)按照震級—距離“影射法”對上式進行修正，得到華南地震基岩加速度峰值的衰減關系

$$\ln a = 8.237 + 0.781M - 2.080\ln(R+25) \qquad \sigma_{\ln a} = 0.65 \qquad (4.8)$$

汪素雲(1988年)給出華南地區基岩加速度峰值的衰減關系爲

$$\ln a = 1.153 + 0.677M - 1.465\ln(R+25) \qquad \sigma_{\ln a} = 0.684 \qquad (4.9)$$

羅俊雄(1991年)給出臺灣地區基岩加速度峰值衰減關系爲

$$\ln a = -4.920 + 1.024M - 1.065\ln(R+R_0) \qquad \sigma_{\ln a} = 0.572 \qquad (4.10)$$

$$R_0=0.0395e^{0.92M}$$

霍俊榮(1989年)給出美國西部的基岩地震加速度峰值衰減關系爲

$$\lg a=-0.935+1.241M-0.046M^2-1.904\lg(D+R_0)\quad \sigma_{\lg a}=0.180 \qquad (4.11)$$

$$R_0=0.3268\mathrm{e}^{0.6135M}$$

霍俊榮等(1992年)考慮了近場高烈度區地震動飽和特性，按照橢圓模型，給出了華南地區的基岩地震加速度峰值衰減關系

長軸 $$\lg a_l=-1.2629+1.4956M-0.0513M^2-2.2252\lg(D+R_{0l}) \qquad (4.12a)$$

$$R_{0l}=0.3618e^{0.6989M}\qquad \sigma_{\lg a_l}=0.247$$

短軸 $$\lg a_s=-2.0301+1.4573M-0.0501M^2-1.9731\lg(D+R_{0s}) \qquad (4.12b)$$

$$R_{0s}=0.1201e^{0.7654M}\qquad \sigma_{\lg a_s}=0.247$$

李焯芬、余演波(1996年)假定華南地區與美國西部地區相同震級相同距離的烈度比值等同于它們對應的地震動衰減的比值，把美國西部的地震動資料轉化爲華南地區的地震動值．按圓形衰減規律，得到

$$\ln a=6.6954+0.8599M-1.87145\ln(D+R_0)-0.0028D\quad \sigma_{\ln a}=0.525$$

$$R_0=22.246e^{0.0292M} \qquad (4.13)$$

D.M.Scott等(1996)在討論香港建築抗震設計時，采用Dahle A.等(1990)在研究板内地震的衰減問題所給出的衰減公式

$$\ln a=\begin{cases}-1.471+0.849M-\ln R-0.00418R & R\leqslant R_0\\ -1.471+0.849M-0.167\ln R_0-0.833\ln R-0.00418R & R>R_0\end{cases} \qquad (4.14)$$

$$R_0=100\mathrm{km}\qquad \sigma_{\ln a}=0.83$$

圖16選取M_S=5、6、7級地震，對部分上述公式給出的衰減曲綫作了對比。當M_S=5時，不同衰減關系給出的衰減曲綫比較離散；M_S=6時，4.14曲綫衰減較緩，其他曲綫比較接近；M_S=7時，4.12*a*與4.14兩條曲綫基本相符，4.12*b*曲綫與其他曲綫相差不多。

本文在計算基岩加速度峰值時，按照公式4.5、4.6、4.7、4.8、4.9、4.10、4.11、4.12、4.13和4.14分別對本區及鄰區25個場點作了地震危險性分析計算和比較，最后結果如表6. 其中對華南以外的其他地區的衰減模型的計算結果僅供參考和對比，至于爲華南地區提供衰減公式的有四位，即汪素雲、周克森、李焯芬和霍俊榮. 按前三位的公式計算得到的25個場點的PGA均差別偏小，未能反映珠江三角洲及其鄰近地區地震活動的差別，也不符合各地地震危險性的實際情況，例如有的計算結果表明，廣州和擔杆島均劃爲150gal以上的地區(如按周克森的公式計算)；有的計算結果則顯示，廣州和擔杆島均爲125gal以下(如按汪素雲、李焯芬的公式計算). 按霍俊榮(中國,華南基岩,即公式4.12*a*、*b*)計算則顯示該區内既有PGA高的地區(如位于外帶的擔杆島)，又有PGA較低的地區(如嶺澳). 這種情況與本區地震活動水平的差异相符. 同時，公式4.12*a*、*b*是按照橢圓模型建立的，還考慮了近場高烈度區地震動峰值飽和特性. 這些方面也是該公式的長處，所以，本文選擇公式4.12*a*、*b*作爲計算依據.

本文還利用不同的烈度衰減關系計算了25個場點的地震烈度(表7). 按照周克森、余演波和黄新輝給出的公式，計算結果比較接近，相互差別不大. 考慮到黄新輝提供的公式爲橢圓形衰減模型，其計算結果與按公式4.12*a*、*b*計算的PGA結果基本匹配，所以本文采用公式4.2作爲計算烈度的依據，給出最后結果.

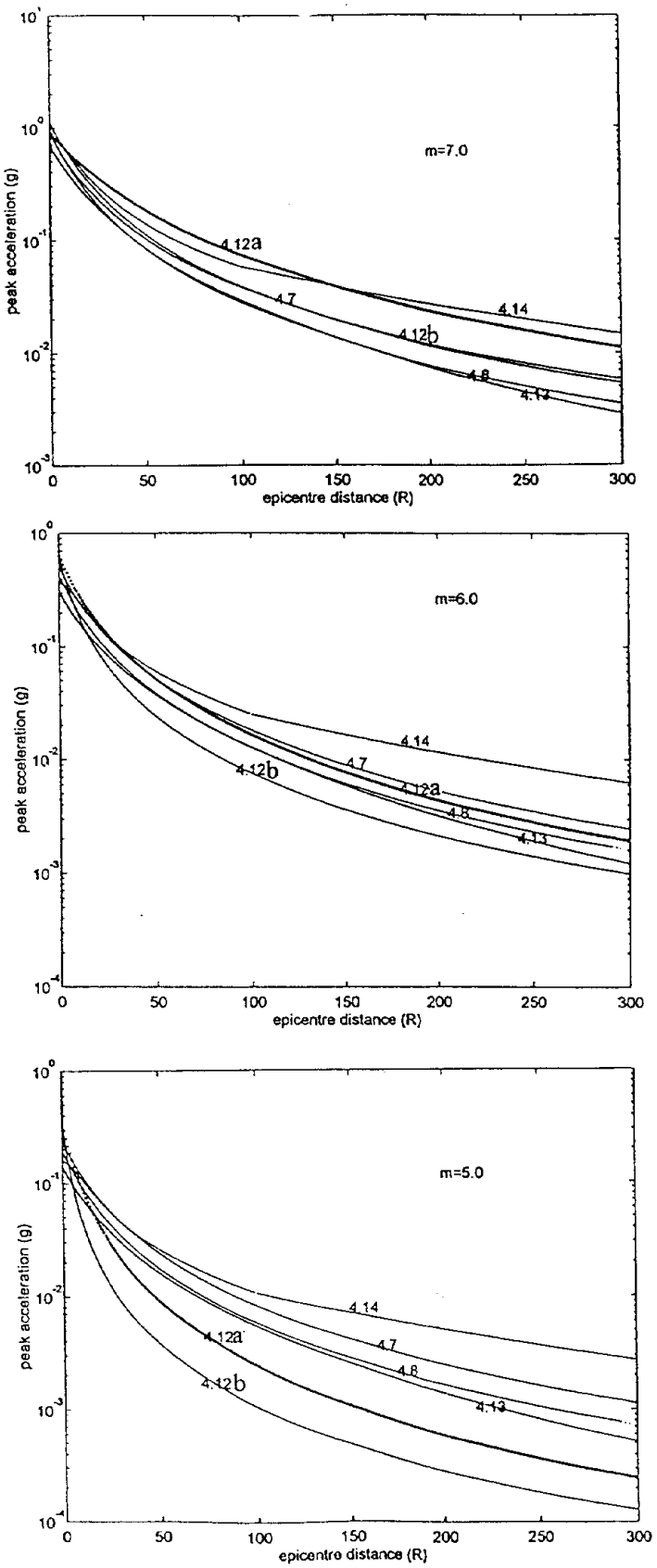

圖16　幾條衰減關系的衰減曲綫

Fig.16　Curves of some attenuation relations of PGA

表 6　采用不同加速度峰值衰減關系得到的 25 個場點 50 年超越概率 10 % 的 PGA 值（單位:gal)

場點	Ambrasseys–Bommer (歐洲)	Joyner–Boore (美國西部,基岩與硬土)	周克森 (美國西部,基岩)	周克森 (中國華南,基岩)	汪素雲 (中國華南,基岩)	羅俊雄等 (中國臺灣,基岩)	霍俊榮等 (中國華南,基岩)	李焯芬–余演波 (中國華南,基岩)	霍俊榮 (美國西部,基岩)	Anders Dahle,etc. (板塊內部)	張大名 (中國華南,基岩)
廣州	97.83	114.31	121.01	159.69	84.64	93.76	76.50	88.39	60.14	92.45	75.56
黃埔	95.41	112.12	117.46	155.15	82.76	91.41	71.15	85.41	57.09	91.17	71.67
九龍	104.90	115.95	125.78	168.29	92.82	105.15	92.70	93.33	66.30	115.42	99.72
香港島	106.07	116.17	126.31	169.10	93.52	106.51	96.32	94.45	68.42	117.54	102.91
沙頭角	102.06	119.70	127.24	168.03	90.19	102.25	80.94	91.41	62.55	105.31	86.39
南丫島	108.65	117.96	131.18	175.11	97.42	110.17	107.41	100.42	76.12	122.86	114.42
萬山島	115.06	123.94	144.69	191.28	104.36	118.27	131.82	112.70	92.62	131.40	136.89
擔杆島	115.51	121.95	145.51	192.79	105.55	117.86	136.38	115.32	96.47	132.04	142.47
二洲島	116.81	123.11	148.90	197.06	107.41	119.63	141.38	118.06	99.27	134.79	149.11
佳篷列島	119.55	126.22	156.30	205.80	110.11	123.75	154.28	125.37	107.76	138.10	161.42
嶺澳	88.24	95.06	98.24	130.88	76.39	85.38	62.27	72.63	46.20	94.09	70.57
羅湖	98.91	113.38	120.39	160.64	87.24	97.06	75.62	86.69	57.07	103.31	81.83
蛇口	97.67	108.53	114.82	153.66	85.76	95.53	78.17	83.93	56.22	104.33	84.39
粉嶺	101.03	114.55	122.90	164.11	89.18	99.71	79.56	88.78	58.87	105.72	86.44
高塘	105.24	122.42	132.50	174.55	94.01	106.99	90.99	96.20	69.25	111.13	95.88
黑咀	101.00	111.50	119.05	158.87	88.94	100.36	86.72	88.01	61.39	109.20	92.01
屯門	100.21	110.72	118.80	159.12	88.89	99.87	85.39	87.51	59.75	109.50	92.06
青衣	102.11	113.10	120.96	162.07	89.65	101.90	86.59	88.97	61.57	112.25	94.01
馬灣	102.13	112.15	121.08	162.30	90.20	101.68	88.14	89.31	61.76	111.97	95.44
煎魚灣	108.35	118.13	130.48	173.64	96.48	110.26	107.74	99.99	76.33	121.51	111.96
內伶仃島	101.61	112.87	120.54	159.85	89.49	101.03	88.22	89.58	63.56	109.39	92.40
淇澳島	101.69	113.41	120.25	160.52	89.51	101.01	89.58	90.30	64.84	109.14	93.02
香洲	105.64	116.09	126.86	168.97	94.34	105.78	101.98	96.74	72.82	116.04	105.49
磨刀門	105.03	115.62	124.56	165.98	92.89	103.55	94.82	94.06	68.45	113.86	98.45
高欄島	109.70	124.31	135.40	179.20	97.60	109.08	97.02	99.78	72.20	117.03	101.52

表7　采用不同烈度衰減關系算得的25個場點50年超越概率10％的地震烈度

場點	Joyner-Boore (美國西部)	周克森 (中國華南)	余演波 (中國華南)	黃新輝 (中國華南)
廣州	6.14	6.44	6.60	6.82
黃埔	6.07	6.36	6.55	6.78
九龍	6.52	6.82	6.98	7.11
香港島	6.57	6.88	7.01	7.14
沙頭角	6.31	6.61	6.79	6.97
南丫島	6.71	7.04	7.12	7.24
萬山島	6.93	7.22	7.30	7.41
擔杆島	7.04	7.34	7.38	7.46
二洲島	7.08	7.38	7.42	7.49
佳蓬列島	7.17	7.49	7.51	7.56
嶺澳	6.12	6.45	6.63	6.82
羅湖	6.24	6.56	6.73	6.92
蛇口	6.29	6.61	6.77	6.96
粉嶺	6.31	6.62	6.79	6.98
高塘	6.46	6.76	6.91	7.06
黑咀	6.41	6.71	6.87	7.04
屯門	6.41	6.71	6.86	7.03
青衣	6.44	6.75	6.90	7.06
馬灣	6.47	6.76	6.91	7.07
煎魚灣	6.67	7.00	7.09	7.22
內伶仃島	6.42	6.72	6.88	7.04
淇澳島	6.42	6.72	6.89	7.05
香洲	6.58	6.89	7.02	7.16
磨刀門	6.48	6.78	6.94	7.10
高欄島	6.49	6.76	6.96	7.11

第五章　地震危險性概率分析

5.1 地震危險性概率分析的基本思路

場點的地震危險性通常用一定年限內地震動超過某一給定的概率值表示。如果有N個地震帶對場點的地震危險性有貢獻，第n個地震帶對場點地震動年超越概率爲$P_n(Z \geqslant z)$，則場點地震動年超越概率可以表示爲:

$$P(Z \geqslant z) = 1 - \prod_{n}^{N}[1 - P_n(Z \geqslant z)] \tag{5.1}$$

式中　Z——地震動參數(或地震烈度)

z——給定的地震動參數值(或地震烈度值)

在地震危險性分析中，最關鍵的步驟是確定第n個地震帶對場點的地震動年超越概率$P_n(Z \geqslant z)$。爲簡單起見，以下公式中參數略去了關于地震帶的角標，所有參數都描述同一地震帶。

在地震危險性的概率分析中，地震活動性參數的統計和分配單元通常采用兩極劃分。地震帶是地震活動性參數的統計單元，它應具有統計上的完整性和地震活動趨勢的一致性。地震時間過程符合分段的泊松過程。在t年內，年平均發生率爲ν，則

$$P_{kt} = \frac{(\nu t)^k}{k!} e^{-\nu} \tag{5.2}$$

式中P_{kt}爲統計區內未來t年內發生k次地震的概率。由此式可以得出未來t年內至少發生一次地震的概率

$$P(t) = 1 - e^{-\nu} \tag{5.3}$$

地震帶內大小地震的比例遵從修正的震級—頻度關系，相應的震級概率密度分布函數爲

$$f_M(M)=\frac{\beta\exp[(M-M_0)]}{1-\exp[(-\beta(M_{uz}-M_0)]} \tag{5.4}$$

式中β=b × ln10，M_{uz}爲地震帶的震級上限。

在地震帶內，可進一步劃分若干潛在震源區。潛在震源區是地震活動性參數的分配單元。爲了如實地反映地震活動的時、空不均勻性，不低估大地震的影響，采用震級分檔的方法，將地震帶內各震級檔的地震年平均發生率，合理地分配到相應的各潛在震源區中。對于地震帶中的第i個潛在震源區，各震級檔Mj的年發生率可以表示爲

$$\nu_{iM_j}=\frac{2\nu\exp[-\beta(M_j-M_0)]sh(-\beta\Delta M)}{1-\exp[-\beta(M_{uz}-M_0)]}f_{iM_j} \tag{5.5}$$

式中　ν——地震帶內地震年平均發生率

ΔM——震級分檔步長

M_j——震級M_0到震級上限M_u的若干檔中第j檔的中心震級

ν_{iM_j}——第i個潛在震源區、第j個震級檔的地震年平均發生率

f_{iM_j}——地震空間分布函數，或稱潛在震源區震級分布的空間權重(W_{iM_j})，其物理意義是一次震級爲$M_j\pm\frac{1}{2}\Delta M$的地震落在第$i$個潛在震源區內的概率。它作爲震級的條件概率，可以反映地震帶內地震强度空間分布的不均勻性，對指定震級的f_{iM_j}在整個地震帶內是歸一化的，即有

$$\sum_{i=1}^{N_s}f_{iM_j}=1 \tag{5.6}$$

式中——N_S爲地震帶內潛在震源區總數。

f_{iM_j}是根據統計方法綜合判斷確定的。

根據分段泊松分布模型和全概率定理，場點地震烈度和地震動參數年超越概率應按下式計算:

$$P(Z\geqslant z)=1-\exp[-\sum_{i=1}^{N_S}\int_{A_i}\int_{\theta}\sum_{j=1}^{N_M}\nu_{iM_j}P(Z\geqslant z|E)f_i(\theta)d\theta dA/A_i]$$

$$=1-\exp[-\frac{2\nu}{\beta}\sum_{i=1}^{N_S}\int_{A_i}\int_{\theta}\sum_{j=1}^{N_M}\nu_{iM_j}P(Z\geqslant z|E)f_M(M)sh(-\frac{1}{2}\Delta M)f_i(\theta)f_{iM_j}d\theta dA/A_i] \quad (5.7)$$

式中 N_M——地震帶震級分檔數

$f_i(\theta)$——第i個潛在震源區的方向性函數

θ——可能的主破裂方向

A_i——第i個潛在震源區的面積

$P(Z\geqslant z|E)$——第i個潛在震源區內發生特定事件時(震級爲$M_j\pm\frac{1}{2}\Delta M$，特定的橢圓長軸取向)，場點地震烈度和地震動參數超過某一給定值的概率。

5.2 衰減關系的不確定性分析

由于地震烈度和地震動衰減關系具有一定的離散性，衰減公式中給出的只是烈度或地震動的期望值，爲了使分析結果更安全、可靠，必須考慮衰減關系的不確定性。在地震危險性的概率計算中，衰減關系的不確定性校正，可以按下列公式進行

$$P(Z\geqslant z)=\int_{-3\sigma}^{3\sigma}P(Z>z|\varepsilon)f(\varepsilon)d\varepsilon \quad (5.8)$$

式中 ε——回歸分析中不確定性的隨機變量

$f(\varepsilon)$——衰減關系中不確定性隨機變量的概率密度函數，一般取均值爲0，標準差爲σ的正態概率密度函數。

衰減關系的校正問題，已經在計算程序中考慮，計算輸出的地震危險性數值已是經過不確定性校正的結果。

假設各年之間場點的地震烈度和地震動參數Z在統計上是獨立的，而各年的年超越概率保持不變，采用伯努利獨立試驗序列，則在T年內地震烈度或地震動參數Z超過某一給定值z的概率爲

$$P_T(Z \geqslant z) = 1 - [1 - P(Z \geqslant z)]^T \tag{5.9}$$

當年超越概率值足夠小(如 $\leqslant 0.05$)時，場點的地震烈度和地震動參數Z的分布可近似取爲

$$P_T(Z \geqslant z) \approx 1 - e^{-P(Z \geqslant z)T} \tag{5.10}$$

場點地震烈度和地震動參數$Z \geqslant z$的復發周期T_Z即爲

$$T_z = \frac{1}{P(Z \geqslant z)} \approx -\frac{T}{\ln[1 - P(Z \geqslant z)]} \tag{5.11}$$

5.3 香港外圍地區地震危險性的對比

按照本課題所確定的地震帶和潛在震源區的劃分方案及其地震活動性參數，對珠江三角洲地區部分場點進行試算，以便與歷年廣東省地震局的學者們所作的地震危險性分析以及《中國地震烈度區劃圖(1990)》相互印證和對比，從而了解到本課題所給出的地震活動性參數和地震動衰減關系是否合理、合適．經過計算，珠江三角洲部分場點的地震基岩水平加速度峰值和地震烈度的結果如表8．本課題對香港外圍地區部分場點的試算結果與十年來其他研究工作者給出的數據相近，對各地地震危險性的評價大體一致，也與《中國地震烈度區劃圖(1990)》的結果相吻合，所以本課題確定的地震活動性參數和地震動衰減關系可以接受，以它們作爲計算依據所得出的結果是可信的．

表 8　珠江三角洲部分場地的基岩加速度峰值和地震烈度

場地	周克森等(1995)		丁原章等(1994)		周克森等(1996)		丁原章等(1987)		張大名等(1995)		周克森等(1987)		黃日恒等(1989)		王振才等(1989)		胡聿賢等(1993)		中國地震烈度區劃圖(1990)	本文計算結果	
	PGA(g)	I	PGA(g)	I	PGA(g)	I	PGA(g)	I	PGA(g)	I	PGA(g)	I	PGA(g)	I	PGA(g)	I	PGA(g)	I	地震基本烈度	PGA(g)	I
廣州	0.0866	6.94																	VII	0.0780	6.82
黃埔			0.0887	6.936															VII	0.0725	6.78
嶺澳					0.0608	6.8													VII	0.0635	6.82
深圳							0.0587	6.4											VII	0.0771	6.92
新會									0.0636										VI	0.0535	6.65
珠海											0.092								VII	0.1040	7.16
磨刀門													0.099						VII	0.0967	7.10
高欄島															0.132				VII	0.0989	7.11
淇澳島																	0.0836	7.17	VII	0.0913	7.05
內伶仃島																	0.0839	7.18	VII	0.0899	7.04
萬山島																			VII	0.1344	7.41
擔杆島																			VIII	0.1390	7.46
二洲島																			VIII	0.1441	7.49
佳蓬列島																			VIII	0.1573	7.56

5.4 香港地區的地震危險性概率分析

根據本課題所確定的地震帶和潛在震源區劃分方案及其地震活動性參數，采用選定的地震烈度和地震動參數衰減關系(公式4.2、4.12)對香港地區840個控制點，進行了計算，結果如下:

1. 基岩加速度峰值

香港地區50年超越概率爲63％、10％、2％的基岩加速度峰值(PGA)等值綫圖分別見圖17－1、2、3。三組等值綫都基本呈近東西向延展，北部地區的基岩加速度峰值相對較低，南部地區相對較高。如以50年超越概率10％的等值綫分布爲例，北部如沙頭角、元朗和屯門等均界于75—85gal之間，而九龍、香港及大嶼山島(大部)則界于90—105gal之間，蒲臺列島一帶基岩加速度峰值高達115gal。最高與最低相差40gal，本區各地PGA值基本在同一檔次中。

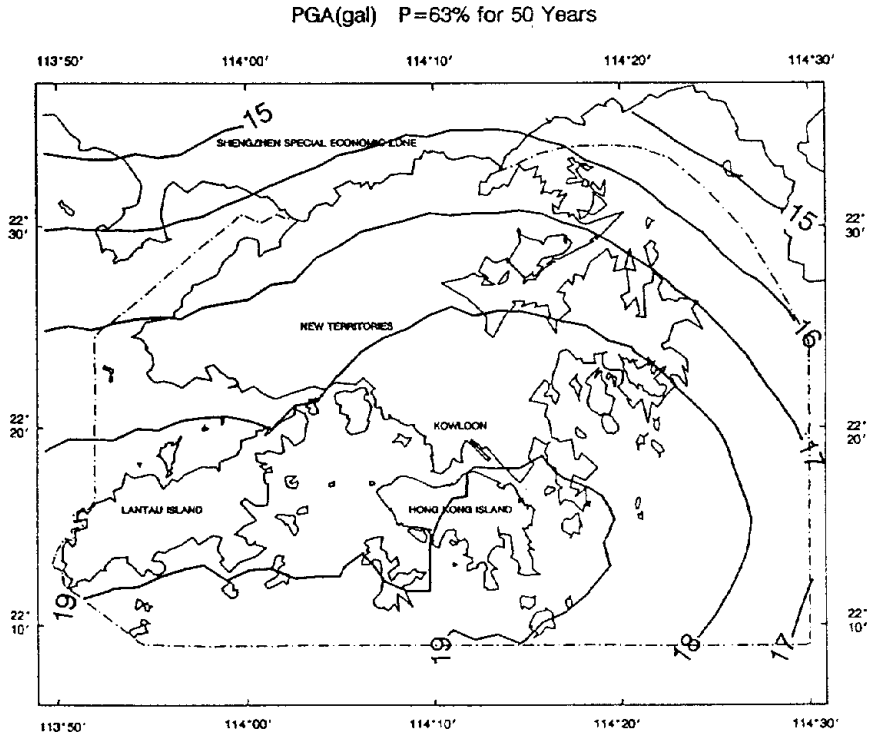

圖17－1　香港地區50年超越概率爲63％的基岩加速度峰值(PGA)等值綫圖

Fig.17-1　Contour map showing the regional distribution of peak ground acceleration in Hong Kong (P=63% for 50years)

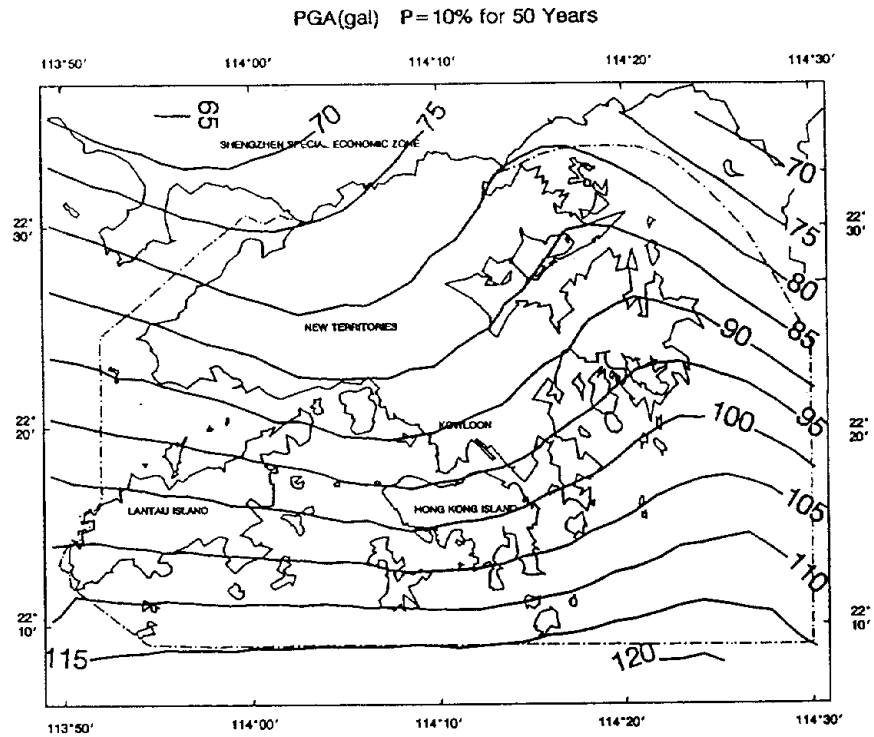

圖17－2　香港地區50年超越概率爲10％的基岩加速度峰值(PGA)等值綫圖

Fig.17-2　Contour map showing the regional distribution of peak ground acceleration in Hong Kong (P=10% for 50years)

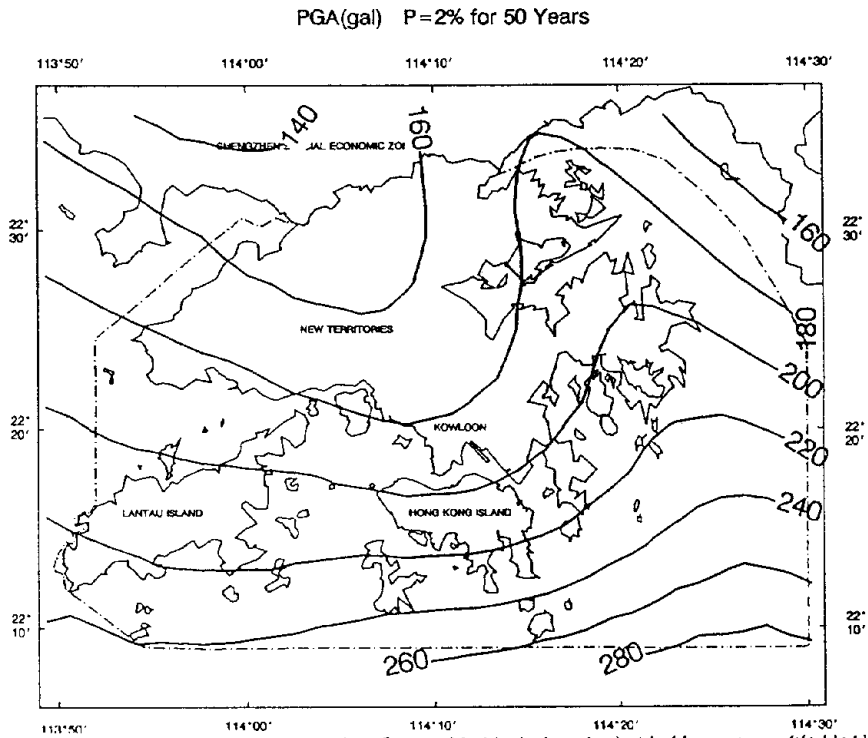

圖17－3　香港地區50年超越概率爲2％的基岩加速度峰值(PGA)等值綫圖

Fig.17-3　Contour map showing the regional distribution of peak ground acceleration in Hong Kong (P=2% for 50years)

爲了具體地表明各潛在震源區對本區場點的基岩加速度峰值(PGA)的貢獻，現以九龍(114°10′E，22°19′N)爲例，給出5個主要潛在震源區對九龍場點的基岩加速度峰值的貢獻(表9，圖18)。

表9　各主要潛在震源區對九龍場點基岩加速度峰值的貢獻

編　號		99	38	23	32	48
潛源名稱		擔杆島	大嶼山	深　圳	大鵬灣	珠江口
基岩加速度峰值	20gal	40.1%	16.5%	22.6%	13.2%	7.7%
	75gal	62.6%	14.2%	14.1%	8.0%	1.2%
	150gal	83.9%	13.6%		2.5%	

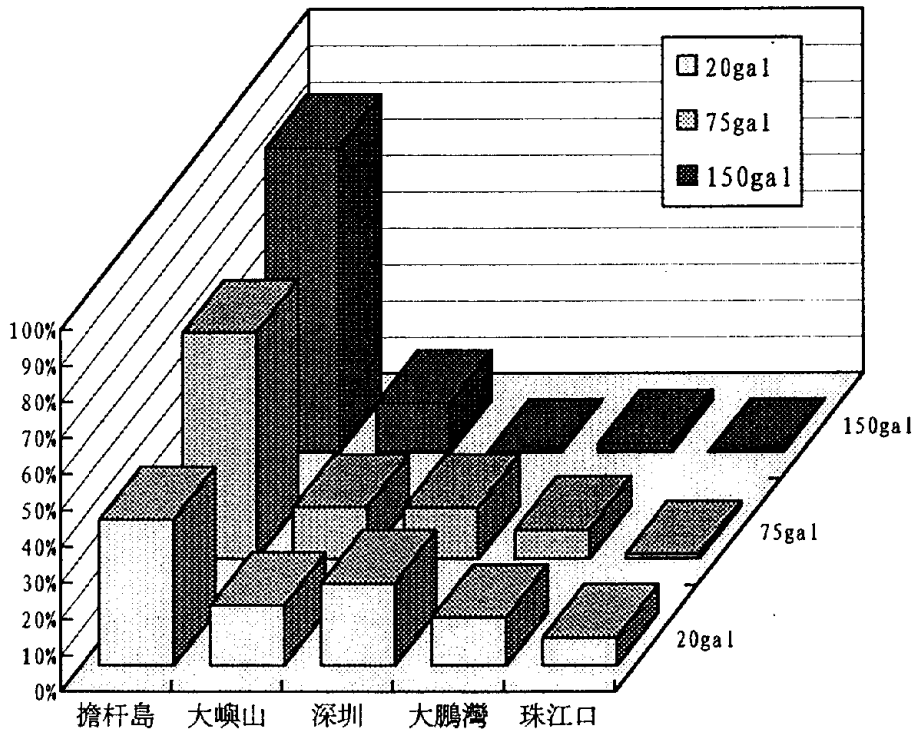

圖18　各主要潛在震源區對九龍場點基岩加速度峰值的貢獻

Fig.18　Devotion of the main potential seismic zones for PGA at Kowloon site

九龍場點的基岩加速度峰值主要由5個潛在震源區的貢獻所致，其中尤其以擔杆島潛源(99)的貢獻最大。不過就20gal而言，香港鄰近的3

個潛在震源區(38、23、32)的貢獻則超過50%．九龍未來50年三種超越概率(63%、10%、2%)相應的基岩加速度峰值分別爲18.82gal、92.70gal、190.58gal．九龍場點基岩加速度峰值(PGA)不同年限的超越概率曲綫如圖19所示，可以從圖中得到1年、20年、50年和100年不同超越概率的PGA值．香港地區其他場點不同年限不同超越概率的PGA值與九龍基本相同．九龍場點PGA的復發周期示于圖20．

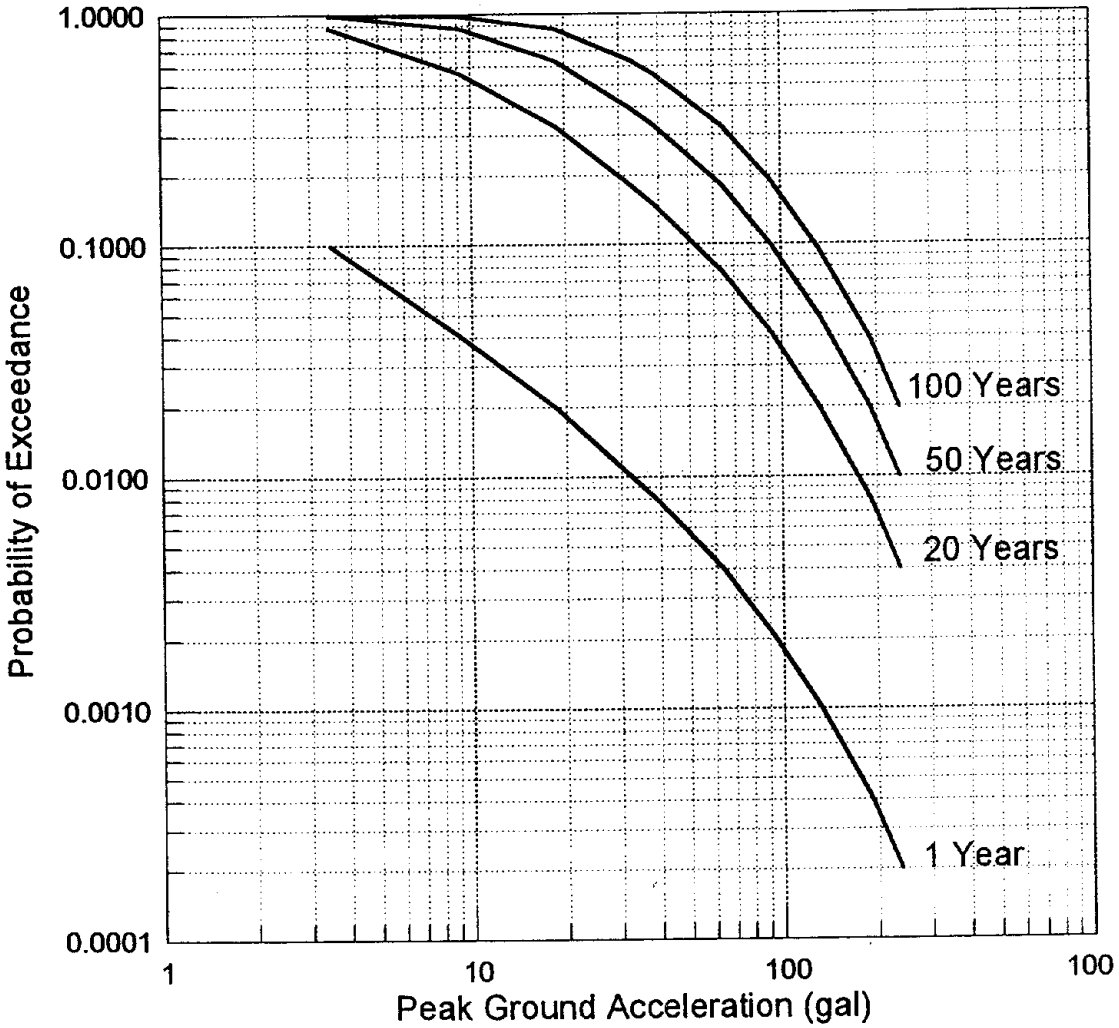

圖19　九龍場點基岩加速度峰值(PGA)不同年限的超越概率曲綫

Fig.19　Probability of exceedance of PGA in 1,20,50 and 100 years at Kowloon site(114°10′E, 22°19′N)

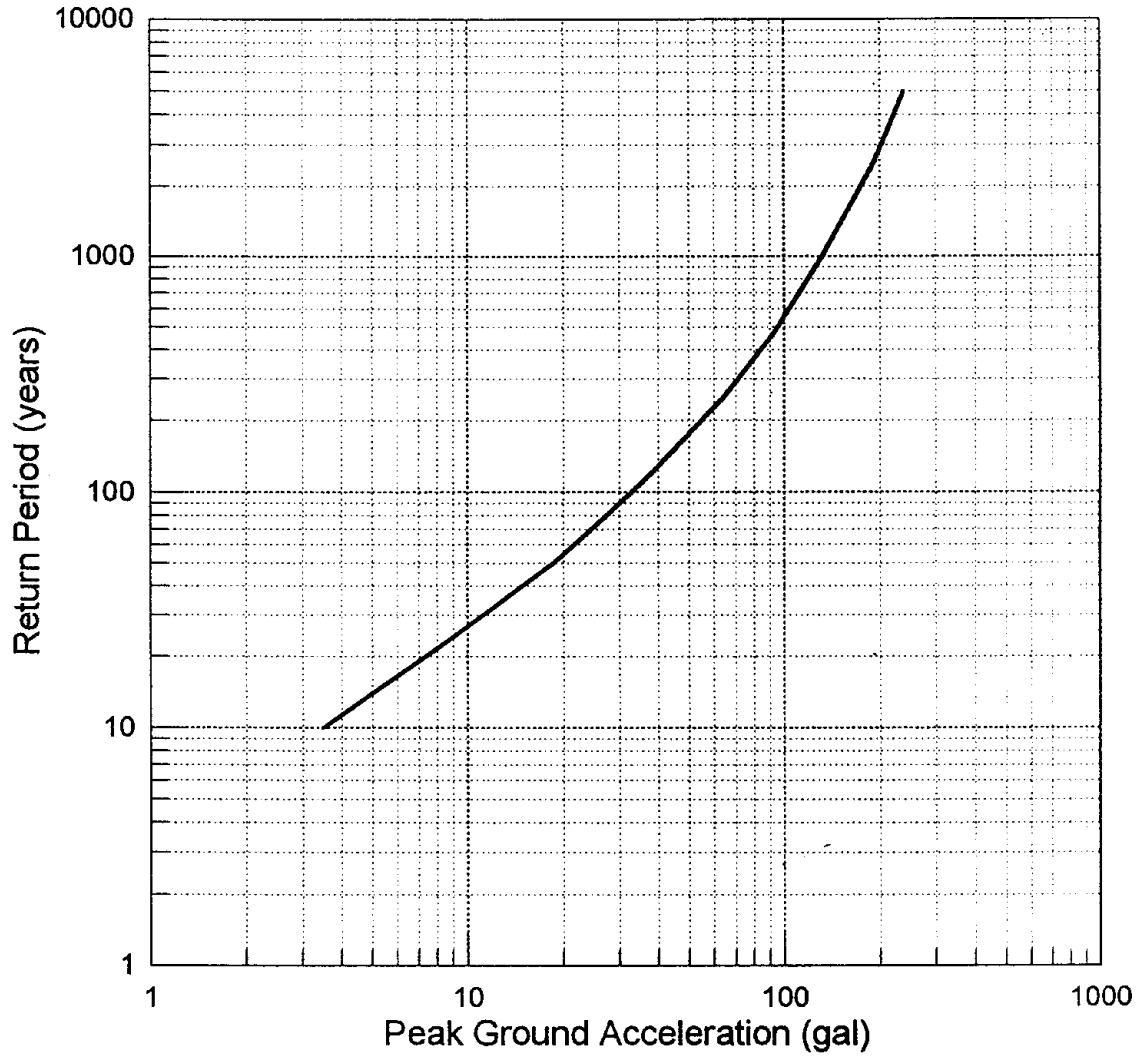

圖20　九龍場點和香港地區PGA的復發周期

Fig.20　Return period of PGA at Kowloon site(114°10′E, 22°19′N)

2. 地震烈度

香港地區50年超越概率分別爲63％、10％和2％的地震烈度等值綫分別示于圖21－1、2、3。50年超越概率爲63％的地震烈度均小于6度。50年超越概率爲10％的地震烈度界于6.95和7.30之間，絶大多數地區爲7度左右。本課題的計算結果表明，香港地區50年超越概率爲10％的地震烈度應確定爲Ⅶ度，與中國地震區劃圖(1990年)所示相符。

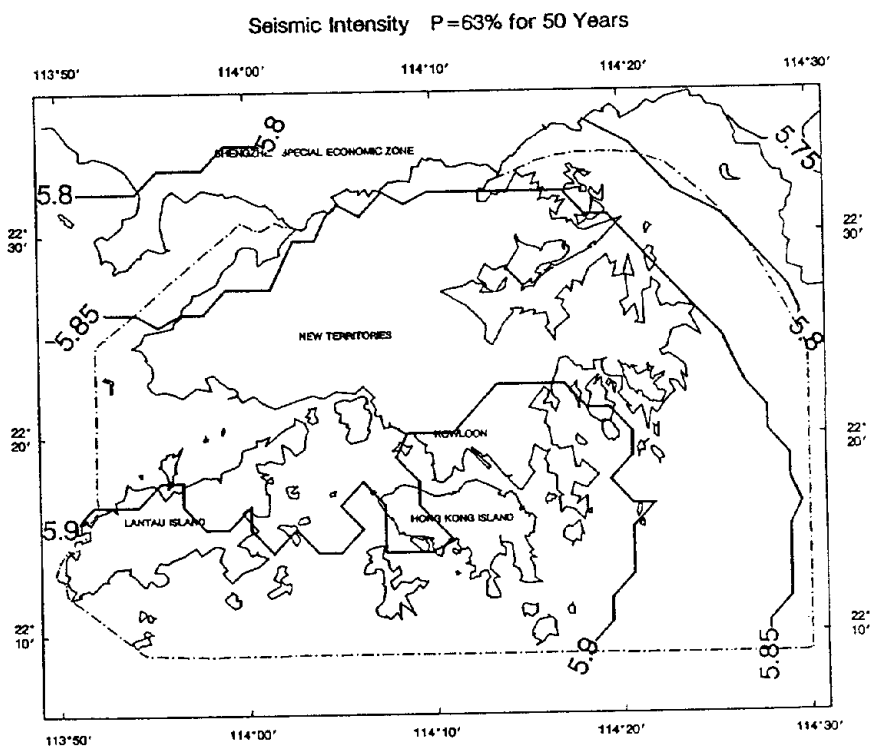

圖21－1　香港地區50年超越概率爲63％的地震烈度等值綫圖

Fig.21-1　Contour map showing the regional distribution of seismic intensity in Hong Kong (P=63% for 50years)

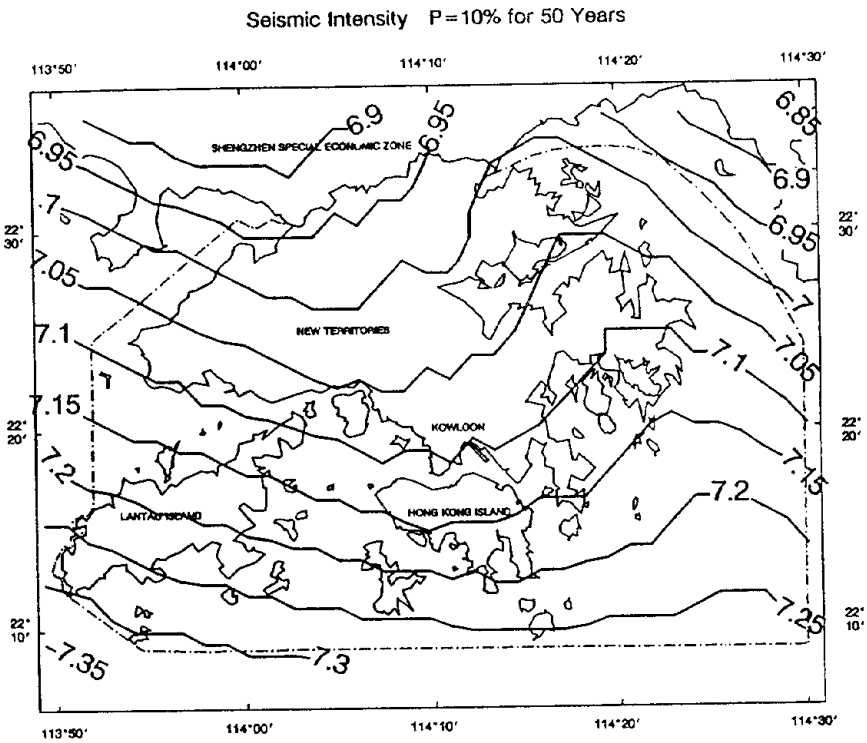

圖21－2　香港地區50年超越概率爲10％的地震烈度等值綫圖

Fig.21-2　Contour map showing the regional distribution of seismic intensity in Hong Kong (P=10% for 50years)

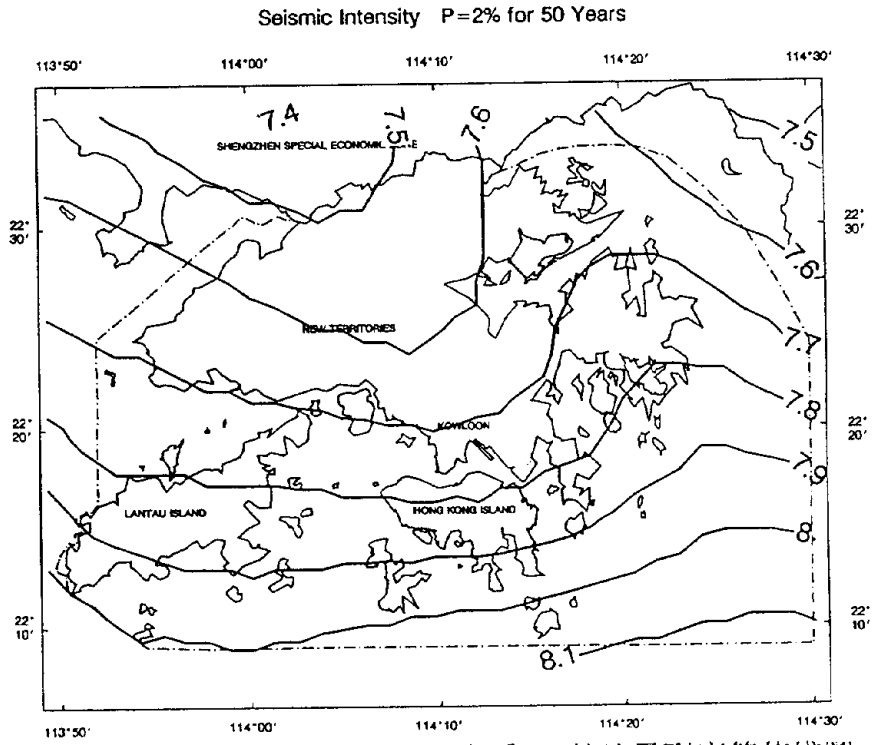

圖21－3　香港地區50年超越概率爲2％的地震烈度等值綫圖

Fig.21-3　Contour map showing the regional distribution of seismic intensity in Hong Kong (P=2% for 50years)

爲了具體地表示各潛在震源對本區烈度的貢獻，現以九龍場點(114°10′E，22°19′N)爲例，給出主要潛在震源的貢獻(表10，圖22)。對于VII度而言，有4個潛源的貢獻最大，對于VI度，則有9個潛源存在不同程度的影響。香港鄰近的4個潛源(23、38、32、48)的貢獻超過50%。

表10　各主要潛在震源區對九龍場點地震烈度的貢獻

編號		99	23	38	32	48	33	82	35	83
潛源名稱		擔杆島	深　圳	大嶼山	大鵬灣	珠江口	惠　陽	紅海灣	中　山	高欄島外
地震烈度	VI	40.1%	14.9%	16.6%	11.8%	11.6%	2.7%	1.8%	0.3%	0.2%
	VII	85.3%	2.8%	11.6%	0.3%					
	VIII	100.0%								

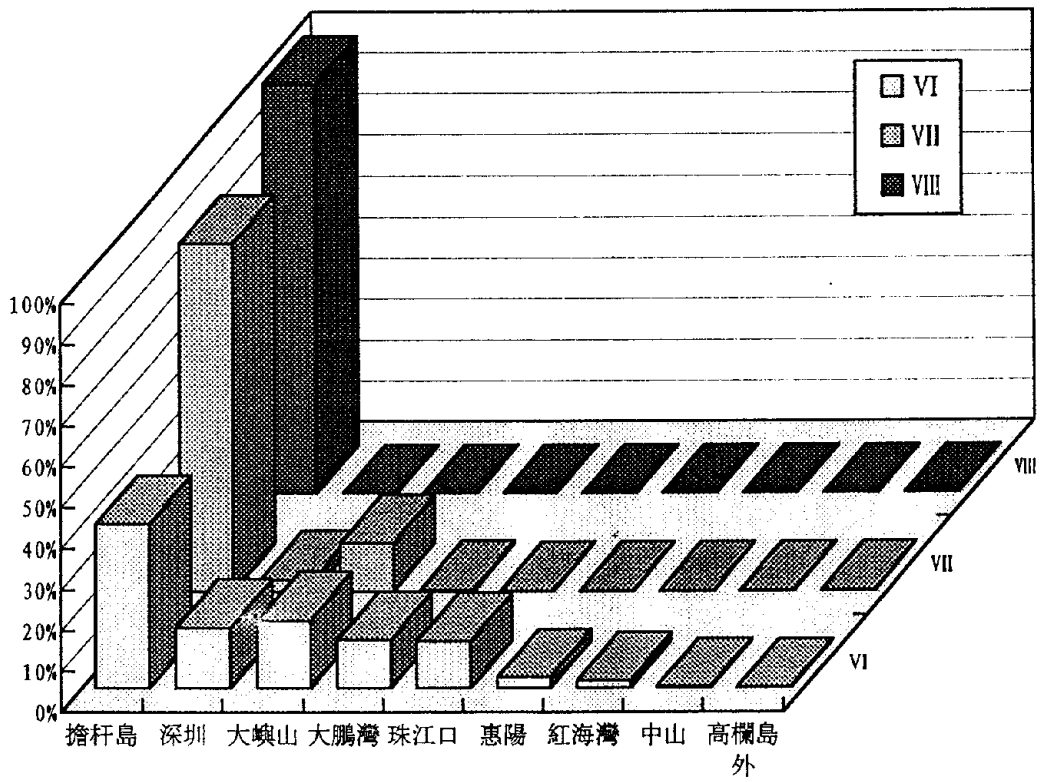

圖22　各主要潛在震源區對九龍場點地震烈度的貢獻

Fig.22　Devotion of the main potential seismic zones for seismic intensity at Kowloon site

九龍未來50年超越概率爲63％、10％和2％的地震烈度分別爲5.91、7.10和7.75. 九龍場點不同年限不同超越概率的地震烈度可以從圖23求得. 圖24爲九龍場點地震烈度的復發周期.

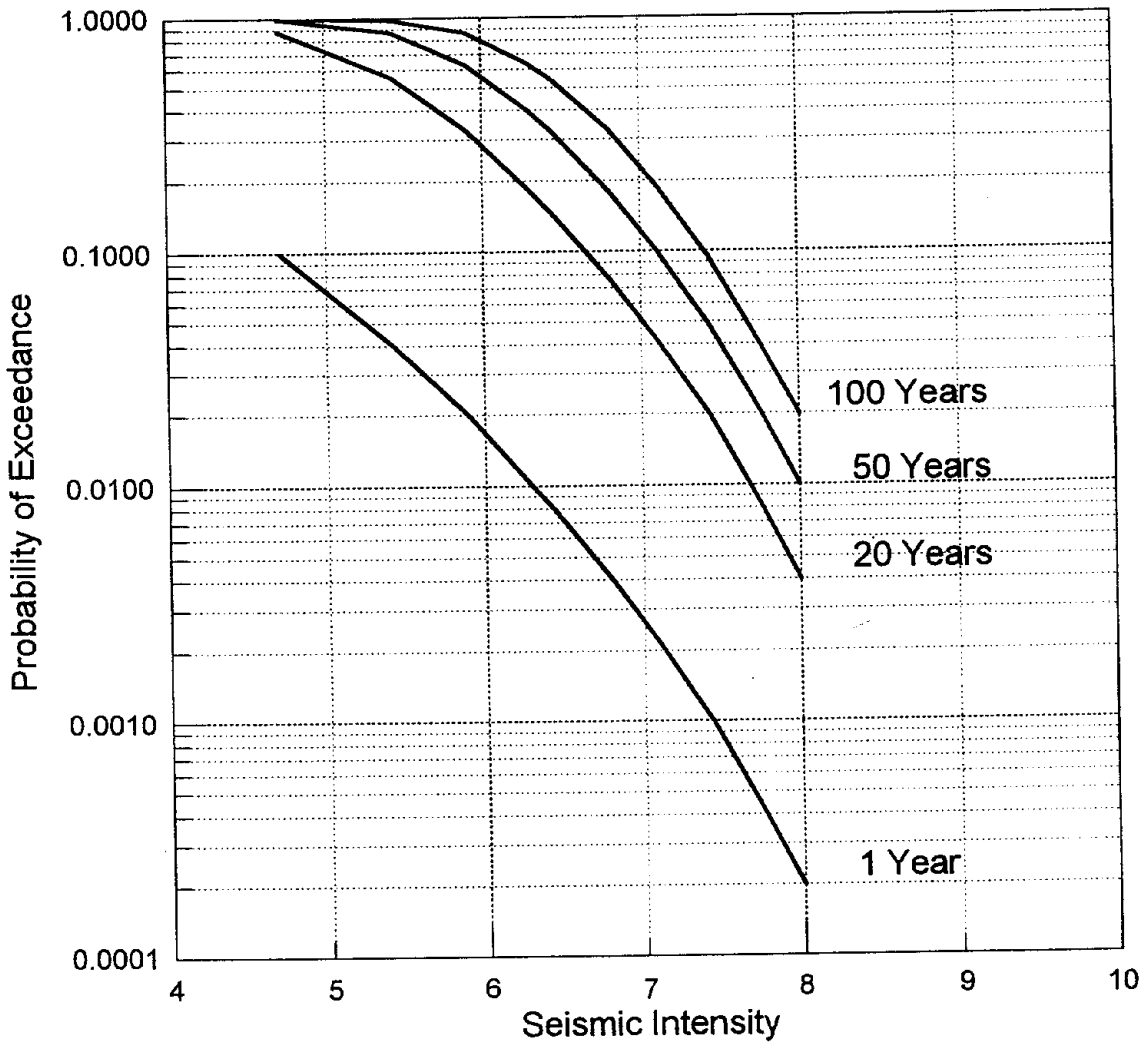

圖23　九龍場點不同年限不同超越概率的地震烈度

Fig.23　Probability of exceedance of seismic intensity in 1,20,50 and 100 years at Kowloon site(114°10′E, 22°19′N)

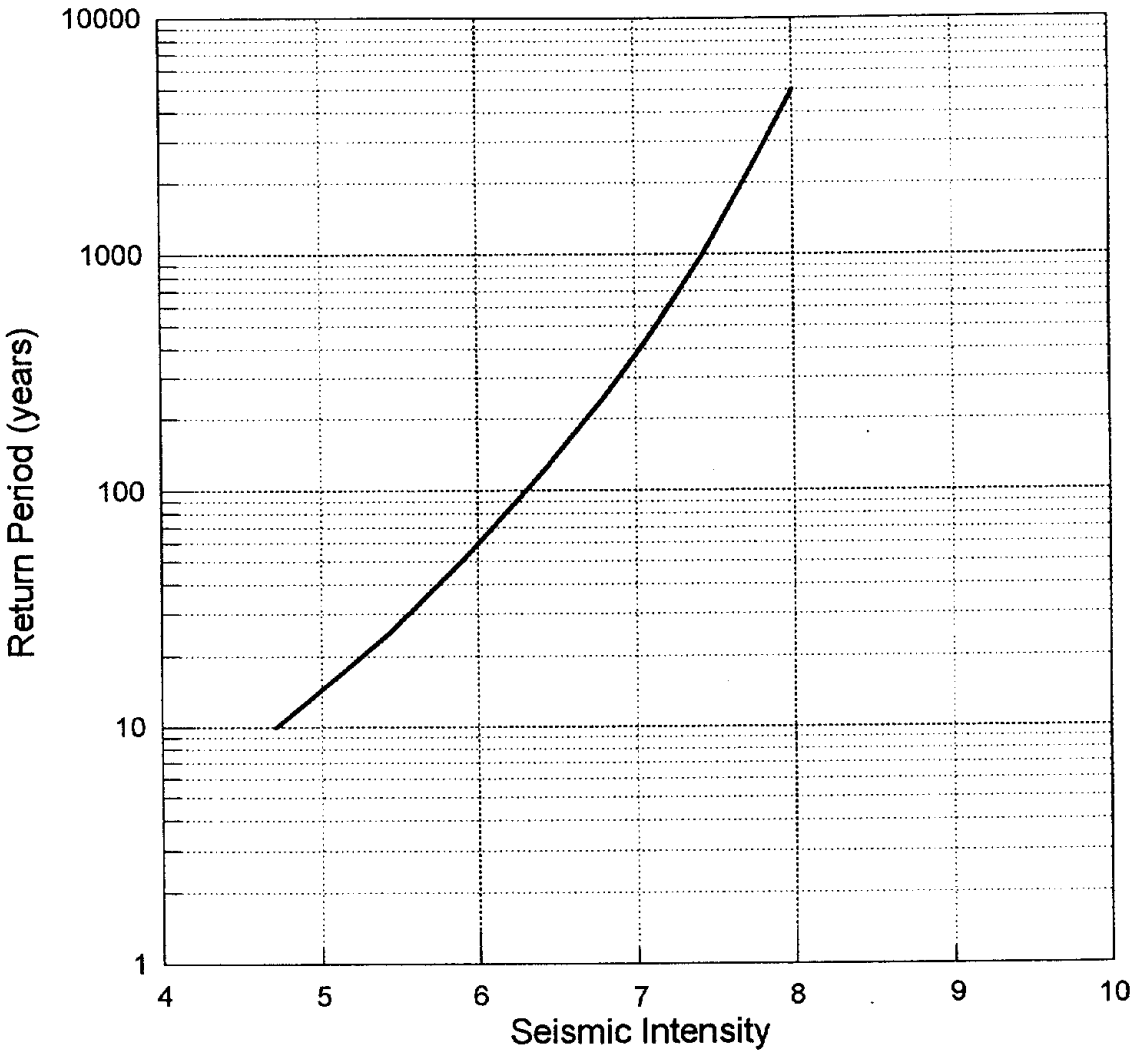

圖24　九龍場點地震烈度的復發周期

Fig.24　Return period of seismic intensity at Kowloon site(114°10′E, 22°19′N)

5.5 不確定性分析

由于地震危險性分析結果取決于計算時所輸入的各種參數，而后者有一定的人爲性，或者説有一定的不可靠性。爲此對計算結果應進行敏感性分析，這也是不確定分析的一個方面。

本研究課題對衰減關系的不確定性校正已在計算程序中予以考慮：基岩加速度衰減關系的離散性符合以$\sigma_{\ln a}$爲標準差的對數正態分布進行校正；烈度衰減關系的離散性符合以σ爲標準差的正態分布。

地震活動性參數是不確定的，目前尚無嚴密的數學公式計算其不確定性的影響。本課題采用讓參數在一定範圍內變化，從而得知地震活動性參數的變化對計算結果的影響程度。

1．潛在震源的劃分與權重

從表6和表7中可以得知，有4個潛在震源對本區的場點基岩加速度峰值和地震烈度的貢獻比較大，即擔杆島潛在震源區(99)、大嶼山潛在震源區(38)、深圳潛在震源區(23)和大鵬灣潛在震源區(32)。它們對峰值加速度爲75gal的影響達98%以上。爲此，本課題對擔杆島潛在震源區(99)的震級上限分別給出兩種方案，即7.0級和7.5級。對其他三個潛在震源區的震級上限也給出兩種方案，第一方案：大嶼山潛在震源區(38)與大鵬灣潛在震源區(32)的震級上限爲6.0級，深圳潛源區(23)爲5.5級，第二方案是把上述三個潛在震源區合并爲一個潛在震源區，震級上限爲6.0級。

同時，除去在第三章給出的潛在震源區權重矩陣(W_1)以外，還另外請專家給出另一組權重矩陣(W_2)，以便相互比較。以下仍然以九龍場點爲例，本文5.4節給出的地震危險性結果是按W_1、擔杆島潛在震源區(99)的震級上限爲7.0級，38、23和32爲三個震級上限分別爲6.0級、5.5級和6.0級的潛在震源區進行計算的，換言之，后三個潛在震源區爲分開的情況。計算結果是：基岩加速度峰值爲92.70gal，地震烈度爲7.11。按其他方案組合成另外7種組合方式，其結果如表11。該表給出的結果表明，不同組合方案對地震烈度的影響不大，烈度值在7.07度與7.37度之間，相差不超過0.3度。對基岩加速度的影響在86gal與116gal之間，相差30gal。本文給出的兩組權重矩陣雖然不完全相同，但是對計算結果影響很小，說明不同專家對本區潛源權重的分配意見基本相同。99號潛源的震級上限爲7.5級比7.0級使PGA增多24—26gal，地震

烈度增加0.2度。38、23與32三個潛源合并，則使PGA和烈度稍有下降，但不超過10gal或烈度0.04度。

表11　不同潛源劃及不同權重的計算結果

組合方案	權重矩陣	99號潛源的震級上限	38、23、32潛源	PGA(gal)	I
1	W_1	7.0	分開	92.70	7.11
2	W_1	7.5	分開	116.78	7.37
3	W_2	7.0	分開	92.71	7.12
4	W_2	7.5	分開	116.35	7.37
5	W_1	7.0	合并	86.14	7.07
6	W_1	7.5	合并	112.87	7.35
7	W_2	7.0	合并	88.32	7.09
8	W_2	7.5	合并	114.62	7.36

2. *b*值

本課題計算方案中的*b*值，外帶定爲0.56，內帶爲0.80。爲了分析b值的影響，對內外帶的*b*值分別加或減0.05。其結果(表12)顯示，*b*值的變化對地震烈度影響較小，約爲 ± 0.08度，對PGA的影響大約爲 ± 10gal以下。

表12　*b*值變化的影響

方案	外帶	內帶	PGA(gal)	I
1	0.56	0.80	92.70	7.11
2	0.61	0.85	84.90	7.03
3	0.51	0.75	101.27	7.19

3. 地震年發生率*v*

本課題按外帶年發生率爲1.38，內帶爲1.05計算。如果分別加或減20%，則結果如表13，所以年發生率變化20%，對地震危險性分析的計算結果影響不大，PGA增減10gal左右，地震烈度爲 ± 0.10度。

表13　地震年發生率ν的影響

方 案	外 帶	內 帶	PGA(gal)	I
1	1.38	1.05	92.70	7.11
2	1.66	1.26	102.03	7.19
3	1.10	0.84	82.06	7.01

4. 橢圓長軸取向

本文計算按橢圓衰減模型，其長軸的取向變化 ± 15°，對地震危險性分析的影響很小(表14)。

表14　橢圓長軸取向的影響

方案	橢圓長軸取向	PGA(gal)	I
1	原方案	92.70	7.11
2	+ 15°	95.79	7.13
3	− 15°	93.63	7.11

5.6 主要結論

經過地震危險性計算和不確定性分析，對香港地區地震危險性的評估意見是:

1. 計算得到，香港地區50年超越概率爲10%的基岩水平加速度峰值界于75gal和115gal之間。本地區中間位置的九龍場點(114°10′E, 22°19′N)爲92.70gal，此數值可以作爲香港地區基岩水平加速度峰值。

2. 香港地區50年超越概率10%的地震烈度爲6.95和7.30之間。鑒于地震烈度的劃分不宜過分精細，所以本地區各場點的地震基本烈度均宜取Ⅶ度爲宜。

參考文獻

1. 黃鎮國等,珠江三角洲形成發育演變,廣州: 科普出版社廣州分社,1982,168-187

2. 胡聿賢、張敏政, 缺乏强震觀測資料地區地震動參數的估算方法《地震工程與工程振動》, 1984(1),1-9

3. 周克森, 重要工程場地的地震小區劃問題, 第一屆兩岸地震學術討論文集, 北京: 地震出版社,1986,300-215

4. 李作明,香港地質簡介《廣東地質》,1987,第2卷第1期

5. 林紀曾等,東南沿海地區地震活動特征的研究,海南島北部地震研究文集,北京: 地震出版社,1988,173-184

6. 姚梅尹等,東南沿海地區幾次歷史地震的考證. 海南島北部地震研究文集,北京: 地震出版社,1988,211-216

7. 汪素雲等,華南地區地震動參數的衰減關系,海南島北部地震文集,北京: 地震出版社,1988,284-293

8. 丁原章等,廣東省地震地質問題《廣東地質》,1989,第四卷第一期,63-73

9. 張虎男等,華南沿海新構造運動與地質環境,北京: 地震出版社,1990,173-234

10. 國家地震局,中國地震烈度區劃圖説明書,地震出版社,1991年

11. 丁原章、梁勞,巴士系構造的地震危險性,華南地震,1992(2),1-13

12. 霍俊榮、胡聿賢,地震動峰值參數衰減規律的研究,地震工程與工程振動,1992,第12卷第2期,1-11

13. 霍俊榮、胡聿賢、馮啓民, 關于通過烈度資料估計地震動的研究,地震工程與工程振動, 1992,第12卷第3期,1-14

14. 丁原章,南海開發工作中的地震問題,華南地震,1994第14卷第1期,1-6

15. 國家地震局,工程場地地震安全性評價工作規範(DB001-94),北京: 地震出版社,1994

16. 丁原章等,香港地區地震危險性問題的回顧

17. Cornell, C.A.(1968). Engineering seismic risk analysis.*Bulletin of the Seismological Society of America*,vol.58,1583-1606.

18. Lau,R(1972). Seismicity of Hong Kong.*Royal Observatory, Hong kong, Technical Note* no.33,30 p.(Reprinted with revisions, 1977).

19. GCO(1991). *Review of Earthquake Data for the Hong Kong Region(GCOPublication No. 1/91)*.Geotechnical Control Office, 115 p.

20. British Geological Survey (1992). A review of the crustal structure and seismotectonics pertinent to Hong Kong.*British Geological Survey Technacal Report* WC/92/17,135p.

21. KW Lai etc.(1992). Spatial and Temporal Characteristics of Major Faults of Hong Kong.

22. Pun,W.K.& Ambraseys,N.N.(1992). Earthquake data review and seismic hazard anslysis for the Hong Kong region.*Earthquake Engineering and Structural Dynamics*,vol.21,pp433-443.

23. Pun,W.K.(1994).Earthquake resistance of buildings in Hong Kong.*Asia Engineer*,Vol.22, No.3,
pp25-28.

24. Scott,D.M.,Pappin,J.W.& Kwork,M.K.Y.(1994).Seismic design of buildings in Hong Kong.*Hong*
Kong Institution of Engineers Transaction,vol.1,no.2,pp37-50.

25. JP Busby etc.(1995).Interpretation of the Regional Gravity Survey of Hong Kong.*Hong Kong Geological*,1(Autumn)52-66

26. Ir,W.K.W.Pun etc.(1996). Determination of Seismic Load For Buildings In Hong Kong

27. Ir.C.K.Lau etc.(1996). Seismic Design of Tsing Ma Bridge.

28. 活斷層研究會編，日本の活斷層圖[付解説]，東京大學出版社，1992.